Master's Programme in Mechanical Engineering - Structural Mechanics -
October 2021

Study of non-linear strain path in sheet metal forming

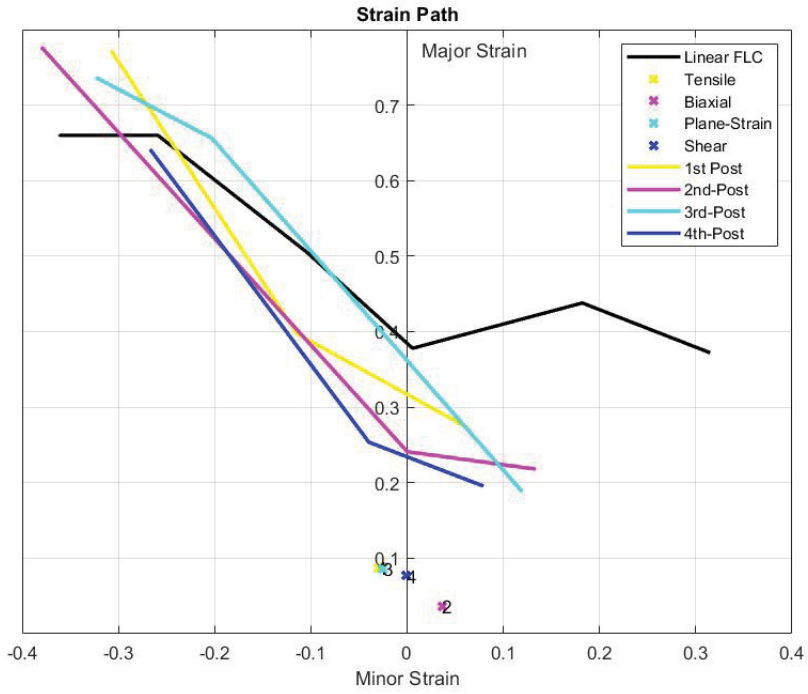

Chandramohan Aisvaran

In collaboration with:

Anton Eriksson

(Master of science in mechanical engineering with emphasis on structural mechanics)

Faculty of Engineering, Blekinge Institute of Technology, 371 79 Karlskrona, Sweden

This thesis is submitted to the Faculty of Engineering at Blekinge Institute of Technology in partial fulfilment of the requirements for the degree of Master's Programme in Mechanical Engineering - Structural Mechanics -. The thesis is equivalent to 20 weeks of full time studies.

The authors declare that they are the sole authors of this thesis and that they have not used any sources other than those listed in the bibliography and identified as references. They further declare that they have not submitted this thesis at any other institution to obtain a degree.

Contact Information:
Author(s):
Chandramohan Aisvaran
E-mail: chai19@student.bth.se

University advisor:
Ph.D. Md Shafiqul Islam
Department of Mechanical Engineering

Faculty of Engineering
Blekinge Institute of Technology
SE–371 79 Karlskrona, Sweden

Internet : www.bth.se
Phone : +46 455 38 50 00
Fax : +46 455 38 50 57

Abstract

At present, Sheet Metal Forming (SMF) is not just limited to increasing demand from automobile industries but also to various other manufacturing industries that utilize sheet metal forming processes. The surplus demands for optimised manufacturing products warrants the need for an extended decisive study on SMF.

One such area of study in SMF is formability. Traditionally, formability is predicted using the conventional Forming Limit Curve (FLC). But when it comes to complex SMF processes, FLC failure model can sometimes overestimate (for low uniaxial straining) or underestimate (for bi-axial straining) failure. This thesis focuses on suitable test procedures to generate non-linear strain paths and prediction of formability using the concept of Generalized Forming Limit Curve (GFLC). Initially, through systematic literature review, two-step process is chosen as the test procedure in this thesis. The test procedure was simulated in LS-Dyna to obtain results which are then used by GFLC concept to predict formability for a bi-linear deformation history. The predicted formability using the concept of GFLC is then compared with the predicted formability using FE-simulation and using experimentation. The found percent error for GFLC prediction compared to that of FE-simulation prediction is 11% and the percent error for GFLC prediction and experimentation prediction is 14%. However, these two predictions can not be used to validate the GFLC prediction. This is because in this thesis GFLC procedure uses data obtained from FE-simulation with GISSMO failure model. Through literature it is identified that the GFLC concept can be applied for multi-linear deformation histories to predict formability and the method to do so is explained in detail in this thesis. Finally it is concluded that the use of GFLC concept in conjunction with the two-step drawing process to predict formability for bi-linear deformation history is acceptable.

Keywords: Non-Linear strain path, Sheet metal forming, Generalized forming limit curve, Formability, CR4 material.

Acknowledgments

This master thesis was conducted at RISE IVF, located in Olofström, Sweden, and at the Mechanical Engineering department of Blekinge Institute of Technology (BTH), from January 2021 to October 2021 to analyse test procedures of non-linear strain paths in sheet metal forming.

First and foremost, I would like to express my sincere gratitude to my primary academic supervisor – Md Shafiqul Islam PhD for the continuous support he has given me to complete this master thesis. I am fortunate to have him as one of my main supervisors because of his patience, guidance, motivation, enthusiasm, and immense knowledge. Secondly, I would like to take this opportunity to convey my appreciation and gratitude to Lluis Pérez Caro PhD, my primary industry supervisor. The completion of this undertaking could not have been possible without his participation and assistance. Both of their contributions are sincerely appreciated and gratefully acknowledged.

I would also like to express my special thanks to Mats Sigvant PhD at Volvo Cars in Olofström, Eva-Lis Odenberger (RISE IVF) PhD, Alexander Barlo PhD candidate (BTH) for giving me useful and beneficial insights during every biweekly meetings. A special note of thanks to Roman Norz, M.Sc, research assistant, Technical University of Munich for providing valuable feedback, support and guidance whenever faced with a problem.

Once again, I would like to express my deep sense of gratitude to Md Shafiqul Islam PhD for giving me this golden opportunity to be a part of the project "PREDICT" [2, 3] financed by the Swedish innovation agency VINNOVA within the "Strategic Vehicle Research and Innovation (FFI) programme (grant number 2020-02986).

Contents

List of Figures

List of Tables

Acronyms

BCC	Body Centered Cubic
BSP	Broken Strain Path
BTH	Blekinge Institute of Technology
CAE	Computational Aided Engineering
CDM	Continuum Damage Models
DIC	Digital Image Correlation
DIEM	Damage Initiation and Evolution Model
DPT	Drawing Depth
DRD	Draw Reverse-Drawing
DRM	Design Research Methodology
DSI	Descriptive Study I
FE	Finite Element
FEM	Finite Element Method
FEA	Finite Element Analysis
FLC	Forming Limit Curve
FLD	Forming Limit Diagram
FLSD	Forming Limit Stress Diagram
FP	Failure Prediction
GISSMO	Generalised Incremental Stress State damage Model
GFLC	Generalized Forming Limit Concept
HS	High Strength
IVF	Institutet för Verkstadsteknisk Forskning (institution for engineering research)

MMC	Modified Mohr-Coulomb Criterion
NL	Non-Linear
NLSP	Non-Linear Strain path
NFLD	Non-Linear Forming Diagram
RC	Research Clarification
RISE	Research Institutes of Sweden
RQ	Research Question
SM	Sheet Metal
SMF	Sheet Metal Forming
TD	Transverse Direction
TDEM	Time Dependent Evaluation Method

Chapter 1

Introduction

1.1 Background

In various industries, manufacturing processes have been evolved and been evolving in order to cater the needs of the society effectively and efficiently. Sheet Metal Forming (SMF) is one such manufacturing process used by various industries. The process where metal sheets are modified to its geometry without removing materials from the sheet is known as Sheet metal forming [1]. SMF based manufacturing process is widely used in the production of automotive body parts, frames of aircraft, house of major home appliances and various fixtures of building [2], [3]. The advancement in various industries which utilized SMF manufacturing process such as automobile industry requires complex products with improvement in weight, toughness and sustainability. Compared to other manufacturing processes SMF offers little material waste enable the production of complex product shapes. However, this requires several steps to obtain the final desired product [1].

During the process of forming the material deforms non proportionally and non-linearly and broken strain paths are seen when changing the directions in which the loads are applied especially during multi-step forming process [1]. In order to reduce the manufacturing cost and time, it is important to analyse the material parameter called formability [4]. The material capability to undergo plastic deformation before rupture is known as formability. Formability of material depends on the number of steps involved in SMF process.

1.2 Problem statement

SMF with multi-step forming processes typically involves non-linear strain paths [5]. There are various test procedures such as uniaxial tests and shear tests involved in sheet metal forming but these tests are not sufficient to understand the effect non-linear strain paths on the material property know as formability [1]. Therefore, it is vital to understand the effect of non-linear strain paths seen in multi-step SMF processes on the formability of sheet metal. This thesis focuses on the test procedures to measure non-linear strain paths with the help of various literatures which focuses on the effect of non-linear strain paths in sheet metal forming processes.

1.3 Project Condition

This thesis has been carried out in association with Anton Eriksson. As both authors are from two different master program, the entirety of the project has been divided between the two authors with certain common parts of the project been present. For the completion of this thesis word findings and results from the thesis work of Eriksson's have been used for support and analysis.

1.4 Aim and Objectives

1.4.1 Aim

The thesis aims on enhancing the knowledge on the implications of non-linear strain paths which is seen in most of the industrial SMF processes and the testing methods that can be utilized to measure the non-linear strain paths. This focus is thereby carried out by the use of three objectives to achieve the above said aim.

1.4.2 Objectives

There are three fundamental objectives this thesis has set to achieve the above-mentioned aim :

- The first objective of this thesis is to carry out a literature review on the existing studies based on measuring the non-linear strain paths and characterization of the material properties such as formability from those tests. The literature review must also include modelling of fracture due the influence of linear and non-linear strains.
- The second objective of this thesis is to predict localized necking for arbitrary deformation history using Generalized Forming limit Concept (GFLC) by implementing metamodeling procedure in a computational software called MATLAB.
- The third objective of the thesis is to simulate the test procedure to compare the predicted formability obtained from GFLC.

1.5 Research Question

The objectives stated in the previous section number of research questions can be formulated to help guide protocol development and study design. The formulated research questions can be seen below. Although this thesis is done in collaboration with anther peer, certain topics are covered in an individual basis. In order to achieve this some of the research questions are carried out and analysed individually.

- What are the testing procedures that can be used to generate non-linear strain paths and characterization of the material properties from those tests? (Carried out by - Student 1)

- Which FE-Software and failure models are primarily used in researches to predict formability and failure? (Carried out by - Student 2)
- How to predict localized necking on arbitrary deformation history using GFLC? Carried out by -Student 1)
- What is the outcome of the metamodeling procedure? (Carried out by - Student 1)
- How do the outcomes from simulation compare to the results obtained from the metamodeling procedure (Carried out by – Student – 1)

The figure 1.1 below, shows the interconnections between the objectives and the formulated research questions.

No	Objectives	Research Question
1	Literature Review on the existing studies based on measuring the non-linear strain paths and characterization of the material properties such as formability from those tests. The literature review must also include modelling of fracture due the influence of linear and nonlinear strains.	What are the testing procedures that can be used to generate non-linear strain paths and characterization of the material properties from those tests? (Carried out by - Student 1)
		Which FE-Software and failure models are primarily used in researches to predict formability and failure? (Carried out by - Student 2)
2	Predict localized necking for arbitrary deformation history using Generalized Forming limit Concept (GFLC) by implementing metamodeling procedure in a computational software called MATLAB.	How to predict localized necking on arbitrary deformation history using GFLC? Carried out by -Student 1)
		What is the outcome of the metamodeling procedure? (Carried out by - Student 1)
3	Simulate the test procedure to compare the predicted formability obtained from GFLC.	How do the outcomes from simulation compare to the results obtained from the metamodeling procedure (Carried out by – Student – 1)

Figure 1.1: Objectives and their corresponding research questions

1.6 Scope

This study initially focuses on the existing test procedures to measure non-linear strain paths by reviewing related papers. As this thesis project is carried out in conjunction with Anton Eriksson as mentioned under Project conditions previously, certain findings and results are used from his thesis work. Accordingly, this thesis does not include literature review on FE–software and fracture models but includes the finding from Anton Eriksson in his thesis. A Metamodeling technique is applied for a test procedure and corresponding results are obtained. Furthermore FE-modelling

of the above test procedure is also carried out in the thesis. Finally, this thesis covers the discussion on the results obtained from both metamodeling and FE-Simulation for the test procedures to measure non-linear strain paths.

1.7 Limitation

Below are few listed limitations faced while conduction this thesis.

- The test procedure, 'Bulging with stepped dies' cannot be carried out as it involves higher investment for constructing different die geometries.
- The test procedure in-plane biaxial tensile test with cruciform specimen would require a higher investment to adapt 4 independent actuators to control the strain path in the central area of the specimen at RISE research facility in Olofstörm.
- Certain test procedures were unable to perform due to limited range of the strain rate in the existing experimental apparatus.
- The prediction of formability using GFLC concept cannot be validated using the results from FE-simulation and experimentation. This is due to the influence of different formability prediction approach by the used failure models.

Chapter 2

Literature Review

2.1 Introduction

This chapter focuses on the literature which highlight on the requirement for test procedures to analyse non-linear strain paths seen in complex sheet metal forming processes and on different test procedures involved in measuring such non-linear strain paths. Test procedures as discussed by the authors have been summarized in detail, providing a clear knowledge and understanding in order to perform Finite Element (FE) simulations and to conduct the experiment with the aid of Digital Image Correlation (DIC).

2.2 Sheet Metal Forming process (SMF)

An industrial manufacturing process called the sheet metal forming process typically involves various stages before finishing the final product [1]. Single step forming process are also available but with the increasing requirement for complex products, multi-step process are widely used. Single step processes typically creates linear strain paths and multistep processes create non-linear strain paths in the material that is undergoing forming [1,4,6].

In this thesis, the effect of non-linear strain paths seen in multi-step SMF process will be the primary focus.

2.2.1 Effect of non-linear strain paths in Sheet Metal Forming

Non-linear loadings have a great effect on level and shape of forming limit curves [6]. This is very commonly faced and seen in industrial processes and have been exhibited by many authors [6]. Nearly all of the studies are based on the use of the M-K model and are systematic and logical in this literature. Forming limits with two types of combined loading have been analysed by Yoshida et al. [7]. The first is a two linear stress paths whereby unloading is included between the first and second loading. Secondly, a loading whereby the strain path is instantaneously changed without unloading. They have exhibited that FLC in strain space rely significantly on the strain path whereas limit stresses formation is only influenced by the second type of loading.

Kuroda and Tvergaard [8] proposed a riveting study to demonstrate dependence on if or not the load on the sheet is removed between two load steps on a non-proportional strain path. For two load steps without unloading, tremendous unsteady

behaviour can be seen in this theoretical analysis based on the M-K model. A quick change of stress point along the yield surface can explain the reason for jumps of FLC. This is in the case for specific strain path. An anisotropic model formed on texture and dislocation structure have been established by Hiwatashi et al. [9] in order for predictions of some experimental tendencies to be better. In order for predictions of AA6111 FLCs to be ameliorated, Chow et al. [10] extended an anisotrophic damage model. The studies are largely concentrated on 6000 series in the case of aluminium alloys, if followed by plane strain or biaxial tension, prestrain in biaxial tension normally reduces the formability; but if followed by biaxial tension, prestrain in uniaxial tension, along the rolling direction, increases the forming limits. Forming limits systematically drops if principal strains after prestraining are rotated. A stress-based forming limit idea was put forward during the early years in the 80s [11] which looks to be independent on strain path changes. Although a stress state can't be measured experimentally, many authors [12], [13] embraced this concept. With a good description of the plastic behaviour of the material (yield criterion and hardening law) [14], experimental forming limit stress diagrams can be achieved indirectly.

There is less experimental data due to the complexity of the procedure regarding effect of changes of strain path. During the 90s, an early experimental work on aluminum alloy 6111 by Graf and Hosford [15] whereby forming limit curves of specimens pre-strained to a few levels in uniaxial, plane strain and biaxial tension, parallel and perpendicular to the rolling direction have been decided. In many research work [15], [10], [16], these experimental data have been used as reference experimental data on a great degree. Traditionally a two-step procedure is done for forming limit curves characterization as it is unfeasible to control strain path changes with the conventional tests. Bulge tests and oversized tensile tests generally used to realize prestrains. Subsequently, on the prestrain sheets, standard Marciniak or Nakajima tests can be performed. Butuc et al. [14] too utilised this 2-step procedure to work out the stress-based forming limits from experimental strain data. Not too long ago, Volk et al. [17] also used this to plot experimental forming limit curves with six prestrains; from uniaxial to equibiaxial. This procedure consumes a lot of time and needs a few experimental devices. Moreover, the measure of the strain path is discontinuous between the 2 steps. Last but not least, curved loading path are seen in actual forming processes without any unloading. Moreover, if the loading procedure really affects the material forming limits, the traditional 2 steps procedure with unloading considered to be unseemly. Therefore, it is inevitable to choose a single test procedure to measure non-linear strain paths.

2.3 Test procedures

There are many test procedures used by various authors to realize non-linear strain paths seen in sheet metal forming processes. Below are few of the test procedures and will be discussed in detail in the following subsections.

Test procedures:

- Cruciform specimen in a conventional Nakajima test setup

- Nakajima testing with modified punch geometry
- Two-step deep-drawing or drawing reverse-drawing process
- Bulging with stepped dies
- In-plane bi-axial test with cruciform specimen

2.3.1 Cruciform Specimen in a conventional Nakajima test

Jocham [18], in his work put forwarded a test procedure which allows the identification of non-linear load paths in a conventional Nakajima test setup with the use of a draw bead tool and a cruciform specimen. He and others utilized preformed Nakajima specimens which were cut using 3D laser in order to generate non-proportional load paths or non-linear load paths [18]. As the specimen's dimensions typically gets reduced with every cutting only certain strain path can be realized with these specimens. Modified Marciniak tool could be used for pre-straining the specimens to solve the above problem [19]. For all width range of Nakajima specimen, uniformly distributed strain area is considerably larger. This method warrants the need for multiple tools. In recent years, yield loci have been evaluated by various authors for the cruciform specimen. There exist various different cruciform geometries in order to determine yield-loci [20-22]. Such cruciform specimens are optimised by considering uniform distribution of strain for a large area. However. when higher strains are applied. These specimens tend to fracture in the areas which are outside the evaluated parts.

Different cruciform specimens should be employed to create nonproportional load paths. In-plane biaxial test is used by Leotoing et al. [23] in order to identify localized necking. Their cruciform specimen is milled to create areas with three different thickness. Efe and Güler [24] in their works also used biaxial apparatus for testing.

In order to strengthen the specimen to achieve higher strain, the arms of the cruciform specimen must be strengthened. Yong and others employed laser deposition to achieve this [25]. A black holder with draw bead which can be adjusted is used by Jocham et al. [18], [26] to generate load-paths which are non-proportional. Jocham's test setup permits all the tests to be carried out in a single conventional Nakajima testing machine. In this test setup the draw bead heights can be adjusted within the range of 0 mm to 7 mm. Various load cases are applied to the test specimen using these draw beads. Norz and Volk used aluminium sheets (AW-5754) of thickness 2 mm where the specimen is indented in the centre [26]. Accordingly, their reduced thickness of 0.7mm in the center warranted that the crack initiates in the evaluation area.

Above critical review on the test procedure to measure non-linear strain paths or non-proportional load paths using a cruciform specimen in conventional Nakajima test shows its applicability in this project.

2.3.2 Modifying Punch Geometry

Krishna et al. [27] and Mathias et al. [28] developed an experimental approach to realize non-linear strain paths in a single experimental step rather than the traditional two step procedure. Both the group of authors modified the punch geometry for the standard Nakajima testing machine. Accordingly, formability of sheet metals can be determined accurately along with different strain paths by adjusting the punch designs. Krishna et al. [27] simulated the new punch designs in the commercial software called LS-DYNA and validated the results using material testing such as tensile test and biaxial formability testing using Institute for Metal Forming Technology (IFU) Nakajima press by replacing the punch with the new punch design. Mathias et al. [28] presented supporting evidence in his paper about the applicability of this new punch geometry approach to realize non-linear strain paths. Both these papers almost presented similar conclusions supporting this test set up.

2.3.3 Two-step deep-drawing or Drawing reverse-drawing process

Christian et al. [29] used a test setup involving two-step deep drawing process to investigate the necking behaviour for Aluminium and two types of steel alloys under non-linear strain paths. Hongzhou and Xin in their work [30], developed a similar test setup based on drawing reverse-drawing process to analyse formability of sheet metal during Sheet metal forming process with the influence of significant non-linear strain paths.

The first operation of the experimental procedure of Christian a beading is brought into the blank [29]. This beading is important to avoid the flow of material in the second operation of Christian's deep drawing step. He created non-linear strains in his second forming operation using an axisymmetrical punch which is connected to the upper die which is said to draw the blank over an elliptical counter punch that is situated on the lower die [29]. The upper punch is the only part which is in contact with the sheet metal specimen in the beginning. Christian et al. performed a strain path which is linear depending on blank shape. Furthermore, sheet specimen meets the elliptical shaped counterpunch during drawing [29]. By performing this Christian changed the strain path to a non-linear strain path. He maintained a constant velocity of 0.085mm/s when moving the lower die towards the upper die. The blank holder is said to be attached to the lower die. Christian et al. [29] applied a uniformly distributed clamping force of 407N by applying the clamping force over 15 equally spaced bolts. To avoid the friction which is said to be an important parameter that affects the sheet metal forming process, Christian et al. [29] put a latex foil of 0.1 mm thickness between the sheet specimen and the die.

Christian et al. [29] used three blank shapes to realize non-linear strain paths of different types. Their specimens were of different widths (340mm, 180mm, 80mm). Furthermore, in order to change the first contact point between the sheet specimen and the lower die Christian used adjustable shims [29]. This clearly resulted in the variation of non-linear strain paths in the specimen. He drew the blank shapes under the elliptical counterpunch with one and four shims. He also validated the test procedure using three different samples [29].

Hongzhou and Xin in their work [30], implemented their experimental setup with drawing reverse-drawing in three procedures. They prepared the specimen in their first procedure [30]. They also prepared three test specimens with different sizes similar to that of Christian et al. [29.] Hongzhou and Xin [30] prepared the specimens by trimming using Electrical Discharge in order to realize varying forming limit strains and strain loading modes. In the second procedure they pre-formed the draw bead [30]. During pre-forming there tends to be difficulties in applying required punch force to fully form the draw bead. Hongzhou preformed the draw bead on a separate press with higher tonnage as the hydraulic press used the typical draw reverse-drawing test is not enough to supply the needed punch force [30]. Honghou and xin, [30] placed the convex draw bead on the die and the concave draw bead on the punch tool. During this preforming procedure, with the central strain measurement region, only a little tension pre-strain and spring back was seen. This can be ignored as the it has a very little impact on the forming limit strain in the following procedure. In the final procedure of Hongzhou and Xin, the blank was fixed between the die and the binder [30]. They also placed 15 equally distributed bolts to apply the clamping force same as Christian et al. [29]. Both the work by Christian and Hongzhou used Digital Image Corelation (DIC) system to measure the data.

2.3.4 Bulging with Stepped dies

In the past 30 years, various experimental procedures have been developed for biaxial tests. Bulge test with elliptical or circular shaped die is considered to be widely used experimental method for biaxial tests which clearly does not include friction [31,32]. Bulging test with circular die is generally used to analyse sheet metals undergoing biaxial tension in order to determine flow stress curves [33,34]. This test clearly shows that biaxial loading case better than uniaxial tensile tests in representing flow stress properties at higher strain levels [35].

Forming Limit Curve (FLC) can be computed using bulging tests with elliptical shaped dies and using the theoretical model, flow stress seen at the poles of the bulging test area can be evaluated [36-38]. An analytical model under the assumption where the surface of the bulged specimen can be approximated to a rotational ellipsoid is proposed and developed by Lăzărescu et al. [39,40]. Lăzărescu et al also determined the corresponding equivalent stress-strain curves [39,40]. Furthermore, William et al. [41] and Lenzen et al. [42] in their works applied stress states which they obtained from bulging test with elliptical shaped dies to determine the yield surfaces. However, its is seen that only linear loading paths could be measured using bulging with elliptical or circular shaped dies.

Zhalehfar et al. [43] in their work used a two-step dome test formed an aluminium alloy in order to investigate non-linear strain paths on the FLC. Sugawara et al. [44] developed a testing apparatus where stretching is done double-action punch to realize non-linear strain paths without unloading. Kuwabara et al. [45-47] developed a test procedure using biaxial tensile test and cruciform test specimen to control the changing load paths continuously in one test. By controlling the four arms it is possible to realize non-linear load paths effectively [48]. Cruciform test specimen with thinner central region must be used to observe higher strain levels in the central area of the test specimen [49-52]. Due to this, cruciform test specimen with biaxial

tensile testing is widely employed to study hardening and yield behaviour of sheet metals.

The sheet was bent into a tubular specimen by Sumita et al. [53] and Kuwabara et al. [54] and tested by combining tension and internal pressure using a servo-controlled tube bulge testing machine developed by Kuwabara et al. [55,56] in order to measure the deformation behaviour of sheet metals under biaxial tension for a large strain range. This method of testing has the potential to measure a tube specimen's elastic-plastic behaviour to a prescribed strain paths from yield to fracture [57,58]. However, there might be a small draw back to this process where, the mechanical properties and the micro-structure of the tested specimen might be impacted due to the involved bending process.

Zhubin et al. [59] developed a novel test procedure to realize continuous non-linear biaxial tensile deformations of sheet metals by bulging with stepped dies. According to their work it can be concluded that non-linear loading paths can be effectively realized using this test procedure [59]. When the bulging process changes from an elliptical step to another elliptical step, the poles thickness and the curvature radius versus bulging height change suddenly. When the difference between the two elliptical sections are greater, more clear non-linear load paths can be seen. Zhubin [59] used the changing cross section of the die cavity for the provided sheet metal and its corresponding relative position with the die to determine non-linear loading path. Zhubin et al. [59] used this test procedure to obtain smooth and abrupt non-linear load paths.

2.3.5 In-plane biaxial test with cruciform specimen

As a means to overcome the downsides of conventional methods, a great alternative would be using the in-plane biaxial tensile test with the cruciform specimen to control the strain path. In order to study the effect of strain path change on the FLCN and to investigate the FLCF under linear strain paths, the presenting authors [60,61] validated the potentiality of the in-plane biaxial tensile test with a cruciform specimen. Initially it can be said that the motion of actuators along the axes can be used to control the strain path throughout the test. It can be said that this is enough to include complete linear and non-linear strain path which is enough to cover the complete forming limit diagram. Moreover, during the change of strain path the measurement of strain is considered to be continuous and unloading on the specimen is not mandatory.

Lastly, complex strain path having a few changes can be predicted for continuous process conditions like temperature and strain rate. The design of the cruciform specimen remains to be the important point for the in-plane biaxial tensile test. In the literature, a great number of cruciform shapes have been put forward, depending on the mechanical behaviour to be acknowledged such as hardening, forming limits and yield locus. Of late, a standardized shape that has been proposed based on the works of Kuwabara et al. [62] is not suitable for forming limit investigations. The reason for this is that there is a very low strain in the central area fracture occurs in the arms. For the establishment of FLCN and FLCF [61] for AA5086, with 4mm starting thickness, a first geometry made from a metal sheet was validated. The correlation between results from conventional Marciniak tests and biaxial tensile tests

for linear strain paths is relatively good for FLCN [6]. In recent times, the author optimized and validated a new shape with a 2mm starting thickness for linear strain paths. [65]. When the thickness is reduced from 4mm to 2 mm, it can be deduced that it permits to analyse the sheet metal over many applications. In the central region a reduction of thickness in imminent for the two geometries. Furthermore, it can be said that the transverse rigidity is reduced by the two arms and strain localization is seen at the junction area between the two perpendicular arms. Song et al. [66] used experimental setup with in-plane biaxial test in their work to investigate forming limit strains at fracture and necking under non-linear strain paths.

2.4 Summary of literatures using the test procedures

This literature review mainly focuses answering the research question 'What are the testing procedures that can be used to generate non-linear strain paths and characterization of the material properties from those tests?'. However the research question related to literature review 'Which FE-Software and failure models are primarily used in researches to predict formability and failure?' will be handles by Anton Eriksson in his thesis. Figure 2.1 and figure 2.2 below shows a summary of literatures that uses the previously discussed test procedures.

Ref	Purpose	Methodology	Findings
Cruciform specimen in a conventional Nakajima test setup.			
18	Identifying nonlinear strain paths	Using Draw bead tools and cruciform specimen in standard Nakajima test	The simulation is almost near the experimental results. Formability predicted using General FLC.
26	Identifying nonlinear strain paths	Cruciform Specimen in standard Nakajima testing machine	The experimental results correspond with the predicted results.
Modifying Punch Geometry for a Nakajima test setup			
27	Identifying nonlinear strain paths in single step	Modelling different punch geometry and simulating the test procedure in LS-DYNA	The results of simulation correspond with the experimental results
28	Identifying nonlinear strain paths in single step	Modelling different punch geometry and simulating the test procedure in LS-DYNA	The results of simulation correspond with the experimental results
Two-step deep-drawing or Drawing reverse-drawing process			
29	Investigating necking behaviour using two-step deep drawing test	Two-step deep drawing method is used to identify nonlinear strain paths with the help of DIC	The experimental methods are validated using other method such as time dependant methods.
30	Analytical approach for forming limit calculations	Comparing the results of the proposed analytical approach with experimental results (results from drawing reverse-drawing process)	The results from analytical approach can be validated using the results from the experiment.

Figure 2.1: Summary of findings 1 of 2

Ref	Purpose	Methodology	Findings
Bulging with stepped dies			
43	Investigating nonlinear strain paths on the FLC	Using two step dome test to compare the results with the results of the analytical method	Both the results agreed.
59	Developing novel test setup with single step to realize nonlinear strain path	Bulging with stepped dies	Feasibility of the proposed novel test procedure is validated.
In-plane biaxial test with a cruciform specimen			
17	Developing one-step procedure to control strain path changes in sheets, without unloading	In-plane biaxial test with independent actuators to control the displacement of the arms of the cruciform specimen	Predictive and experimental forming limits are severely influenced by pre-strains. Premature necking is seen when applying higher strain
65	Identifying Forming limit strains under the influence of nonlinear strain path	In-plane biaxial test with independent actuators to control the displacement of the arms of the cruciform specimen	Comparing the Forming limit under linear strain path with nonlinear strain paths.

Figure 2.2: Summary of finding 2 of 2

Chapter 3

Theory

3.1 Introduction

The following chapter introduces the theories that are utilized for basic understanding of the problem and analysis of the thesis.

3.2 Formability

A metal sheet can only be deformed to a certain extent in SMF manufacturing processes. Formability refers to the ability of a sheet metal to bend to a required shape without local necking or fracturing. The forming limit diagram (FLD) or forming limit curve (FLC) is the most widely used technique for evaluating sheet metal formability. An FLD is a diagram containing major and minor strains that can differentiate between protected points and those that are necked or broken. Forming limit curve at necking (FLCN) or FLC depicts the transition from the safe to necked points, whereas forming limit curve at fracture (FLCF) or fracture forming limit line (FFL) depicts the transition from safe to fractured points in SMF process. Sheet metal formability is influenced by a variety of factors, including structural properties and process parameters such as strain path, strain rate, temperature, etc. In order to completely optimize the formability of the material, the design and optimization of forming process using computational instruments, such as FE analyses, require a more precise prediction of material formability.

3.3 Forming Limit Curve (FLC)

Various factors are used in computing the moment of fracture. When a function based on stress and strain reaches a critical value, a fracture occurs. The majority of the parameters are based on plastic strains concentration [66-68]. From various techniques of analysis of formability, the concept of a forming limit diagram, also called forming limit curve, especially in the context of complex drawn – parts appear to be very beneficial [69-72]. Keeler and Backofen [73] and Goodwin [74] established forming limit curve, which has since become a common feature in the optimization of sheet-metal forming processes [75]. As stated by Marciniak et al. [76], forming limit curve reports local necking and tearing that is a curve dependent material property on the state of the strain, but not on the boundary conditions. As a result, the goal in designing sheet-metal forming is to ensure that strains observed in the

sheet do not come near this limit curve [77-81], underline that in the event that the material properties or process conditions vary slightly, a safe forming zone with an acceptable margin between it and the limit curve must be marked . The majority of works address empirical methods for determining forming limit curve, but with the emergence of computational methods, numerical models based on ductile fracture parameters for predicting forming limit curves [66,75,76] have become more popular. Other models, for example, the one introduced by Hill [82] on localised necking and, diffuse necking introduced by Swift [79], and the development of thickness imperfection model done by Marciniak and Kuczynski [83] are utilized as well. However, since forecasting forming limit curves requires complicated equations, its practical use is minimal [81].

3.4 Forming limit curve and its role in assessment of sheet formability

A forming limit curve is a graphical representation of limit strains which cannot be exceeded during sheet – metal forming. It is presented in the system of the in – plane principal strains: major strain ϕ_1 and minor strain ϕ_2. A forming limit curve minimum occurs at or near the major strain axis. Marciniak et al . [77] notices that the curve intercepts the major strain axis at approximately the value of strain - hardening exponent n. As n decreases, the height of the curve also decreases. A sheet metal exposed to strains that lie above the curve will fracture, while strains underneath the curve are safe to apply to the metal. Usually, two curves are plotted on the diagram. One of them is the Forming Limit Curve at Fracture (FLCF) and the second one, which lies slightly below FLCF, is Forming Limit Curve at Neck (FLCN). Figure 3.1 presents their location in FLD. The space between them is the zone where the metal can be safe or may crack, so in practice it is worth avoiding this zone. When the strains from this zone are applied to the metal, necking is likely to occur.

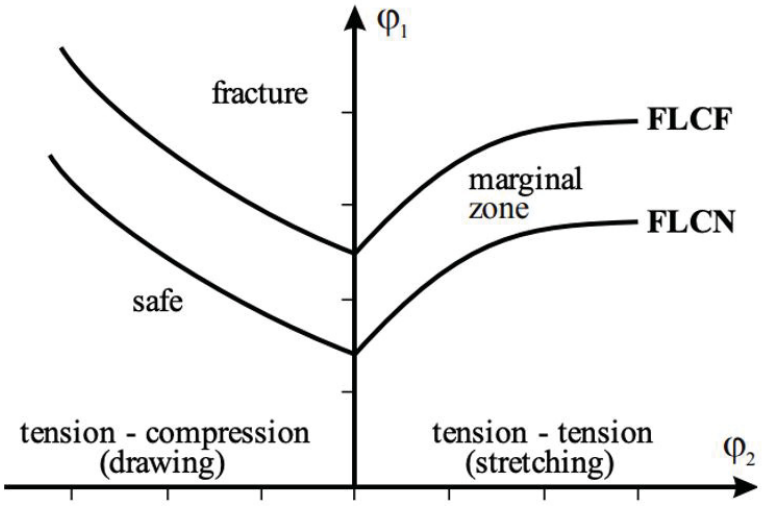

Figure 3.1: Forming Limit Diagram (FLD)

FLD is used in sheet - metal forming for predicting the forming behaviour of sheet metal and making a decision if any improvements in the forming process are needed. To do this the strains in the drawn - part (ϕ_{d-p}) are compared with the limit strains (ϕ_l). If the strains in the drawn - part are much smaller than the limit strains ($\phi_{d-p} \ll \phi_1$) it means that it is possible to use the sheet with lower formability. If the strains in the drawn - part are only slightly smaller than the limit strains ($\phi_{d-p}<\phi_1$) it means that no changes are needed. And if the strains in the drawn - part significantly exceed the limit strains ($\phi_{d-p} \geq phi_1$) it is necessary to change forming conditions (e.g. improve lubrication) or choose the sheet with higher formability or introduce changes in design (e.g. increase fillet radius).

3.5 Determination of FLC

Theoretically [87,88] or empirically, FLCs are usually tested using a set of experiments. Strains are introduced to metal samples of various shapes in experiments to simulate varying strain conditions. A hemispherical punch is typically used to stretch the samples before a crack occurs. Each and every sample is covered with a grid pattern just before the forming process, often a circular grid printed on the sheet metal by the electro-chemical grid marking method. Circles change to ellipses as a result of plastic deformation. Computation of major and minor strains for various strain states permit the development of forming limit diagram as a line at which cracking begins. Strain values are measured using the diameter of the circle before deformation (d0), as well as the main d1 and minor d2 axes of the ellipse in the region of localised necking or fracturing (see Figure 3.2).

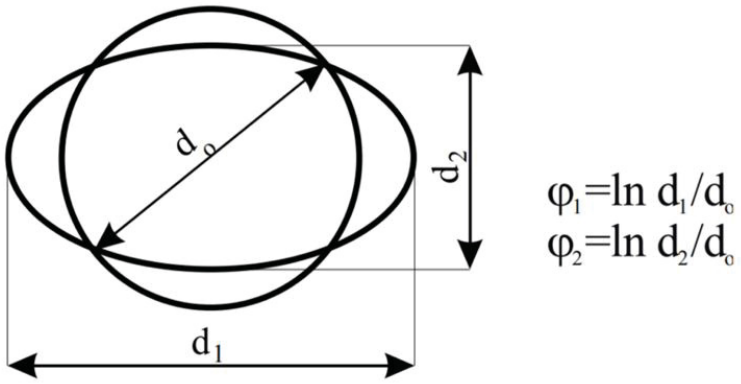

Figure 3.2: Scheme of measuring deformation

3.6 Forming Limit Stress-based Diagram (FLSD)

The Forming Limit Diagram (FLD) method is a practical approach in the forming processes for the analysis of the formability of sheet metals that is proven to be true only in cases of proportional loading, in which the ratio between the principal stresses are kept constant throughout the whole forming process. The manufacturing

of complex work pieces in an industrial application is usually done in terms of multi-step processes, in which the effect of the non-proportional strain history on the Forming Limit Diagram can be troublesome [89]. Hence, the FLD cannot be used under such circumstances for the prediction of formability in SMF. Moreover, the fact that Forming Limit Diagram is only applicable to linear strain ratios has been shown by a few authors that have used the Forming Limit Stress Diagram approach [90-92].

The information acquired from total deformation paths for the crack initiating area was used by ARRIEUX [93] to present the method of determining the FLSD. This was done by using Nakajima FLD tests. Stress-based FLD for forming limit investigation of both proportional and non-proportional loading was utilized by STOUGHTON [94]. By utilizing numerical results of forming tests in the FEM, the forming limit stresses can be obtained. While reaching the FLD-failure criterion, the numerically computed stresses can be assessed in regular increases in the necking area. In order to determine the FLSD, UTHAISANGSUK et al. [95] used finite element simulation of Nakajima tests. The evaluation of the maximum stresses of these elements is done when the strains from the crack-critical elements in the simulation reach the forming limit curve (FLD criterion). In the study of forming limit diagram and forming limit stress diagram of aluminium alloy 1060 under linear and non-linear strain paths studied by FANG et al. [96], the effects of the material's yield criteria on the forming limit stress diagram are analysed by comparing Hill's 48, Hill's 79 and Hosford non-quadratic criteria.

The resulting stress-based curves appears to be affected in a small extent by changes to strain path when strain-based forming limit curves are changed into stress-based forming limit curves [94]. Therefore, one could map the corresponding strain path dependant FLC points to stress-based FLC. This characteristic allows forming limit stress diagrams to be an appealing substitute to forming limit diagrams for necking instability prediction under arbitrary loading.

Transformation between stress and strain states

The transformation between the stress and strain states are carried out with the use of the formula of Stoughton. Here, the thickness stress (σ_1) of the sheet metal is omitted by assuming a plane stress condition. The ratio σ between minor true stresses σ_2 and major true stresses σ_1 is expressed as:

$$\sigma = \sigma_2/\sigma_1 \tag{3.1}$$

According to plastic theory, effective stress (σ) is a function of material parameters and stress tensor components. In this case effective stress can be written as:

$$\sigma \equiv \sigma(\sigma_2, \sigma_1) \tag{3.2}$$

The above relation can be expressed as:

$$\sigma \equiv \sigma_1 \phi(\alpha) \tag{3.3}$$

Where ϕ (α) is a function of material parameters.

Accordingly, the ratio (ρ) between the minor true strain increment ($d_{\epsilon 2}$) and major true strain increment ($d_{\epsilon 1}$) can be written as:

$$\rho = d_{\epsilon 2}/d_{\epsilon 1} \tag{3.4}$$

The effective strain can be expressed as the time integral of the increment of effective strain. It is written as:

$$\overline{\epsilon} = \int d\overline{\epsilon} = \int \lambda(\rho) d\epsilon_1 \tag{3.5}$$

Where $\lambda(\rho)$ is a function of material parameters.

The relation between effective strain and effective stress can be written as shown below:

$$\overline{\sigma} = \overline{\sigma\epsilon} \tag{3.6}$$

Therefore,

$$\alpha = \alpha(\rho) \tag{3.7}$$

Using the above relations, the strain states can be transformed into stress states. When there is an initial strain state due to pre-strain and a final strain state due to second stage, then principal stresses at the end of second stage can be written as:

$$\sigma_1 = \frac{\overline{\sigma}[\overline{\epsilon}(\epsilon_{1i}, \epsilon_{2,i}) + \overline{\epsilon}(\epsilon_{1f} - \epsilon_{1i}, \epsilon_{2f} - \epsilon_{2i})]}{\Phi[\alpha(\epsilon_{2f} - \epsilon_{2i})/(\epsilon_{1f} - \epsilon_{1i})]} \tag{3.8}$$

$$\sigma_2 = \alpha \frac{(\epsilon_{2f} - \epsilon_{2i})}{(\epsilon_{1f} - \epsilon_{1i})} \tag{3.9}$$

Using the above stated relations, each point in the strain based FLC can be mapped out into stress based FLC.

3.7 Initiation of Necking in SMF

Choosing an acceptable criterion is the most challenging part of defining the experimental forming limit strains at necking. Previous studies have described a variety of methods for determining the initiation of necking, which can be separated into three categories:

- Position-dependent methods
- Time-dependent methods
- Time-position-dependent methods

3.7.1 Position-dependent methods

In Nakajima and Marciniak experiments, the standard ISO 12004-2: 2008 offers a position-dependent approach for estimating the forming limit strains. The strain variations in the specimen prior to the occurrence of a crack are used to determine this criterion. The DIC method can be used to obtain position values and strains (ϵ_1, ϵ_2) for each section point on the specimen's surface [97]. See figure 3.3

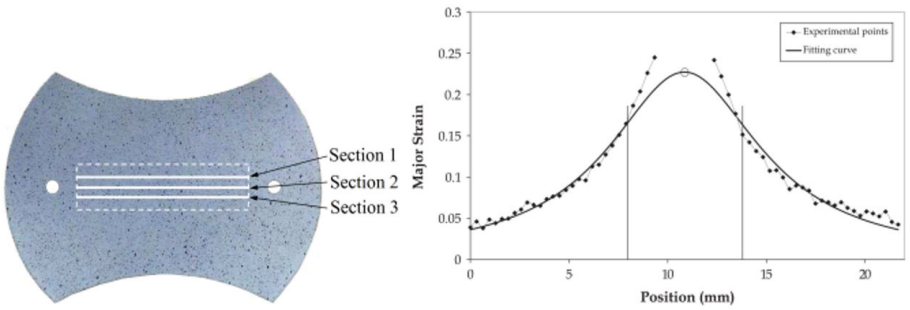

(a) Cross sections (b) Major strain distribution along section

Figure 3.3: ISO 12004-2 standard method [32]

3.7.2 Time-dependent methods

A study of strain rate in the field of necking and eventual cracking is used in the time-dependent evaluation process [98]. Throughout all the stages involved in the SMF processes, the strain rate values are determined. The strain rate increases in the necking zone when necking begins, then decreases beyond the necking zone. Figure 3.4 depicts how strain rates progress within and beyond the necking area. Figure 3.5 shows a detailed study of the rate of change of strain rate. At the start of the procedure, a linear characteristic rate of change of strain rate is shown, and then it increases. The rate of change of strain rate is used to determine a linear regression coefficient. The linear regression coefficient increases as the homogeneous plastic deformation continues, reaching a maximal value at the beginning of necking. The rate of change of strain rate drops dramatically after necking, while the linear regression coefficient rises. The initiation of necking is shown by the highest value of the linear regression coefficient curve, and the corresponding major and minor strain values reflect the FLCN data point.

3.7.3 Time-Position-dependent method

The time-position-based method, also known as the flat-valley method [99], is a hybrid method that is time and position dependent. In the traditional Nakajima test, Figure 3.6 depicts the longitudinal displacement of the exterior surface of the specimen along a segment perpendicular to the failure zone at various times prior to fracture. As an example, the plane-strain stress is used. The outside surface of the sheet metal deforms earlier in the SMF process because of the curvature induced by the punch. Later, this curve flattens in a specific area, forming a necking valley

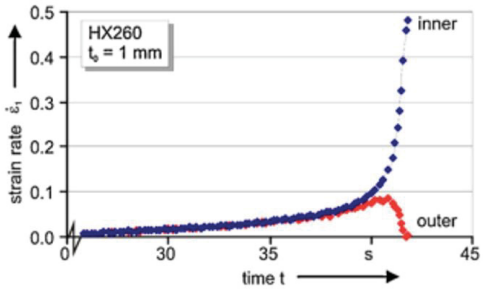

Figure 3.4: Strain rate progress inside and outside the necking region [33]

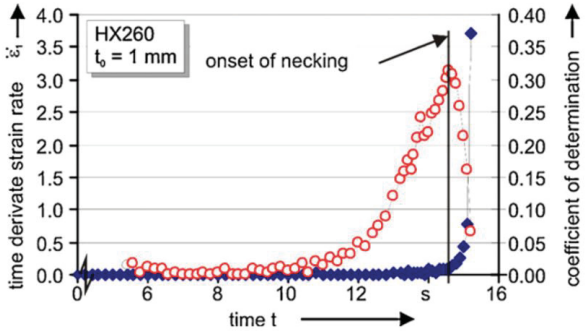

Figure 3.5: Realizing the Onset of necking using Time dependant method [33]

(stage 222) that gradually deepens before the sheet metal fractures. The profiles are roughly smooth at the start of necking, and the sheet is unable to deform with the curvature exerted by the punch, indicating the onset of plastic instability.

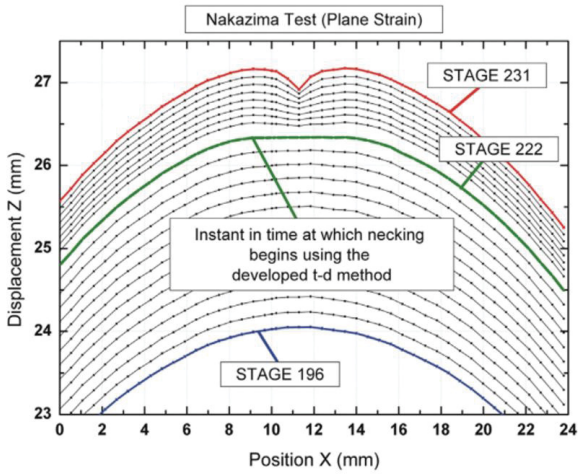

Figure 3.6: Time dependant method - position based [34]

3.8 Generalized Forming Limit Concept (GFLC)

The feasible prediction of localized necking or unacceptable wrinkling is one of the major goals of SMF simulations. The analysis of Forming Limit Curves is the most commonly used failure criteria (FLCs). In post-processing, the computed true strains 1 and 2 are compared to theoretically or empirically obtained FLCs. The international standard ISO 12004-2 [18] specifies two distinct experimental procedures for determining FLCs: the Nakajima test [21] and the Marciniak [21]. The failed specimens are examined using the so-called cross section method, which is also the standard assessment approach, to determine local instabilities. Because the forming limit strains are reassessed, this approach is reliable but not always correct. Furthermore, it is sometimes unsuitable when there are several necking zones. Recent advancement in photogrammetric technology has made it feasible to record the whole experiment and directly pinpoint the beginning of necking. Thus the previously discussed time dependent method is used.

Conventional FLCs are only relevant to forming processes with virtually linear and uninterrupted strain pathways. Many forming procedures with variable loading directions, such as two-step forming operations, are unlikely to provide these proportional loading circumstances. As a result, a number of writers have proposed increased stress-based criteria. Because the computed forming limits are highly dependent on the applied stress-strain relationship, these stress-based analysis techniques have a decreased robustness. A phenomenological strain-based method was proposed by Ofenheimer et al. [15], Volk et al. [19], and others. The basic concept is to use metamodeling to parameterize bi-linear strain increases. The evaluation approach is extremely resilient and straightforward to apply in commercial software applications with reasonable experimental effort. However, the method is restricted to two-step forming processes. For arbitrary deformation histories, Volk et al. [19] developed the so-called generalized forming limit concept (GFLC). Using FLC predictions made using the analysis if bi-linear experiments GFLC concept can be generalized for the arbitrary deformation histories.

The principal ideas and applied theories in GFLC have been discussed in details in the following subsections.

3.8.1 FLD for Bi-Linear deformation history

Thinning rate is an appropriate physical metric for detecting localized necking [19]. High thinning rates will result from the concentration of residual plastic deformation in tiny shear zones, whereas outside the shear bands thinning rates will remain constant. This impact is used in the method to detect the beginning of instability [21]. The initial stage of deformation is steady and almost homogenous. During instable deformation and before fracture development, localized necking occurs. Using the least squares approach, two linear trendlines are fitted to the stable and instable regions. The starting instability is defined as the point where these two straight lines cross. This time-dependent evaluation approach may also be used to determine the remaining forming limits in two-step forming processes.

3.8.2 Parameterization

The presence of two linear strain increments at deformation states will allow each forming limit strains to be parameteried as a function of strain path length and strain ratio. As reference data, the FLC of a linear strain path is used. The unique strain route length $l_{FLC}(\beta)$ intersects with the common FLC at each strain ratio $\beta = (\epsilon_2/\epsilon_1)$ of the starting instability. Each strain path length ratio β_{pre} and β_{pos} of the first and second forming operations, respectively ($\lambda = 1/l_{FLC}$), is computed continuously for a corresponding strain ratio ßpre and ßpost. The so-called total strain route length can be viewed as a measure of depleted formability in this context. Following this, the metamodel for the total strain path length ratio can be formulated as follow:

$$\lambda = f(l_{pre}, \beta_{pre}, l_{pos}, \beta_{pos}) = \lambda_{pre} + \lambda_{pos} = \frac{l_{pre}(\beta_{pre})}{l_{FLC}(\beta_{pre})} + \frac{l_{pos}(\beta_{pos})}{l_{FLC}(\beta_{pos})} \tag{3.10}$$

3.8.3 Metamodeling

A metamodel, sometimes known as a surrogate model, is a model of another model, and metamodeling is considered to be the process of creating such model. Thus, metamodeling is the study, building, and development of the models, rules, constraints, frames, and theories that are relevant and beneficial for modeling a certain class of issues [54].

Using the presented parametrization in the previous section it is possible to create a procedure based on metamodeling to evaluate bilinear deformation history. This metamodeling procedure, based on isoparametric approximation, utilizes the transformation of 4 node Lagrange elements of FEM.

3.8.4 Principle of equivalent preforming

With respect to improving the forecast quality for sheet metal forming simulations, the reliable application of FLC to non-linear deformation histories is of considerable importance. The provided metamodeling using experimental data may directly forecast the available formability on bi-linear deformation histories. For a given post-strain, the corresponding pre-strain in that direction may also be computed. It should be clear from this that the points that contain the same pre-strain values have the same residual formability in the given post-forming direction. According to principle of equivalent preforming, all these points portray the same remaining formability.

According to the theory, one can say that there is only one specific point exists with linear strain path that is when ($\beta_{pre} = \beta_{post}$) [32]. Furthermore, it also states that the points which underwent equivalent pre-forming have significantly varying amount of effective plastic strain. One can transform a bi-linear deformation history into linear strain path by applying this theory and this methodology can be repeated for any number of bi-linear deformation histories. Using this theory and the discussed GFLC concept for bi-linear deformation history, one can extend the concept to analyze the remaining formability for arbitrary number of non-linear deformation histories with unlimited linear strain increments.

One can divide the multi non-linear deformation history into various segments of deformation histories that are bi-linear. Furthermore, these formulated bilinear deformation histories can be further reduced to its corresponding linear strain paths. Using this method of iteration, it is possible to simplify multi non-linear deformation history to a bi-linear deformation history. Finally, the metamodel of bi-linear deformation histories may be used to forecast the remaining formability of the final post-forming. This concept can further be used to evaluate formability for deformation histories that multi step and with changing number of forming direction.

3.9 Yield Criterion

A yield criterion is a theory that defines the elasticity limit of a material and the beginning of plastic deformation under all feasible stress combination. This defined elastic limit is an important factor that plays a major role in SMF processes as plastic zone is the mostly required for SMF. Depending on the material continuum it is possible to categorize the yield criterion into two:

- Isotropic yield criterion
- Anisotropic yield criterion

The production stage of SMF involves multi directional rolling operations. Homogeneous means that the material has the same, or very similar, mechanical properties in all directions with respect to the rolling direction (longitudinal, transverse, and diagonal), i.e. yield stresses and R-values. As isotropic yield criterion considers material to be completely homogeneous, SMF requires anisotropic yield criterion. Hill48 and Barlat yld200 are two anisotropic yield criterion that can be applied in SMF processes. In this thesis Barlat yld2000 is used for the FE-simulations provided by RISE. Barlat yld2000 material model was specifically chosen as the CR4 material that is being studied can be considered as anisotropic.

3.9.1 Barlat yld2000

Barlat et al. initially described the yield criterion Barlat yld2000, as a plane-stress yield function that is non-quadratic specifically for anisotropic material. Due to the limitation in the initially developed Barlat89 and Barlat yld96, the currently used Barlat yld 2000 is developed. Barlat89 follows isotropic material properties and this material model can only be used for Lagrangian shell elements. The Barlat Yld96 function does not cause any problems when implementing plane stress in FE code and produces decent simulation results. However, because of the relative convexity of the Yld96 function, numerical issues may be a concern in the 3D situation (Barlat et al., 2003). Another disadvantage is the difficulty in estimating strain rates for FEM simulations analytically. The Barlat 2000 have eight material parameters. These material parameters are calibrated to uniaxial tests in rolling direction, transverse direction and diagonal direction, and a balanced bi-axial test.

3.10 Failure models

A simplified failure model can be represented according the equation given below [72].

$$D \int_0^{\epsilon_f} f(\sigma, \epsilon, \dot{\epsilon}, T, ...) d\bar{\epsilon}^p \leq 1 \tag{3.11}$$

where,
ϵ_f - Plastic strain at fracture
$d\bar{\epsilon}^p$ - Plastic strain increment
f - Scaling function
σ - Stress state
ϵ - Strain state
$\dot{\epsilon}$ - Strain rate
T - Temperature
D - Damage indicator

3.10.1 Generalised Incremental Stress-State damage Model (GISSMO)

Daimler[8] and DYNAmore jointly created this numerical failure model called Generalised Incremental Stress-State damage Model (GISSMO). The model utilizes incremental damage accumulation in order to predict ductile failure.

GISSMO failure model is based on two conceptualization.

1. **Damage** - Damage in SM usually refers to the physical processes of void nucleation, development, and coalescence that starts following the beginning of necking at high stresses. The damage evolution in GISSMO starts when the plastic limit is exceeded. Therefore it can be understood that damage is referred differently in GISSMO.

2. **Regularisation** - In terms of GISSMO, regularization entails prescribing a material parameter as a function of mesh size to increase the model's mesh independence. This is a really effective approach of dealing with the issue. The fundamental concept is to keep track of how much energy is wasted during fracture formation and propagation.

Chapter 4

Method

4.1 Introduction

Initially this chapter focuses on the general methodology used to carryout this Masters thesis. Secondly, the methodology used to create GFLC in metamodeling is discussed in detail. Finally, methods involved in FE-simulations are clearly laid out.

4.2 Design Research Methodology (DRM)

This is a research-oriented thesis which is based on reviews of existing literatures, designing, and formulating various models. Therefore, one can conclude that this thesis is based on design research. The most commonly used methodology or framework for carrying out design research is called Design Research Methodology (DRM) by authors Blessings and Chakrabarti [5] and this methodology will be employed in this thesis. DRM technique can help if used flexibly, as the authors indicate, to make design analysis more efficient and successful. There are 4 stages involved in DR-methodology. The figure 4.1 shows the framework of Design Research Methodology.

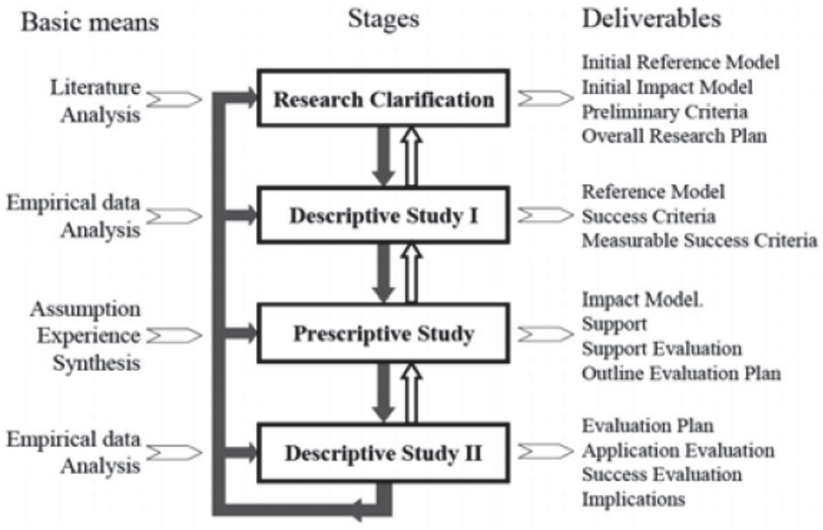

Figure 4.1: Design Research Methodology [6]

4.2.1 Research Clarification

Most of the design research project begins with the Research Clarification(RC), which attempts to identify and refine a research issue that is academically viable. To do so, you'll need to have a sense of the present state of knowledge in your chosen field. According to Blessing et al., RC is the primary stage which helps to create a stable plat form of understanding throughout the project and help making clarifications at later phases of the project too.

There are six steps involved in successfully utilizing RC.

- Step 1 - Identifying the broad range of subjects that are of interest for the project. Here one would formulate the problem along with intended research goals.
- Step 2 - Increasing knowledge regarding existing in research for the project and formulationg potential research gaps if present.
- Step 3 - At this step suitable research question are formulated.
- Step 4 - There are seven different types of research in DRM. One of such choice is chosen. For this thesis research type two is selected and can be seen in figure 4.2
- Step 5 - At this step, the project scope is defined.
- Step 6 - At this final stage of RC the research plan is formulated.

Research Clarification	Descriptive Study I	Prescriptive Study	Descriptive Study II
1. Review-based →	Comprehensive		
2. Review-based →	Comprehensive →	Initial	
3. Review-based →	Review-based →	Comprehensive →	Initial
4. Review-based →	Review-based →	Review-based → Initial/ Comprehensive	Comprehensive
5. Review-based →	Comprehensive →	Comprehensive →	Initial
6. Review-based →	Review-based →	Comprehensive →	Comprehensive
7. Review-based →	Comprehensive →	Comprehensive →	Comprehensive

Figure 4.2: Research types in DRM [6]

While carrying out this thesis under the stage of RC, above described 6 steps were utilized and integrated. As a result of these 6 steps, background, aim and objectives and research questions were formulated.

4.2.2 Descriptive Study I (DSI)

The researcher has a defined aim and focus in the Descriptive Study I (DSI), and the goal is to create a thorough enough description of the existing situation to decide which elements should be addressed to enhance task clarity.

There are 5 steps involved in formulating DSI.

- Step 1 - At this step literature review is carried out. Here, one should assess the current degree of knowledge in the subject under study and where extra or new information is required to provide an appropriate response to the major questions stated in the RC stage.
- Step 2 - At this step various interested areas are identified and defined while the research question are refined.
- Step 3 - Planning and listening the details of the suitable activities and experiments for the project.
- Step 4 - This step is where the empirical study takes place, where the obtained data are analysed.
- Step 5 - The main goal of this step is obtaining the findings and conclusions from various research and putting them together to form a comprehensive knowledge of the DSI.

4.2.3 Prescriptive Study

In this stage based on the understanding and finding from the previous DSI stage, suitable support is developed. This is 3rd stage in DRM is the final stage in this research thesis. The primary objectives are achieved in this stage for this report.

4.3 Literature review

The review of literature is an important part of academic study. Knowledge progress must, at its core, be based on previous effort. We need to know where the knowledge frontier is in order to drive it forward. We may gain a better understanding of the breadth and depth of the current body of work by reading relevant literature and identifying gaps to investigate. We can test a certain hypothesis and/or generate new ideas by summarizing, evaluating, and synthesizing a collection of relevant material. We may also use a criterion to assess the validity and quality of previous work, revealing flaws, inconsistencies, and contradictions. Literature reviews, like scientific investigations, should be legitimate, dependable, and reproducible.

In this report a systematic literature review is conducted. Typically there are 8 steps involved in conducting a systematic literature review. These steps are explained below.

- Formulation of research question - A suitable research question must be formulated stating the need for a literature review.

- Development of research protocol - A detailed plan of how the study will be conducted should be prepared.
- Identifying literature - Conducting a search for suitable literature supporting or related to the area under study.
- Selection of studies based on the protocol - Different choice of studies must be chosen to produce a comparative study.
- Appraising the selected studies.
- Extracting information from the literature.
- Analysing the extracted information.
- Interpreting the results - Finally the compiled literature review is written.

4.4 Metamodeling of GFLC

GFLC concept is used to predict remaining formability for multi-linear deformation histories and is mainly applied for two-step SMF processes. The principle idea behind this concept is formulated from the work of Volk et al [12] and is presented in Chapter 3. Here in this section detailed description of the employed methodlogy is stated.

One can divide the multi non-linear deformation history into various segments of deformation histories that are bi-linear. Furthermore, these formulated bi-linear deformation histories can be further reduced to its corresponding linear strain paths. Using this method of iteration, it is possible to simplify multi non-linear deformation history to a bi-linear deformation history.

4.4.1 Step involved in prediction of formability for bi-linear deformation history

There are three main steps to follow in order to predict the remaining formability for bi-linear deformation history.

1. **Step 1 - FLD for Bilinear deformation histories.** In this step three set of data points are obtained.

   FLC - linear FLC data of the material is used.

   Pre-strain - Four specimens from the same material are pre-strained up to 8-10% towards shear, tension, plane strain, and biaxial directions there by creating 4 set of data points for 4 pre-strained specimens.

   Post-strain paths - Each of the above four pre-strained specimens are cut to obtain Nakajima specimens for post-straining using Nakajima testing machine. These cut specimens are then post-strained and its corresponding post-strain paths are obtained.

Note - These data are usually obtained from experimentation, but in this project these values are obtained from FE-simulation using the models provided by RISE. This is further explained in the next section.

2. **Step 2 - Parmeterization of the obtained values.** In this step initial calculations are made. Using the theory and mathematical formulations mentioned in section 3.8.2. The following parameters are initially computed and used in the further in the procedure.

   (a) Pre-strain ratio

   (b) Pre-strain path length ratio

   (c) Post-strain ratio

   (d) Post-strain path length ratio

   These parameters are obtained using the obtained data points in the previous step.

3. **Step 3 - Metamodeling** This step is used to evaluate bi-linear deformation histories in this thesis. This step follows in an order as stated below.

   (a) **The transformation of 4 node Lagrange element** - This strategy is initially applied to formulate a diagram with 4 experimental or in this case simulated nodes and added 6 extra nodes based on the traditional FLC. This can be seen in results chapter.

   (b) **Isoparametric approximation** Using the above formulated diagram further calculations are carried out. The interested preforming condition is used to compute variables in the shape functions. Later post-strain path length ratio for in interested pre-strain condition is formulated using this theory of isoparametric approximation and the calculated shape function for any suitable post strain ratio.

   (c) **Error correction** The calculated post-strain path length ratio for any post-strain ratio needs correction as the the information total strain path should be 1 for a pure linear strain path' is not used. Therefore $\Delta\lambda$ is introduced which is obtained from the following formula.

$$\Delta\lambda = 1 - (\lambda_{pre}(\beta_{pre}) + \lambda_{cal}(\beta_{pre})) \tag{4.1}$$

   Furthermore, $\Delta\lambda$ is added to the calculated post strain path length ratio for the chosen post strain ratio to obtain the final Post strain path length ratio value.

4.5 FE - Simulation

Various simulations have been carried out in LS-DYNA using the models (simulation model and material model) provided by RISE. There are 4 different testing procedure which are simulated.

- Tensile test
- Plane strain test
- Shear test
- Nakajima test

Each of these test procedure was simulated and a model was created and provided by RISE. Furthermore, material model for each test is also provided for specimens of 3 different cross sections (50mm, 100mm and 200mm) by RISE.

The steps involved in utilizing those models in obtaining the corresponding results are shown below.

1. Initially Provided models for the test procedures were analysed by opening them in *LS-PrePost*.
2. Then, *INCLUDE keyword file is analysed to check if the corresponding components of the tests have been included.
3. Following, the KEYWORD file is then opened in LS-RUN and simulation is carried out.
4. Initially each test is carried out without including failure models (GISSMO)
5. Later GISSMO failure model is included in the *INCLUDE keyword file and each test were simulated again.

The results for these simulations are mentioned in appendix 1.

Above lists shows, the primarily utilized steps in performing simulations in this thesis. Few Steps described below shows how FE-Simulations are carried out to obtained data to predict the exhausted formability using GFLC concept.

Steps involved in obtaining data for GFLC concept

1. Twelve specimens were pre-strained and provided by RISE. These specimens were of 3 different cross-section and are pre-strained by either tensile, plane strain, shear or bi-axial test for upto 8-10%.
2. These pre-strained specimens are then included in the Nakajima test model in the *INCLUDE keyword file and simulated.
3. FLC for material is experimentally determined and provided by RISE.
4. Pre-strain values are obtained from RISE along with the pre-strained specimen.
5. Once the simulation is completed results are obtained.

Steps involved in obtaining the results from LS-DYNA are explained in the following steps

1. Once the simulation is complete the key word file is opened to analyse the model.
2. Other than the specimen, other parts of the simulations are hidden to visually see how the specimen has deformed.
3. Suitable parameters are chosen in the *Fringe Component* to obtain certain results.
4. Next, under the *History* option in LS-DYNA, an element is chosen in the middle of the specimen to extract relevent plots.
5. To obtain further set of results and graphs *XY Plot* option in LS-DYNA is used.

4.6 Validation

An interested prestraining condition is chosen and the parameters such as pre-strain ratio and pre-strain path length ratio are obtained Experimentally. Furthermore, this experimentally,pre-strained specimen is then post strained to obtain post-stain ratio and post strain path length ratio. Using the experimentally obtained pre-strain ratio and pre-strain path length ratio, post-strain path length ratio is predicted for the said post-strain ratio.

Chapter 5

Results and Analysis

This chapter presents the results obtained from literature review, FE-simulation and GFLC procedure.

5.1 Literature Review

This section will present the findings of the research question: *What are the testing procedures that can be used to generate non-linear strain paths and characterization of the material properties from those tests?*

Figure 5.1 and figure 5.2 below list the main findings related to the literature and test procedures.

Ref	Purpose	Methodology	Findings
Cruciform specimen in a conventional Nakajima test setup.			
18	Identifying nonlinear strain paths	Using Draw bead tools and cruciform specimen in standard Nakajima test	The simulation is almost near the experimental results. Formability predicted using General FLC.
26	Identifying nonlinear strain paths	Cruciform Specimen in standard Nakajima testing machine	The experimental results correspond with the predicted results.
Modifying Punch Geometry for a Nakajima test setup			
27	Identifying nonlinear strain paths in single step	Modelling different punch geometry and simulating the test procedure in LS-DYNA	The results of simulation correspond with the experimental results
28	Identifying nonlinear strain paths in single step	Modelling different punch geometry and simulating the test procedure in LS-DYNA	The results of simulation correspond with the experimental results
Two-step deep-drawing or Drawing reverse-drawing process			
29	Investigating necking behaviour using two-step deep drawing test	Two-step deep drawing method is used to identify nonlinear strain paths with the help of DIC	The experimental methods are validated using other method such as time dependant methods.
30	Analytical approach for forming limit calculations	Comparing the results of the proposed analytical approach with experimental results (results from drawing reverse-drawing process)	The results from analytical approach can be validated using the results from the experiment.

Figure 5.1: Finding 1 of 2

Ref	Purpose	Methodology	Findings
		Bulging with stepped dies	
43	Investigating nonlinear strain paths on the FLC	Using two step dome test to compare the results with the results of the analytical method	Both the results agreed.
59	Developing novel test setup with single step to realize nonlinear strain path	Bulging with stepped dies	Feasibility of the proposed novel test procedure is validated.
		In-plane biaxial test with a cruciform specimen	
17	Developing one-step procedure to control strain path changes in sheets, without unloading	In-plane biaxial test with independent actuators to control the displacement of the arms of the cruciform specimen	Predictive and experimental forming limits are severely influenced by pre-strains. Premature necking is seen when applying higher strain
65	Identifying Forming limit strains under the influence of nonlinear strain path	In-plane biaxial test with independent actuators to control the displacement of the arms of the cruciform specimen	Comparing the Forming limit under linear strain path with nonlinear strain paths.

Figure 5.2: Effective Plastic Strain

5.2 Finite Element Analysis [FEA]

This section includes results obtained from FE-Simulations carried out in LS-Dyna. Initially, The four specimens are pre-strained in tensile, shear, plane strain and biaxial directions and the corresponding results are shown. It is followed by the results obtained after post -straining the pre-strained specimen in different directions with the use of different specimen width and Nakajima test. The material parameters used for CR4 in the simulation are seen in table 5.1

Material Parameters CR4												
Material	ρ	E	v	σ_0	σ_{45}	σ_{90}	σ_{biax}	M	R_0	R_{45}	R_{90}	R_{biax}
CR4	7.8e-9	2.1e+5	0.3	156.6	160	156	187	4.5	1.805	1.336	1.876	0.982

Table 5.1: Material parameters of CR4

Following figure5.3 shows how the pre-strain specimen is cut in order to apply post-strain in Nakajima testing. Here simulating the first specimen of 200mm in nakajima testing will provide biaxial post straining. Similarly specimen of 100mm will provide plane-straining and specimen of 50mm will provide uniaxial post straining.

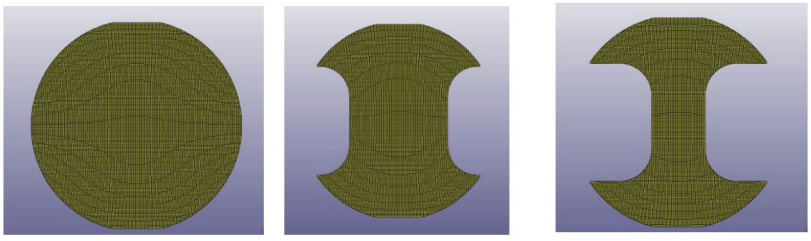

Figure 5.3: Specimen geometry 200mm, 100mm and 50mm

5.2.1 Forming Limit Curve

in order to verify Generalised Forming Limit Concept(GFLC), certain experimental values are necessary. FE-Simulation are carried out in order to acquire most of required data points. First, FLC for material, CR4 is obtained experimentally at RISE IVF, Olofström. This FLC curve is further used in metamodeling technique in GFLC. Figure 5.4 shows the obtained FLC.

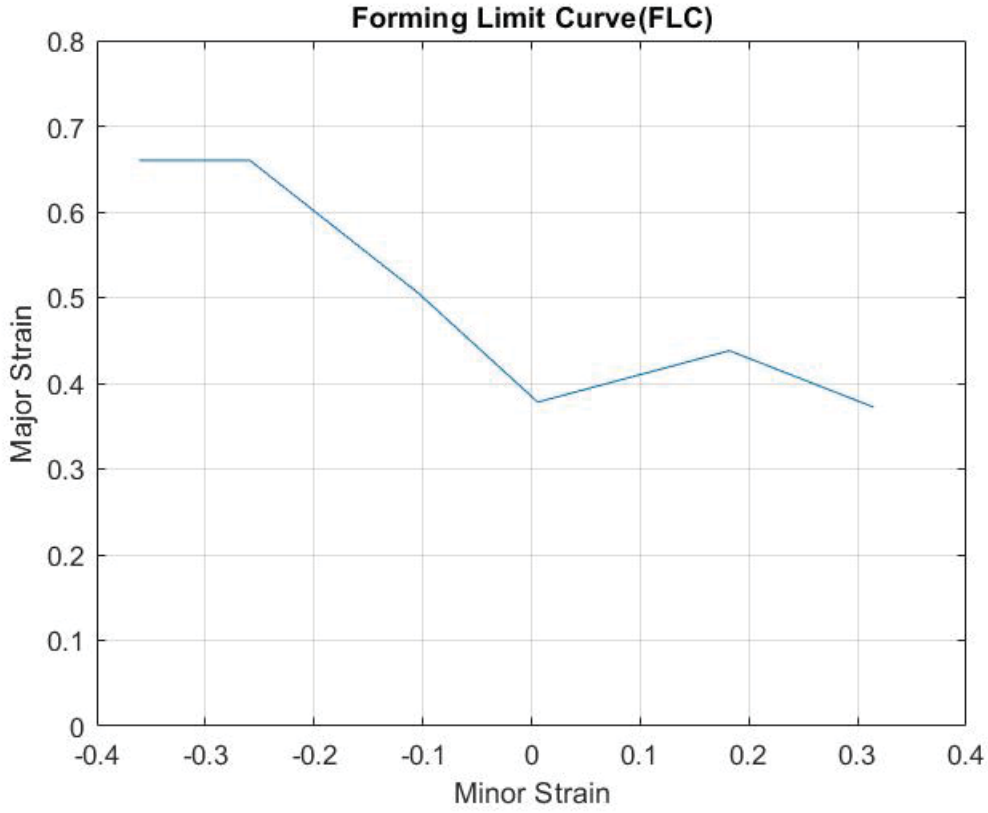

Figure 5.4: Experimentally obtained FLC for CR4 material.

5.2.2 Pre-straining of specimens

In order to predict formability using the concept of GFLC its required to have a minimum of four pre-strains. Therefore, the specimens are pre-strained upto 8-10% towards shear, tension, plane strain and bi-axial directions. See figure5.5

5.2.3 Post-Straining the pre-strained Specimen

The pre-strained specimens were cut to produce Nakajima test geometries of 50mm, 100mm and 200mm as shown in figure5.3. Post-straining the pre-strained specimen can be grouped in two 4 types as per their respective pre-straining directions.The groups are as follow:

1. Post-straining the pre-strained specimen in Tension direction.

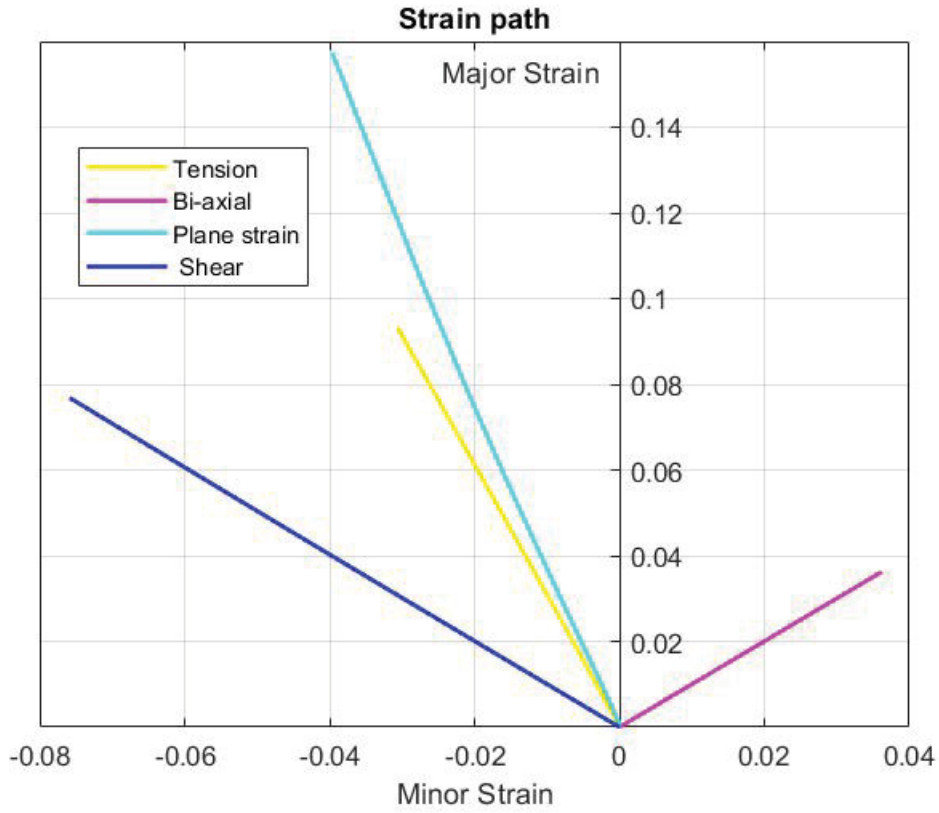

Figure 5.5: Four different Pre-straining in LS-Dyna

2. Post-straining the pre-strained specimen in Plane strain direction.
3. Post-straining the pre-strained specimen in Shear direction.
4. Post-straining the pre-strained specimen in Bi-axial direction

Initially, the pre-strained specimens 50mm, 100mm and 200mm in tension direction is used in the Nakajima testing to produce post straining in uni-axial, plane-strain and bi-axial directions respectively. Continuing the procedure for other three types of pre-strained specimens, post-strain paths or post FLC for each pre-strained specimen is formulated.

Post-straining the pre-strained specimen (Tension direction)

Once the FE-Simulation is completed, strain paths for each geometries were imported into MATLAB to produce the strain paths as shown in figure 5.6.

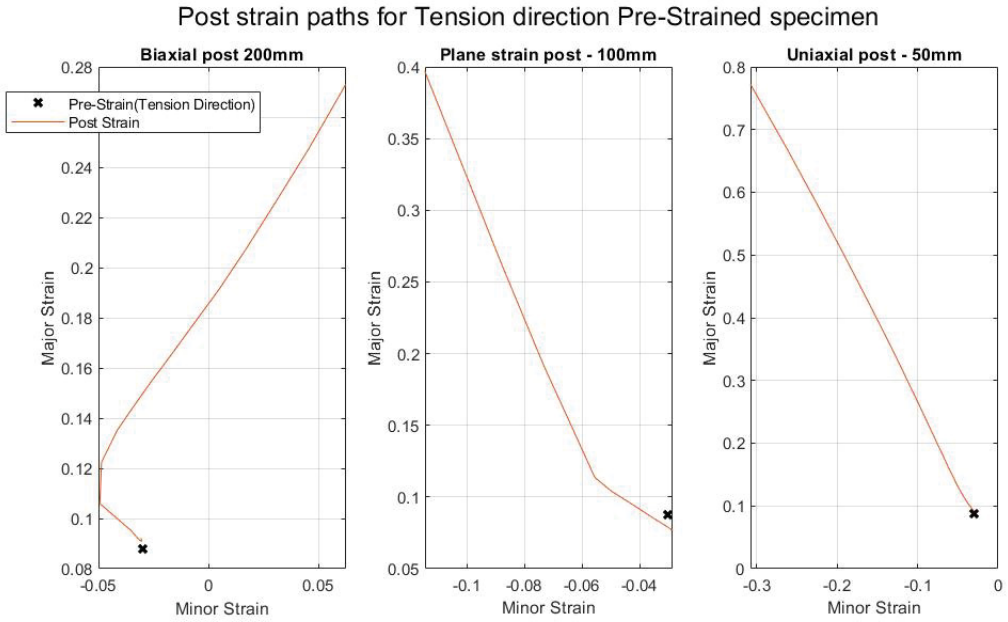

Figure 5.6: Three different post straining for Tensile pre-strained specimen

Using the above data points it is possible to obtain the post FLC for the pre-strained specimen in tensile direction. This will be referred to as 1st Post FLC for for further discussions. See figure 5.7.

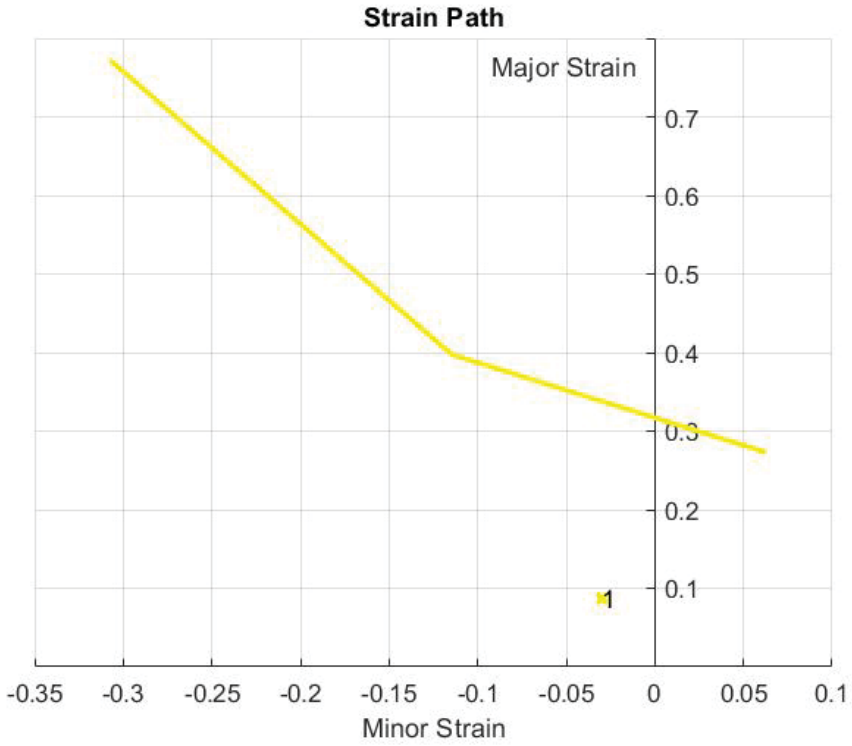

Figure 5.7: First post FLC

Post-straining the pre-strained specimen (Bi-axial direction)

Once the FE-Simulation is completed, strain paths for each geometries were imported into MATLAB to produce the strain paths as shown in figure 5.8.

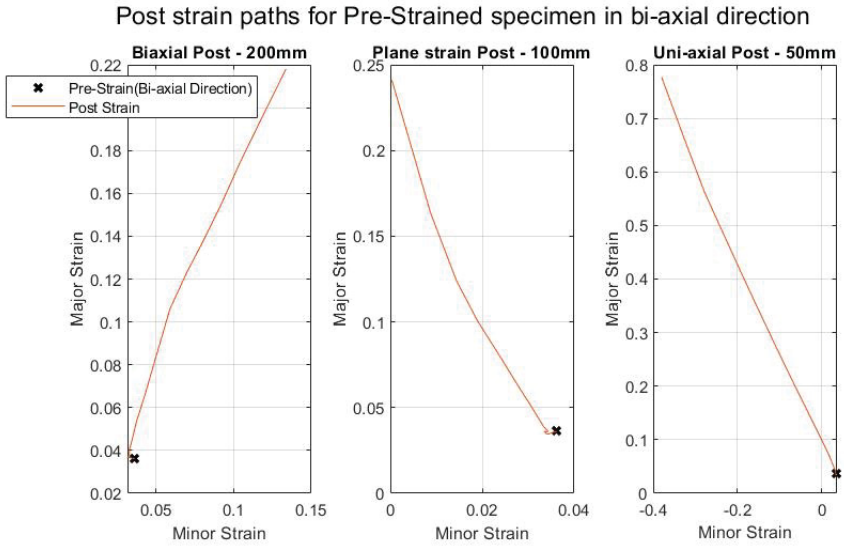

Figure 5.8: Three different post straining for Bi-axial pre-strained specimen

Using the above data points it is possible to obtain the post FLC for the pre-strained specimen in bi-axial direction. This will be referred to as 2nd Post FLC for for further discussions. See figure 5.9.

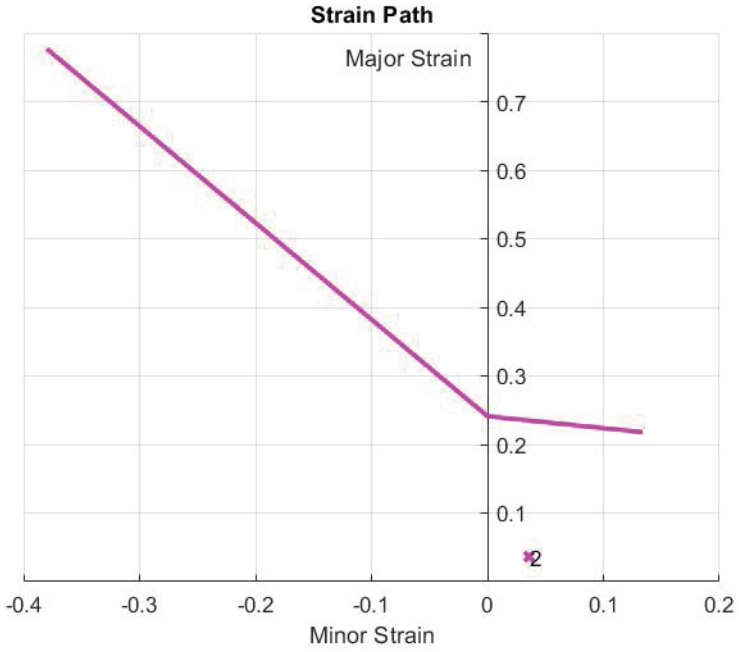

Figure 5.9: Second post FLC

Post-straining the pre-strained specimen (Plane-strain direction)

Once the FE-Simulation is completed, strain paths for each geometries were imported into MATLAB to produce the strain paths as shown in figure 5.10.

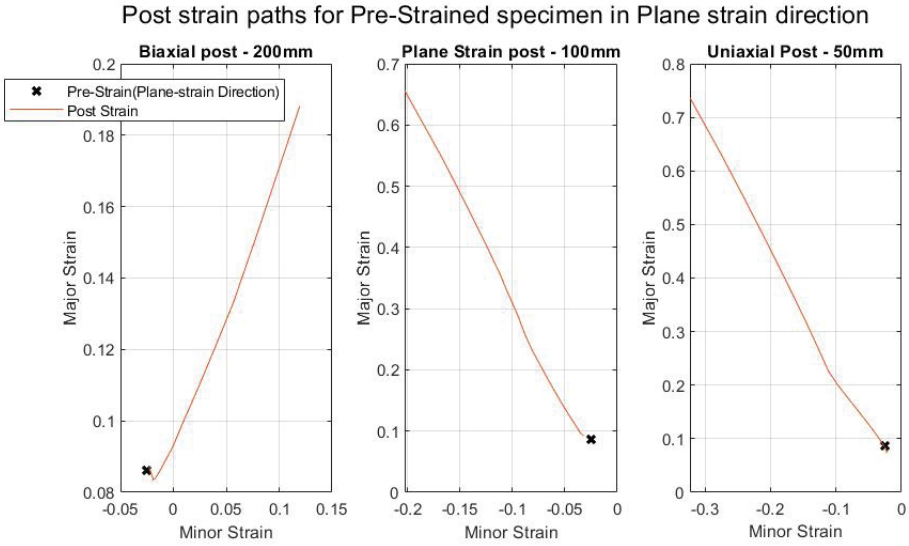

Figure 5.10: Three different post straining for Plane-strain direction pre-strained specimen

Using the above data points it is possible to obtain the post FLC for the pre-strained specimen in plane-strain direction. This will be referred to as 3rd Post FLC for for further discussions. See figure 5.11.

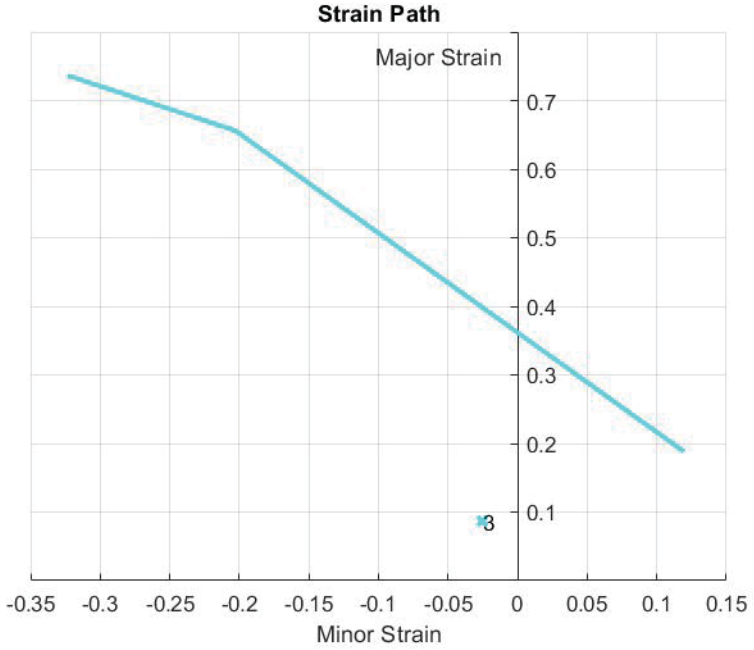

Figure 5.11: Third post FLC

Post-straining the pre-strained specimen (Shear direction)

Once the FE-Simulation is completed, strain paths for each geometries were imported into MATLAB to produce the strain paths as shown in figure 5.12.

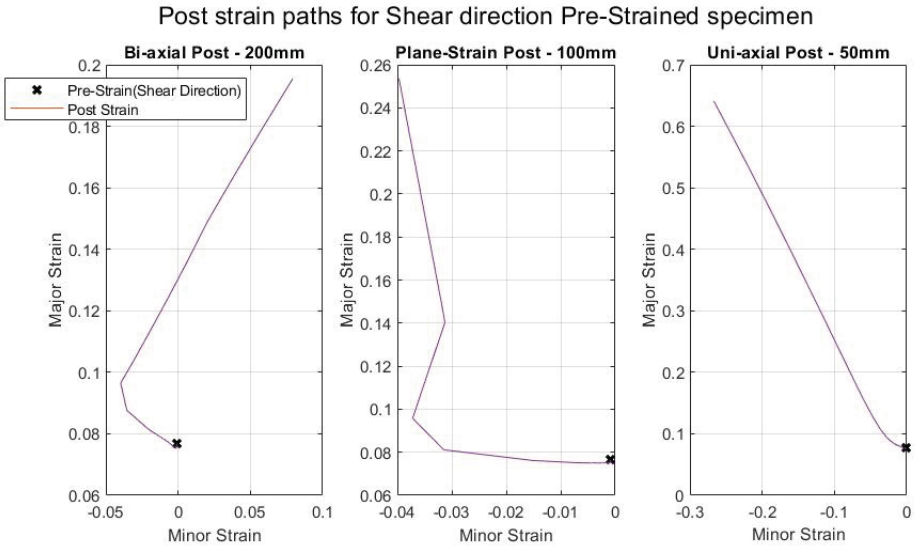

Figure 5.12: Three different post straining for Shear pre-strained specimen

Using the above data points it is possible to obtain the post FLC for the pre-strained specimen in shear direction. This will be referred to as 4th Post FLC for for further discussions. See figure 5.13.

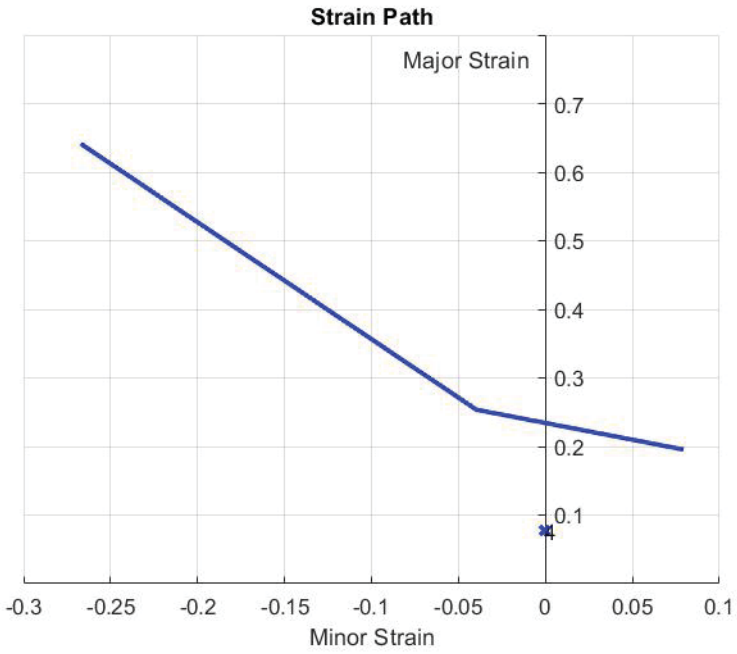

Figure 5.13: Fourth post FLC

5.3 Prediction of Formability using GFLC

5.3.1 Forming Limit Diagrams (FLD)

Initially, Forming Limit Diagrams for tbe material CR4 is compiled and is shown in figure 5.14. Using the forming limit diagrams, it is possible to parameterize it and obtain certain parameters.

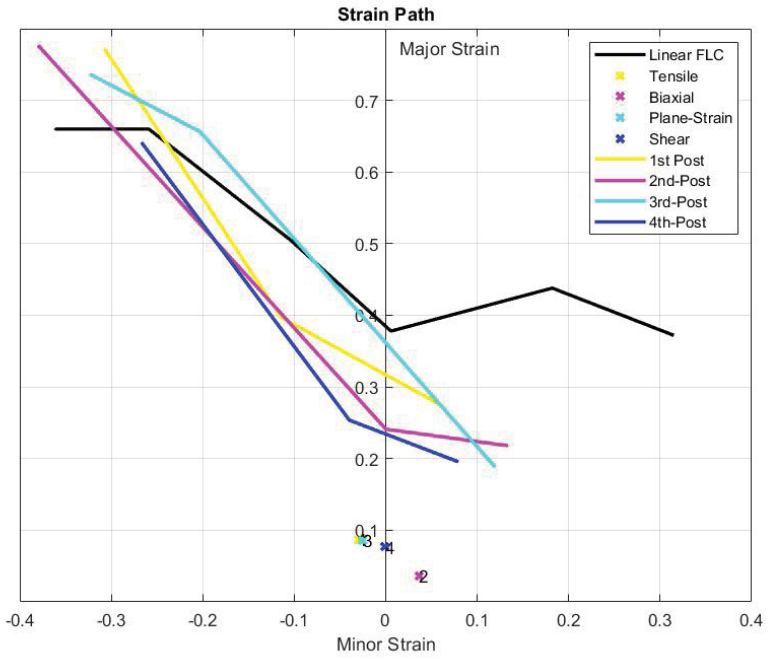

Figure 5.14: Forming limit diagrams for CR4 material

5.3.2 Parameterization

Following parameterization, pre-strain ratio and pre-strain path ratio are calculated for the 4 different pre-straining. Tensile pre-strain is referred to as a the first node, bi-axial pre-strain as the 2nd node, plane strain pre-strain as the 3rd node and finally, shear pre-strain is considered as the 4th node. Please refer to table 5.2 for the calculated pre-strain and pre-strain path values for the four nodes.

Nodes	Pre-strain Ratio(β_{pre})	Pre-Strain path length ratio(λ_{pre})
1	-0.3425	0.1438
2	0.9989	0.1051
3	-0.2942	0.1516
4	-0.0119	0.1967

Table 5.2: Parameterised Value

5.3.3 Metamodeling

This section contains all the results from metamodeling procedure. In order to predict formability, parameters such as pre-strain ratio, pre-strain path length ratio and post strain ratio of the interested specimen are important and is very much needed. If one knows values of the parameters for the pre-forming conditions, one could approximate the remaining formability based on the expected post strain ratio. In this thesis two prestraining conditions are used to predict formability separately.

First, interested pre-strain ratio and pre-strain path length ratio are calculated using FE-simulation and is shown below.

Pre-Strain Ratio(β_{pre})	Pre-Strain Path ratio (λ_{pre})	Post-strain ratio (β_{pos})
0.9985	0.1857	0

Table 5.3: Interested parameters - FE-Simulation

Second, interested pre-strain ratio and pre-strain path length ratio are calculated using results obtained from experimentation and is shown below.

Pre-Strain Ratio(β_{pre})	Pre-Strain Path ratio (λ_{pre})	Post-strain ratio (β_{pos})
-0.7452	0.1512	-0.3401

Table 5.4: Interested parameters - Experimentation

These values such as β_{pre} and λ_{pre} are calculated using the data points obtained from FE-Simulation and experimentation.

For the first pre-forming condition, the specimen is pre-strained in bi-axial direction for upto 16%. See figure 5.15 which shows the pre-straining and corresponding post straining obtained from FE-simulation which will later be used to predict formability.

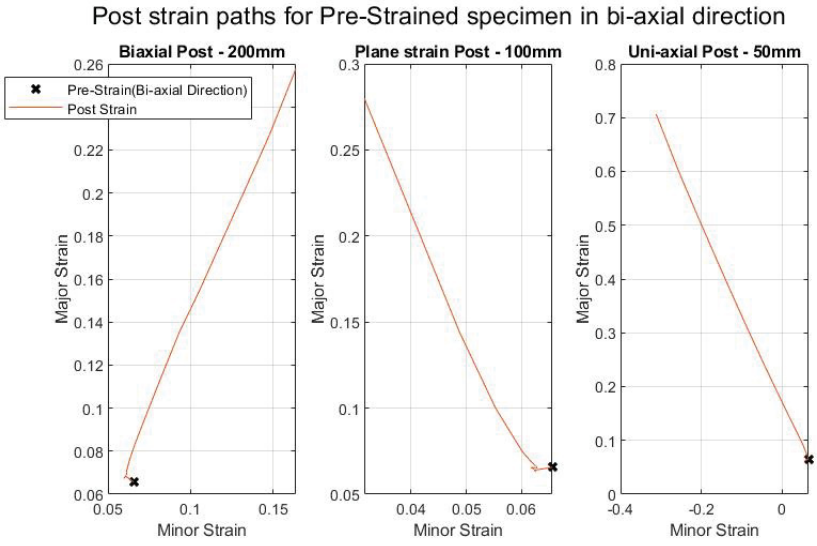

Figure 5.15: Pre-strain and post Straining

For the second pre-forming condition, the specimen is pre-strained in uni-axial direction. See figure 5.16 which shows the pre-straining and corresponding post straining obtained from experimentation which will later be used to predict formability.

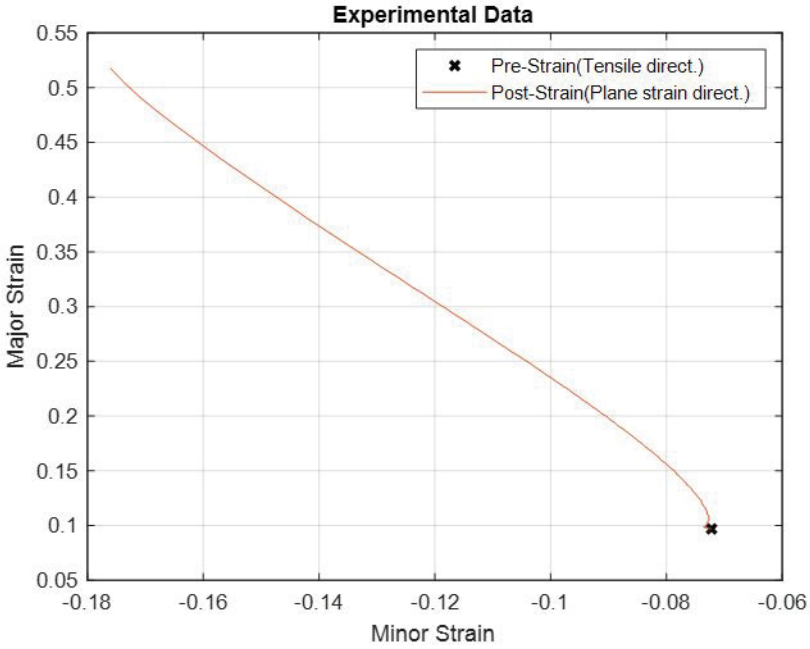

Figure 5.16: Pre-strain and post Straining - Experimental

Here it can be seen that there is only one post-strain data is presented due to the presence of time constraint.

Transformation of four node lagrange element

For first pre-straing condition (table 5.3), once parameterization is completed, strategy based isoparametric approximation by the use of the transformation of a four-node Lagrange element of FEM is applied. See figure 5.17.

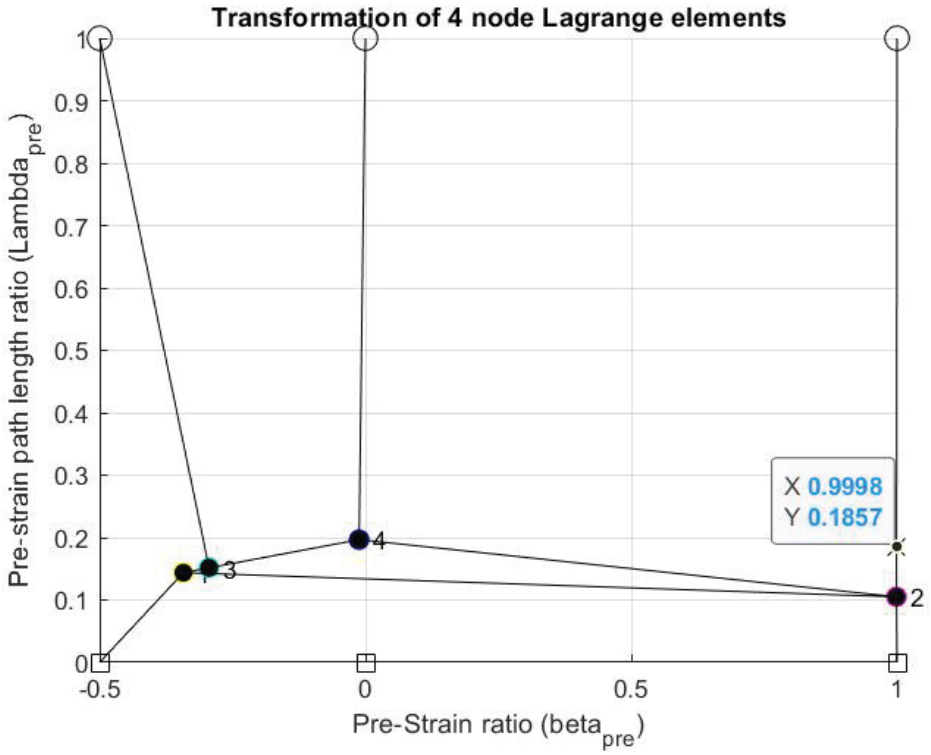

Figure 5.17: Transformation of four node Lagrange Elements

Next, using the theory of isoparametric approximation, post FLC for the interested pre-straining conditions stated in table 5.3can be computed. Figure 5.18 corresponds to the calculated post FLC which will be used to predict the exhausted formability after correction.

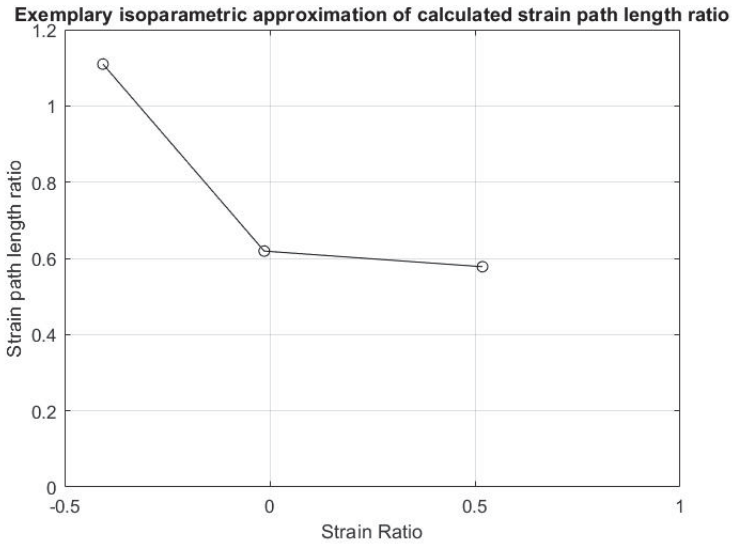

Figure 5.18: Isoparametric Approximation - strain ratio VS calculated strain path ratio

For second pre-straing condition (table 5.3), once parameterization is completed, strategy based isoparametric approximation by the use of the transformation of a four-node Lagrange element of FEM is applied. See figure 5.19.

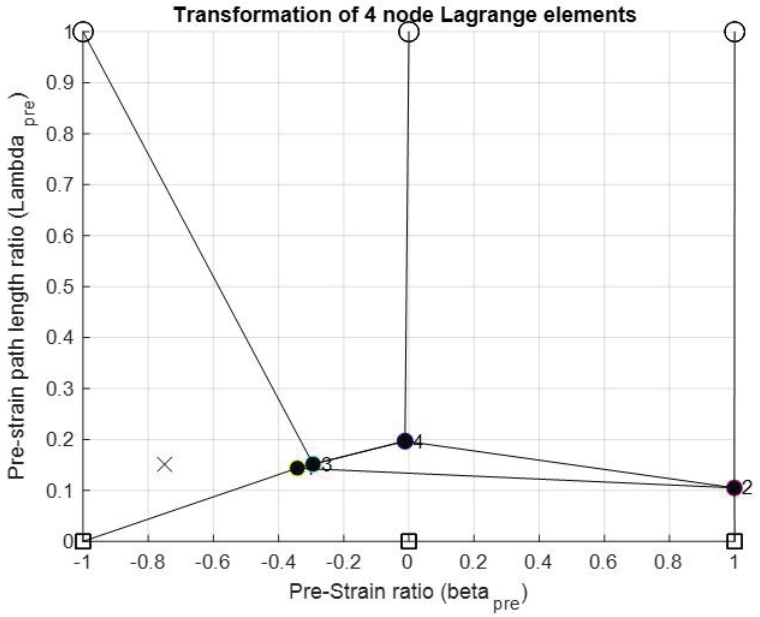

Figure 5.19: Transformation of four node Lagrange Elements

Next, using the theory of isoparametric approximation, post FLC for the interested pre-straining conditions stated in table 5.4can be computed. Figure 5.20 corresponds to the calculated post FLC which will be used to predict the exhausted formability after correction.

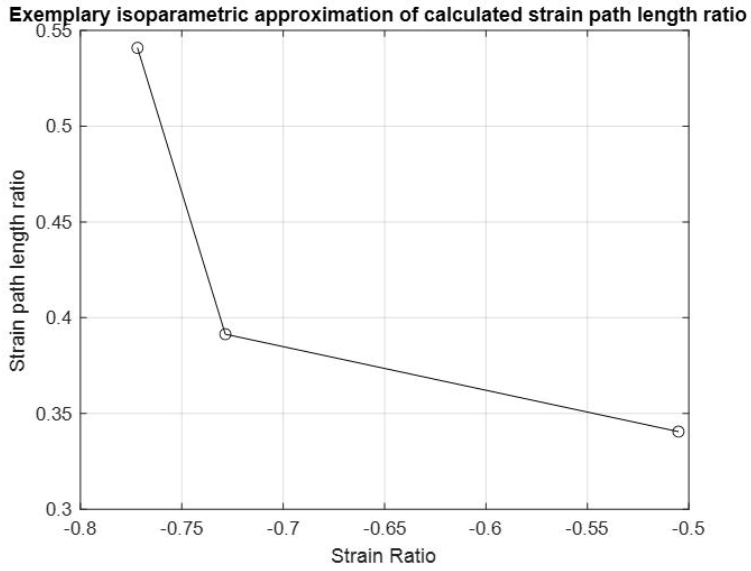

Figure 5.20: Isoparametric Approximation - strain ratio VS calculated strain path ratio

Exhausted Formability

For first pre-straining condition the correction is computed as discussed in the theory section. The computed parameters are shown in the table below.

Parameter	Value
$\lambda_{cal}(\beta_{pos})$	0.5408
$\lambda_{cal}(\beta_{pre})$	0.6180
$\Delta\lambda$	0.2735

Table 5.5: Parameters calculated to carry out correction

Finally λ_{pos} at corresponding β_{pos} is calculated using the following formula:

$$\lambda_{pos}(\beta_{pos}) = \lambda_{cal}(\beta_{pos}) + \Delta\lambda \tag{5.1}$$

Total strain path or exhausted formability λ is calculated as per eqquation 3.10.

$$TotalStrainPath, \lambda = 0.8916 + 0.1857 = 1.0773 \tag{5.2}$$

For second pre-straining condition the correction is computed as discussed in the theory section. The computed parameters are shown in the table below.

Parameter	Value
$\lambda_{cal}(\beta_{pos})$	0.3029
$\lambda_{cal}(\beta_{pre})$	0.4487
$\Delta\lambda$	0.4062

Table 5.6: Parameters calculated to carry out correction

Total strain path or exhausted formability λ is calculated as per equation 3.10.

$$TotalStrainPath, \lambda = 0.7091 + 0.1512 = 0.8603 \tag{5.3}$$

5.4 Validation

In this section computed exhausted formability using GFLC will be verified with the computed exhausted formability obtained from FE-simulation and experimentation.

5.4.1 First pre-forming condition - FE-simulation

Obtained post FLC curve using FE-Simulation is shown in figure 5.21.

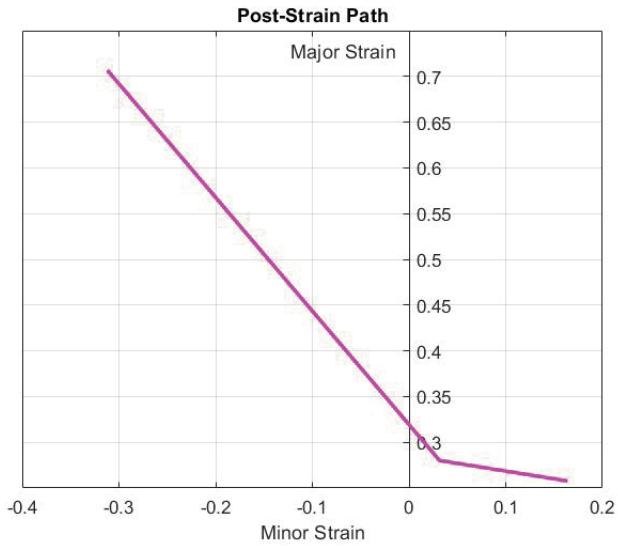

Figure 5.21: Post-Strain path length ratio obtained from FE-Simulation

Corresponding strain ratio vs strain path length ratio, graph is plotted and shown in figure 5.22.

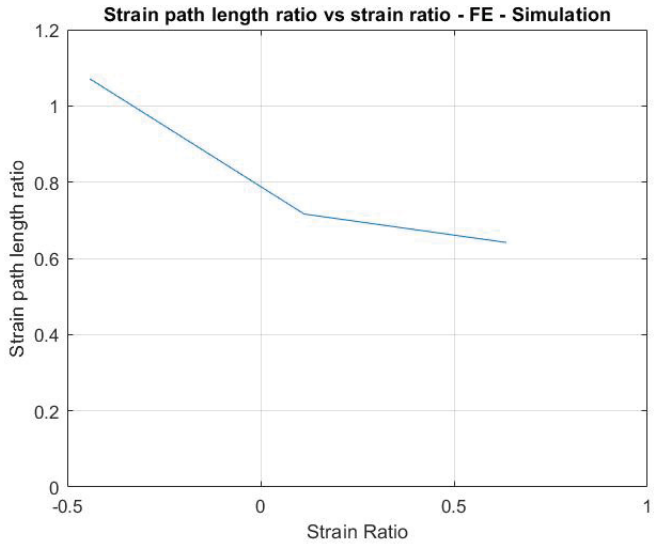

Figure 5.22: Fe-Simulation - strain ratio VS calculated strain path ratio

Finally total strain path from FE-simulation is shown below.

$$TotalStrainPath, \lambda = 0.7884 + 0.1857 = 0.9414 \tag{5.4}$$

5.4.2 Second pre-forming condition - Experimentation

The experimentation contains one post straining which is used to calculate exhausted formability to compare with the prediction made by GFLC. This value is obtained using the method of parameterization.

Post-strain path length ratio = 0.8516

$$TotalStrainPath, \lambda = 0.8516 + 0.1512 = 1.0028 \tag{5.5}$$

Chapter 6

Discussion

6.1 Introduction

This chapter provides detailed discussions based on the obtained results for key findings. These discussions are categorized into different section.

6.2 Literature review

The thesis begins with raising the first research question: *'What are the testing procedures that can be used to generate non-linear strain paths and characterization of the material properties from those tests?'*. As per the research question, a systematic literature review is conducted and a list of test procedures were identified from existing research works.

A list of five test procedures that can be utilized to generate non-linear strain paths is identified from the literature review are as follows.

6.2.1 Cruciform specimen in a conventional Nakajima test setup

Jocham [18], in his work put forward a test procedure which allows the identification of non-linear load paths in a conventional Nakajima test setup with the use of a draw bead tool and a cruciform specimen. The use of draw beads in this procedure will allow one to apply non-proportional load paths which is needed to realize non-linear strain paths. It is identified that this test procedure can be carried out in a single conventional Nakajima testing machine. This procedure uses draw bead tools which provides difficulty in manufacturing and altering the existing Nakajima test machine. Hence, this procedure is not used in this thesis.

6.2.2 Nakajima test with modified punch geometry

Krishna et al. [27] and Mathias et al. [28] developed an experimental approach to realize non-linear strain paths in a single experimental step rather than the traditional two-step procedure. Both the group of authors modified the punch geometry for the standard Nakajima testing machine. This test procedure was used by Anton Eriksson in his thesis as this project was carried out in cooperation with his thesis [100].

6.2.3 Two-step deep-drawing or Drawing reverse-drawing process

Hongzhou and Xin in their work [30], developed a similar test setup based on drawing reverse-drawing process to analyse formability of sheet metal during Sheet metal forming process with the influence of significant non-linear strain paths. This test procedure is easy implement in experimentation and FE-Simulation. Furthermore, GFLC concept utilizes this two-step procedure to evaluate formability for non linear deformation histories. All these factors made this test procedure as a suitable candidate to work on this thesis.

6.2.4 Bulging with stepped dies

Zhubin et al. [59] developed a novel test procedure to realize continuous non-linear bi-axial tensile deformations of sheet metals by bulging with stepped dies. According to their work, it can be concluded that non-linear loading paths can be effectively realized using this test procedure [59]. The use of stepped die, requires modifications to the existing Nakajima test machine. Thus the setting up cost is high. Therefore, this test procedure is not used in this thesis.

6.2.5 In-plane biaxial test with cruciform specimen

As a mean to overcome the downsides of conventional methods, a great alternative would be using the in-plane biaxial tensile test with the cruciform specimen to control the strain path. In order to study the effect of strain path change on the Forming Limit Curve at Necking (FLCN) and to investigate the Forming Limit Curve at Failure (FLCF) under linear strain paths, the authors[60,61] validated the potentiality of the in-plane biaxial tensile test with a cruciform specimen. This test procedure utilizes actuators to control the strain paths which provides difficulty, hence this test procedure is not used further in this thesis.

6.3 FE-Simulations

This section focuses on the discussion based on the results obtained from FEA that are used to predict formability using GFLC.

Initially the specimen are pre-strained upto 8-10% in 4 different directions. Once the specimen are pre-formed, they were cut to different specimen dimensions of 200mm, 100mm and 50mm as Nakajima geometries for Post straining.

According to the theory, the post strain must begin when pre-strain ends. But this was not the case seen in the simulations (See figure 5.6). Accordingly, one can notice the second graph in that figure shows the described problem. This issue may have occurred due to trimming of specimen to Nakajima geometry after the pre-strain and due to retraction of the specimen (due to elasticity). In order to overcome this phenomenon, an average value of the three pre-strains is calculated to obtain the suitable pre-strain value.

Performing the Nakajima test for the same specimen with different dimentions as shown in figure 5.3, enabled to produce three different types of post-straining that are used to formulate the post FLC for each pre-strained specimen. The point at which each of these post straining fails (localization) is obtained to produce post FLC for each pre-straining. Pre-strain and its corresponding post FLC's or in other words bi-linear deformation histories are shown in figure 5.7, 5.9, 5.11 and 5.13.

6.4 Prediction of Formability using GFLC

Initially, the experimentally obtained linear FLC for CR4 material is used along with the strain paths obtained from FE-simulations to produce the forming limit diagram shown in figure 5.14. From the graph one can see linear FLC, and 4 sets of strain paths with each containing 3 bi-linear deformation history produces a total of 12 bi-linear deformation histories. These individual bi-linear histories are parameterised in the next step to produce important parameters that are used later on in the thesis according to equation 3.10. As a result of parameterization, the strain ratio and total strain path length ratio can be used to indicate each forming limit strain. Based on the results of the experiments and simulations, it is determined that deformation histories have a significant impact on forming limitations.

Following, the parameterization of the results (bi-linear deformation history), a metamodeling procedure is established to evaluate formability for any bi-linear deformation history. Isoparametric approximation strategy using four node Lagrange element transformation is the strategy behind the metamodeling (See figure 5.17). The diagram consists of 4 Fe-Simulated pre-strain points and 6 additional nodes that are created based on the conventional FLC. Here, pre-strain path length of 0 refers to the whole FLC is available for post straining. Whereas, if the pre-strain path length is 1 then, it is understood that there is no remaining formability. Using figure 5.17 it is possible to investigate, the interested preforming conditions which belongs to any of the domains. In figure 5.17 and 5.19 element formation is not optimal (The element arrangement is odd for a reader). This is due to the pre-straining range that is used in the simulation. As the specimen were pre-strained between 8-10%, the primary middle element could not be produced to create a proper element formation. In order to avoid this, pre-straining could be done over a larger range. This also provided difficulty as strain localization is seen at higher strains in simulation.

Following that, it is understood from the theory that it is possible to predict post strain path length ratio provided that pre-strain ratio, pre-strain path length ratio and post-strain ratio are known. For this case, a specimen is pre-strained in LS-Dyna upto 16% bi-axially later in order to validate the predicted post strain path length ratio obtained from metamodeling, The pre-strained specimen are post-strained in three different directions to produce post FLC in LS-Dyna. Furthermore, another preforming condition where pre-straining is also conducted experimentally in the uniaxial direction is also used to predict formability. Then, experimentally pre-formed specimen is post strained in plane-strain direction experimentally to validate the predicted formability.

Next, isoparametric approximation strategy is applied to calculate post strain path length ratio for interested preforming condition shown in table 5.3 The created

post-strain path length ratio vs strain ratio graph is seen in figure 5.18. As stated in table 5.3, post strain path length is to be predicted when the post strain ratio is 0. Accordingly using figure 5.18, post-strain path length ratio is calculated. So far it is to be noted that a theory is not yet taken into consideration. This theory says that the total strain path length must always be equal to one if the strain path is linear, that is when pre-strain ratio is the same as post-strain ratio. Taking this into consideration, a small correction of $\Delta\lambda$ is calculated and added with the calculated post strain path length ratio to predict the correct post strain path length ratio. Finally, post strain path length ratio is calculated to be 0.8916 at the given post strain ratio.

Similarly, isoparametric approximation strategy is applied to calculate post strain path length ratio for interested preforming condition shown in table 5.4.The created post-strain path length ratio vs strain ratio graph is seen in figure 5.20. As stated in table 5.4, post strain path length is to be predicted when the post strain ratio is 0.3401. Accordingly, using figure 5.20, post-strain path length ratio is calculated. So far, it is to be noted that a theory is not yet taken into consideration. This theory says that the total strain path length must always be equal to one if the strain path is linear that is when pre-strain ratio is the same as post-strain ratio. Taking this into consideration, a small correction of $\Delta\lambda$ is calculated and added with the calculated post strain path length ratio to predict the correct post strain path length ratio. Finally, post strain path length ratio is calculated to be 0.7091 at the given post strain ratio.

The validation for predicted formability for the first preforming condition is completed using the computed post strain path length ratio obtained from FE-simulation (See figure 5.22). Accordingly post-strain path length ratio when post strain ratio is zero is computed and is 0.7884. Comparing the obtained values for the post-strain path length ratio from the concept of GFLC and FE-simulation, the error is identified to be 11%. It is understood that FE-simulation in LS-Dyna utilizes the procedure based on GISSMO to predict formability. Due to the difference in approach between GISSMO and GFLC, it is not possible to validate the results from GFLC and FE-simulation.

The validation for predicted formability for the second preforming condition is completed using the computed post strain path length ratio obtained from experimentation and its value is 0.8516. Comparing obtained values for the post-strain path length ratio from the concept of GFLC and experimentation, the error is identified to be 14%. Although experimental results are used to validate, most of the calculations made in GFLC procedure utilizes data obtained from FE-simulation (4 pre-strain and post-strain) with GISSMO failure model, thereby rendering this validation faulty.

The number of tests used to characterize the forming limit diagram for many bi-linear deformation histories affects the strategy's prediction accuracy. Therefore it is recommended to have more base points or bi-linear deformations to increase the prediction accuracy.

Following the prediction of formability for a bi-linear deformation history, one can generalize to predict for multi-linear deformation history as multi-linear deformation history is a combination of an arbitrary number of bi-linear deformation history.

Chapter 7

Conclusions

This thesis focuses on generation and prediction of non-linear strain paths in Sheet metal forming. According to literature review, there are many test procedures for generating non-linear strain paths in sheet metal forming and five test procedures were described in detail in this thesis. Based on the described test procedures, it can be concluded that all these test procedures are used to generate non-linear strain paths but they all follow one of the two conventional test methods (Two-step test procedure and Nakajima test procedure) on a more integrated level. There are various advantages and disadvantages corresponding to each test procedure. Taking these into consideration, it can be concluded that the choice of test procedure depends on the expected outcome from the test procedure. Therefore, it can be said, that there is not one best test procedure to realize non-linear strain paths. Two step procedure is chosen for this thesis.

This thesis is carried out in cooperation with the thesis of Anton Eriksson [100]. According to the literature review conducted by him, regarding FE-Software and Failure models, it is concluded that LS-Dyna is suitable for sheet metal forming simulations. Furthermore, according to Anton Eriksson's statement ("In LS-DYNA the DIEM and GISSMO model seems promising, but other models as the GFLC or PIVS are also interesting models to look further into."-[100]) it is concluded that failure prediction using GISSMO failure model and GFLC is most appropriate for this thesis. Most important factor that was understood in the simulation is the influence of friction. We can draw a conclusion here that in order to obtain acceptable results from FE-Simulation, one should opt out friction.

GFLC concept put forwarded by Volk et. al can be said to be an easy procedure with careful handling can provide results. The number of tests used to characterize the forming limit diagram for many bi-linear deformation histories affects the strategy's prediction accuracy. The used 4 bilinear increments (base points) that are calculated using Barlat yld200 yield criterion and GISSMO failure model in LS-Dyna is sufficient enough to predict formability but does not provide results that are accurate. Therefore it is recommended to increase the number of base points to increase the prediction accuracy.

The validation for the obtained exhausted formability for a bi-linear deformation history using GFLC is carried out in conjunction with FE-simulation and also with experimentation. Its is important to note that it is not sensible to validate GFLC prediction using the results obtained GISSMO as both the methods compute formability differently. The results for the pre-straining condition obtained from experimentation also can not be used to validate GFLC prediction in this case. This is because the

used 4 bi-linear FLC for GFLC procedure are obtained from FE-simulation which utilizes GISSMO. As a result it can be said that, in order to validate results from GFLC one should obtain the required data from experimentation.

SMF and non-linear strain paths are considered to be vast area of studies which cannot be covered or completed in one project alone. This project has covered only a small portion of a wide subject area that is currently in study. As a result, looking at a wider picture it can be concluded that the project lack the maturity level for a completed understanding of non-linear strain paths however, the thesis can be said that it has achieved its objectives stated earlier.

Chapter 8

Future Works

This section will provide the readers with the important areas to look into for future work. This thesis studies a subject that has a broader area which provides possibilities to carryout various future work.

First area for suggested future works focuses on the test procedures to generate non-linear strain paths. There are 5 test procedures identified in this thesis to realize non-linear strain paths but the traditional two-step test procedure is only is used in this thesis. This provides opportunity to carry out other test procedures.

The second area for future work is the application of experimentation to obtain data that is used for formability prediction using GFLC. In this thesis FE-simulations are used to obtain these data used in GFLC. Thereby, not providing the opportunity for validation. If one were to obtain these data from experimentation, then it can be used to validate for the suitable preforming condition, which is also obtained from experimentation.

Finally, the third suggested area for future work, is the generalization of the described GFLC approach to predict formability for multi-linear deformation history.

Bibliography

[1] W. Volk and J. Suh, 'Prediction of formability for non-linear deformation history using generalized forming limit concept (GFLC)', Melbourne, Australia, 2013, pp. 556–561, doi: 10.1063/1.4850035.

[2] C. B. Smith and R. S. Mishra, 'Fundamentals of Formability', in Friction Stir Processing for Enhanced Low Temperature Formability, Elsevier, 2014, pp. 7–9.

[3] J. Pilthammar, 'Elastic press and die deformations in sheet metal forming simulations', 2017.

[4] Pilthammar, J. (2017). Elastic press and die deformations in sheet metal forming simulations (Doctoral dissertation, Blekinge Tekniska Högskola).

[5] Björklund, O., Govik, A., & Nilsson, L. (2014). Prediction of fracture in a dual-phase steel subjected to non-linear straining. Journal of Materials Processing Technology, 214(11), 2748-2758.

[6] A. Barata Da Rocha, F. Barlat, and J.M. Jalinier. Prediction of the forming limit diagrams of anisotropic sheets in linear and non-linear loading. Materials Science and Engineering,1984, 68:151–164

[7] K. Yoshida, T. Kuwabara, and M. Kuroda. Path-dependence of the forming limit stresses in a sheet metal. International Journal of Plasticity, 2007. 23:361–384.

[8] M. Kuroda and V. Tvergaard. Effect of strain path change on limits to ductility of anisotropic metal sheets. International Journal of Mechanical Sciences, 42:867–887, 2000.

[9] S. Hiwatashi, A. Van Bael, P. Van Houtte, and C. Teodosiu. Prediction of forming limit strains under strain-path changes : application of an anisotropic model based on texture and dislocation structure. International Journal of Plasticity, 14:647–669, 1998.

[10] C.L. Chow, L.G. Yu, W.H. Tai, and M.Y. Demeri. Prediction of forming limit diagrams for AL6111-t4 under non-proportional loading. International Journal of Mechanical Sciences, 43:471–486, 2001.

[11] R. Arrieux, C. Bedrin, and M. Boivin. Determination of an intrinsic forming limit stress diagram for isotropic sheets. In Proceedings of the 12th IDDRG congress, pages 61–71, Santa Margherita, 1982.

[12] T. B. Stoughton. A general forming limit criterion for sheet metal forming. International Journal of Mechanical Sciences, 42:1–27, 2000.

[13] T.B. Stoughton and J.W. Yoon. Sheet metal formability analysis for anisotropic materials under non-proportional loading. International Journal of Mechanical Sciences, 47:1972–2002, 2005.

[14] M.C. Butuc, J.J. Gracio, and A. Barata Da Rocha. An experimental and theoretical analysis on the application of stress-based forming limit criterion. International Journal of Mechanical Sciences, 48:414–429, 2006.

[15] A. Graf and W. Hosford. The influence of strain-path changes on forming limit diagrams of al 6111 t4. International Journal of Mechanical Science, 36:897–910, 1994.

[16] R. Uppaluri, N. Venkata Reddy, and P.M. Dixit. An analytical approach for the prediction of forming limit curves subjected to combined strain paths. International Journal of Mechanical Sciences, 53:365–373, 2011.

[17] W. Volk, H. Hoffmann, J. Suh, and J. Kim. Failure prediction for non-linear strain paths in sheet metal forming. CIRP Annals – Manufacturing Technology, 61:259–262, 2012.

[18] Jocham D., Gaber C., Böttcher O. and Volk W.: Prediction of formability for multi-linear strain paths. Proc. Of FTF 2015:59-64, 2015

[19] Weinschenk A., Volk W.: FEA-based development of a new tool for systematic experimental validation of non-linear strain paths and design of test specimens, AIP Conf. Proc. 1896, 020009, DOI: 10.10.63/1.5007966, 2017

[20] Pascoe K.J., de Villiers J.W.R.: Low cycle fatigue of steels under biaxial straining, Journal of Strain Analysis, 2:117-126, 1967

[21] Merklein M., Biasutti M.: Development of a biaxial tensile machine for chracterization of sheet metals, Journal of Materials Processing Technology, 213:939-946, DOI: 10.1016/j.matprotec.2012.12.005, 2013

[22] Kuwabara T., Ikead S., Kuroda K.: Measurement and analysis of differential work hardening in cold-rolled steel sheet under biaxial tension, Journal of Material Processing Technology, 80-81:517-523, 1998

[23] Leotoing L., Guines D., Zhang S., Ragneau E.: A cruciform shape to study the influence of strain paths on forming limit curves, Key Engineering Materials, 554-557:41-46, DOI: 10.4028/www.scientific.net/KEM.554-557.41, 2013

[24] Güler B., Efe M.: Large Strain Cruciform Biaxial Testing for FLC Detection, AIP Conf. Proc., 1896-020018, DOI: 10.1063/1.5007975, 2017

[25] Yong H., Min J., Lin J., Carsley E. J., Stoughton T.B.: Cruciform specimen design for large plastic strain during tensile testing, IOP Conf. Series: Journal of Physics: Conf. Series, 1063, DOI: 10.1088/1742-6596/1063/1/012160, 2018

[26] Jocham D., Gaber C., Böttcher O., Wiedemann P., Volk, W.: Experimental prediction of sheet metal formability of AW-5754 for non-linear strain paths by using a cruciform specimen and a blank holder with adjustable draw beads on a sheet metal testing machine, Int J Mater Form10:597-605, 2017

[27] R. Norz and W. Volk, "Investigation of non-proportional load paths by using a cruciform specimen in a conventional Nakajima test", IOP Conference Series: Materials Science and Engineering, vol. 651, p. 012020, 2019. Available: 10.1088/1757-899x/651/1/012020.

[28] K. Saxena, D. Kumar and J. Mukhopadhyay, "A novel experimental approach for detection of forming limits considering non linear strain paths", in International Deep Drawing Research Group, Shanghai, China, 2015.

[29] M. Liewald and K. Drotleff, "Novel Punch Design for non-linear Strain Path Generation and Evaluation Methods", Key Engineering Materials, vol. 639, pp. 317-324, 2015. Available: 10.4028/www.scientific.net/kem.639.317.

[30] C. Gaber, D. Jocham, H. Weiss, O. Böttcher and W. Volk, "Evaluation of non-linear strain paths using Generalized Forming Limit Concept and a modification of the Time Dependent Evaluation Method", International Journal of Material

Forming, vol. 10, no. 3, pp. 345-351, 2016. Available: 10.1007/s12289-016-1283-x.

[31] H. Li, G. Li, G. Gao, W. Zhang and X. Wu, "A formability evaluation method for sheet metal forming with non-linear strain path change", International Journal of Material Forming, vol. 11, no. 2, pp. 199-211, 2017. Available: 10.1007/s12289-017-1342-y.

[32] Olsen TY. Machines for ductility testing. Proc Am Soc Test Mater 1920;20:398–403.

[33] ISO 16808 Metallic materials – sheet and strip – determination of biaxial stress-strain curve by means of bulge test with optical measuring systems. Int Organ Stand 2014:2014.

[34] Reis LC, Prates PA, Oliveira MC, Santos AD, Fernandes J V. Anisotropy and plastic flow in the circular bulge test. Int J Mech Sci 2017;128–129:70–93. doi:10.1016/j.ijmecsci.2017.04.007.

[35] Chen K, Scales M, Kyriakides S. Material hardening of a high ductility aluminium alloy from a bulge test. Int J Mech Sci 2018;138–139:476–88. doi:10.1016/j.ijmecsci.2018.02.00

[36] Janbakhsh M, Djavanroodi F, Riahi M. Utilization of bulge and uniaxial tensile tests for determination of flow stress curves of selected anisotropic alloys. Proc Inst Mech Eng Part L J Mater Des Appl 2013;227:38–51. doi:10.1177/1464420712451963.

[37] Yousif MI, Duncan JL, Johnson W. Plastic deformation and failure of thin elliptical diaphragms. Int J Mech Sci 1970;12:959–72. doi:10.1016/0020-7403(70)90036-6.

[38] Chan KC, Chow KK. Analysis of hot limit strains of a superplastic 5083 aluminum alloy under biaxial tension. Int J Mech Sci 2002;44:1467–78. doi:10.1016/S0020-7403(02)00037-1.

[39] Abu-Farha F, Verma R, Hector LG. High temperature composite forming limit diagrams of four magnesium AZ31B sheets obtained by pneumatic stretching. J Mater Process Technol 2012;212:1414–29.

[40] Lazarescu L, Nicodim IP, Comsa DS, Banabic D. A procedure for the evaluation of flow stress of sheet metal by hydraulic bulge test using elliptical dies. Key Eng Mater 2012;504–506:107–12.

[41] Lăzărescu L, Comşa DS, Nicodim I, Ciobanu I, Banabic D. Characterization of plastic behaviour of sheet metals by hydraulic bulge test. Trans Nonferrous Met Soc China 2012;22:275–9.

[42] Williams BW, Boyle KP. Characterization of anisotropic yield surfaces for titanium sheet using hydrostatic bulging with elliptical dies. Int J Mech Sci 2016;114:315–29.

[43] Lenzen M, Merklein M. Improvement of numerical modelling considering plane strain material characterization with an elliptic hydraulic bulge test. J Manuf Mater Process 2018;2:6.

[44] Zhalehfar F, Hashemi R, Hosseinipour SJ. Experimental and theoretical investigation of strain path change effect on forming limit diagram of AA5083. Int J Adv Manuf Technol 2014;76:1343–52.

[45] Sugawara F, Yoshida K, Kuwabara T, Taomoto N, Yanagi N. Forming limit prediction of sheet metals subjected to combined loading using forming limit stress curve. AIP Conf. Proc. 2010;1315:383–8.

[46] Kuwabara T, Ikeda S, Kuroda K. Measurement and analysis of differential work hardening in cold-rolled steel sheet under biaxial tension. J Mater Process Technol 1998;80–81:517–23.

[47] Kuwabara T. Effect of anisotropic yield functions on the accuracy of springback simulation. AIP Conf. Proc. 2004 2004;712:887–92.

[48] Kuwabara T, Nakajima T. Material modeling of 980MPa dual phase steel sheet based on biaxial tensile test and in-plane stress reversal test. J Solid Mech Mater Eng 2011;5:709–20.

[49] Kuroda M, Tvergaard V. Use of abrupt strain path change for determining subsequent yield surface: illustrations of basic idea. Acta Mater 1999;47:3879–90.

[50] Yu Y, Wan M, Wu XD, Bin Zhou X. Design of a cruciform biaxial tensile specimen for limit strain analysis by FEM. J Mater Process Technol 2002;123:67–70.

[51] Leotoing L, Guines D, Zidane I, Ragneau E. Cruciform shape benefits for experimental and numerical evaluation of sheet metal formability. J Mater Process Technol 2013;213:856–63.

[52] Liu W, Guines D, Leotoing L, Ragneau E. Identification of sheet metal hardening for large strains with an in-plane biaxial tensile test and a dedicated cross specimen. Int J Mech Sci 2015;101–102:387–98.

[53] Leotoing L, Guines D. Investigations of the effect of strain path changes on forming limit curves using an in-plane biaxial tensile test. Int J Mech Sci 2015;99:21–8.

[54] Sumita T, Kuwabara T, Hayashida Y. Measurement of work hardening behavior of pure titanium sheet using a servo-controlled tube bulge testing apparatus. AIP Conf Proc 2011;1353:1423–8.

[55] Kuwabara T, Sugawara F. Multiaxial tube expansion test method for measurement of sheet metal deformation behavior under biaxial tension for a large strain range. Int J Plast 2013;45:103–18.

[56] Kuwabara T, Ishiki M, Kuroda M, Takahashi S. Yield locus and work hardening behavior of a thin-walled steel tube subjected to combined tension-internal pressure. J Phys IV 2003;105:347–54.

[57] Kuwabara T, Yoshida K, Narihara K, Takahashi S. Anisotropic plastic deformation of extruded aluminum alloy tube under axial forces and internal pressure. Int J Plast 2005;21:101–17.

[58] Yoshida K, Kuwabara T, Narihara K, Takahashi S. Experimental verification of the path-independence of forming limit stresses. Int J Form Process 2005;8:283–98.

[59] Yoshida K, Kuwabara T. Effect of strain hardening behavior on forming limit stresses of steel tube subjected to nonproportional loading paths. Int J Plast 2007;23:1260– 84.

[60] Z. He, H. Zhu, Y. Lin, D. Politis, L. Wang and S. Yuan, "A novel test method for continuous non-linear biaxial tensile deformation of sheet metals by bulging with stepped-dies", International Journal of Mechanical Sciences, vol. 169, p. 105321, 2020. Available: 10.1016/j.ijmecsci.2019.105321.

[61] L. Leotoing and D. Guines. Investigations of the effect of strain path changes on forming limit curves using an in-plane biaxial tensile test. International Journal of Mechanical Sciences, 99:21–28, 2015.

[62] X. Song, L. Leotoing, D. Guines, and E. Ragneau. Investigation of the forming limit strains at fracture of AA5086 sheets using an in-plane biaxial tensile test. Engineering Fracture Mechanics, 163:130–140, 2016.

[63] T. Kuwabara, S. Ikeda, and K. Kuroda. Measurement and analysis of differential work hardening in cold-rolled steel sheet under biaxial tension. Journal of

Materials Processing Technology, 80-81:517–523, 1998.

[64] L. Leotoing, D. Guines, I. Zidane, and E. Ragneau. Cruciform shape benefits for experimental and numerical evaluation of sheet metal formability. Journal of Materials Processing Technology, 213(6):856–863, 2013.

[65] X. Song, L. Leotoing, D. Guines, and E. Ragneau. Characterization of forming limits at fracture with an optimized cruciform specimen: Application to DP600 steel sheets. International Journal of Mechanical Sciences, 126:35–43, 2017.

[66] X. Song, L. Leotoing, D. Guines and E. Ragneau, "Effect of continuous strain path changes on forming limit strains of DP600", Strain, vol. 55, no. 6, 2019.

[67] L. Wang and T. Lee, "The effect of yield criteria on the forming limit curve prediction and the deep drawing process simulation", International Journal of Machine Tools and Manufacture, vol. 46, no. 9, pp. 988-995, 2006.

[68] Tvergaard V., Legarth B.N. Effect of Anisotropic Plasticity on Mixed Mode Interface Crack Growth. In: Gdoutos E.E. (eds) Fracture of Nano and Engineering Materials and Structures. Springer, Dordrecht, 2006

[69] S. Stören and J. Rice, "Localized necking in thin sheets", Journal of the Mechanics and Physics of Solids, vol. 23, no. 6, pp. 421-441, 1975. Available: 10.1016/0022-5096(75)90004-6.).

[70] Hecker SS. Simple technique for determining forming limit curves. Sheet Met Ind 1975; 52: 671–676.

[71] J. Gronostajski, A. Dolny, Determination of forming limit curves by means of Marciniak punch. Memor. Sci. Rev. Metal. 4, 570–578 (1980).

[72] R. Narayanasamy and C. Narayanan, "Forming, fracture and wrinkling limit diagram for if steel sheets of different thickness", Materials & Design, vol. 29, no. 7, pp. 1467-1475, 2008. Available: 10.1016/j.matdes.2006.09.017.

[73] K. S. Raghavan, Metall. Trans. A 26, 2075–2084 (1995).

[74] S.P. Keeler, W. A. Backofen, Trans. ASM 56, 25–48 (1963).

[75] G.M. Goodwin, SAE, no 680093, 380-387 (1968).

[76] ASTM E2218 - 02(2008) Standard Test Method for Determining Forming Limit Curves

[77] Z. Marciniak, J. Duncan and S. Hu, Mechanics of sheet metal forming. Oxford: Butterworth-Heinemann, 2005.

[78] D. Banabic, H. Aretz, L. Paraianu, P. Jurco, Model. Simul. Mater. Sci. Eng. 13, 759-769 (2005).

[79] D. Banabic, H. J. Bunge, K. Pöhland, A.E. Tekkaya, Formability of Metallic Materials. Springer, Berlin 2000.

[80] J. Slota, E. Spisak, Metalurgia 4, 249–253 (2005).

[81] Y. M. Huang, Y. W. Tsai, C. L. Li, J. Mater. Process Technol. 201, 385–389 (2008).

[82] J. Winowiecka, W. Wieckowski, M. Zawadzki, Comp. Mater. Sci. 77, 108-113 (2013).

[83] H. Takuda, K. Mori, N. Hatta, J. Mater. Process. Technol. 95, 116–121 (1999).

[84] [29] T. Pepelnjak, K. Kuzman, J. Achiev. Mater. Manuf. Eng. 20, 375-378 (2007).

[85] H.W. Swift, J. Mech. Phys. Solids 1, 1–18 (1952).

[86] R. Hill, Proc. Roy. Soc. London 193A, 197–281 (1948).

[87] Z. Marciniak, K. Kuczynski, Int. J. Mech. Sci. 9, 609 – 620(1967).

[88] S. Ahmadi, A. R. Eivani, A. Akbarzadeh, Comput. Mater. Sci. 44, 1252–1257 (2009).

[89] T. B. Stoughton, X. Zhu, Int. J. Plast

[90] HE Min, LI Fu-guo, WANG Zhi-gang. Forming limit stress diagram prediction of aluminum alloy 5052 based on GTN model parameters determined by in situ tensile test [J]. Chinese Journal of Aeronautics, 2011

[91] CHEN M H, GAO L, ZUO D W, WANG M. Application of the forming limit stress diagram to forming limit prediction for the multi-step forming of auto panels [J]. Materials Processing Technology, 2007

[92] PANICH S, BARLAT F, UTHAISANGSUK V, SURANUNTCHAI S, JIRATHEARANAT S. Experimental and theoretical formability analysis using strain and stress-based forming limit diagram for advanced high strength steels [J]. Materials & Design, 2013

[93] ARRIEUX R. Determination and use of the forming limit stress diagrams in sheet metal forming [J]. Journal of Materials Processing Technology, 1995

[94] STOUGHTON T B. A general forming limit criterion for sheet metal forming [J]. International Journal of Mechanical Sciences, 2000

[95] UTHAISANGSUK V, PRAHL U, BLECK W. Stress based failure criterion for formability characterisation of metastable steels [J]. Computational Materials Science, 2007

[96] FANG Gang, LIU Qing-jun, LEI Li-ping, ZENG Pan. Comparative analysis between stress- and strain-based forming limit diagrams for aluminium alloy sheet 1060 [J]. Transactions of Nonferrous Metals Society of China

[97] International standard ISO 12004-2: 2008 metallic materials - sheet and strip - determination of forming-limit curves - part 2: Determination of forming-limit curve in the laboratory, 2008.

[98] M. Merklein, A. Kuppert, and M. Geiger. Time dependent determination of forming limit diagrams. CIRP Annals-Manufacturing Technology, 59(1):295– 298, 2010.

[99] A.J. Mart´ınez-Donaire, F.J. Garc´ıa-Lomas, and C. Vallellano. New approaches to detect the onset of localised necking in sheets under through-thickness strain gradients. Materials and Design, 57:135–145, 2014

[100] A. Eriksson, 'Non-Linear strain paths in Sheet Metal Forming', Dissertation, 2021.

Appendix A

FE-Simulation results

A.0.1 Tensile test

Findings of FE-simulation of Tensile test are categorized in two two section based on the inclusion of failure model, GISSMO.

Tensile test without Failure Model (GISSMO)

All the test results corresponding to tensile test without failure models are shown below. Initially, effective strain path seen in the specimen at the end of the simulation is shown in figure A.1. Continuously, Von Mises stresses seen in the specimen at the end of the simulation is shown in figure A.2. Next, minor strain and major strain of the specimen at the end of the simulation is shown in figure A.3 and figure A.4 respectively.

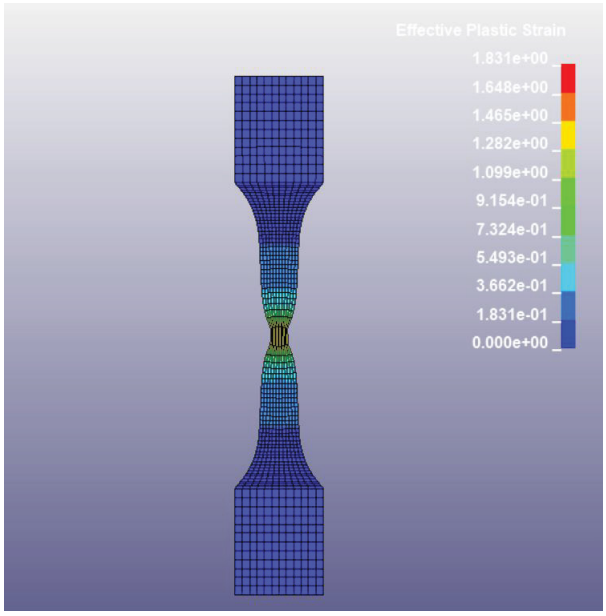

Figure A.1: Effective Plastic Strain

In addition to results based on fringes shown from figure A.1 - A.4, few graphs corresponding to strains and strain paths have been plotted and show below with further details. Minor strain Vs time graph for the entire simulation is shown in figure A.5. Furthermore figure A.6 corresponds to major strain vs time graph.

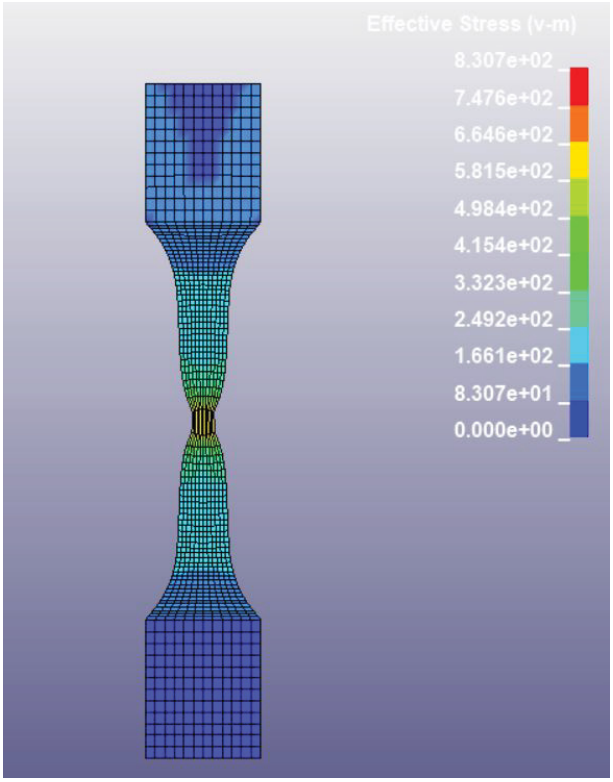

Figure A.2: Von Mises Stress

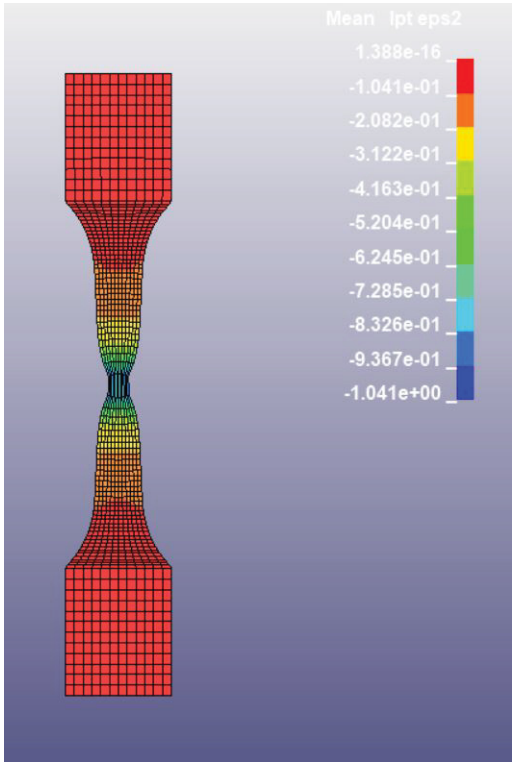

Figure A.3: Minor Strain

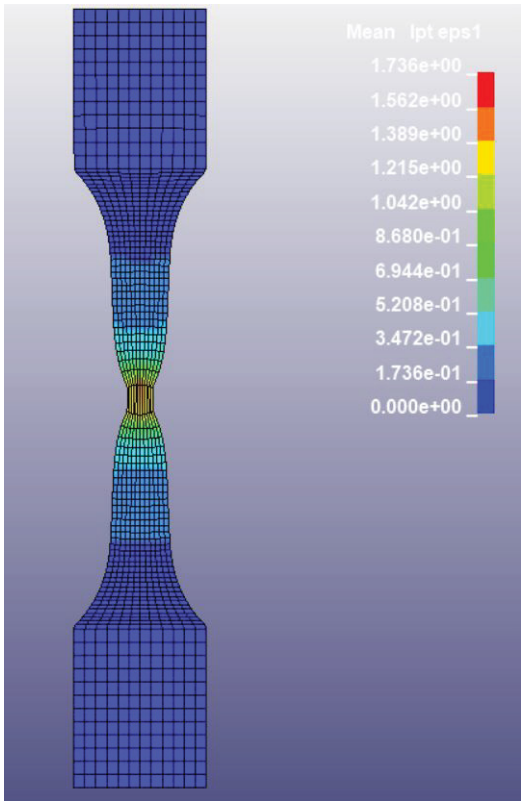

Figure A.4: Major Strain

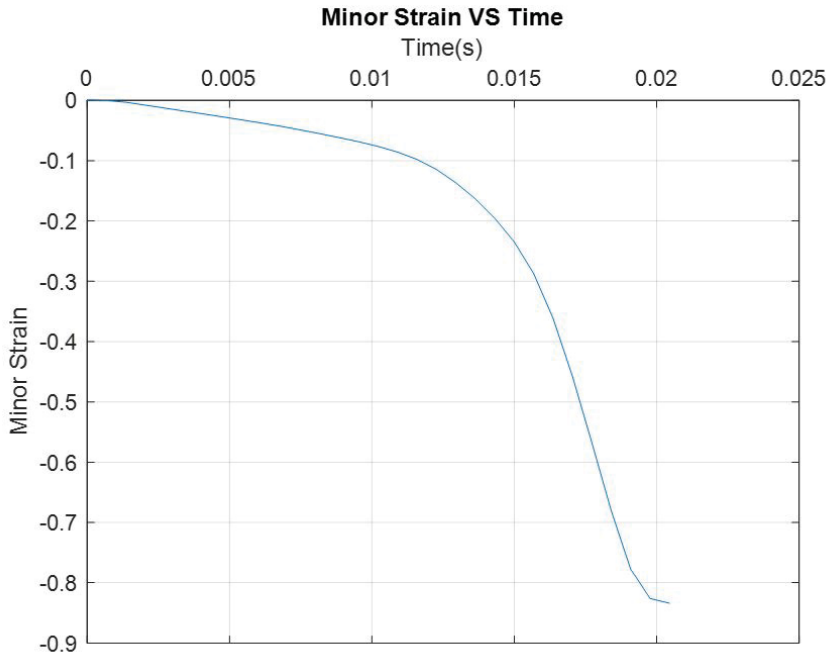

Figure A.5: Minor Strain VS Time

Finally, the observed strain path for the element in center for tensile testing FE-simulation is shown is figure A.7.

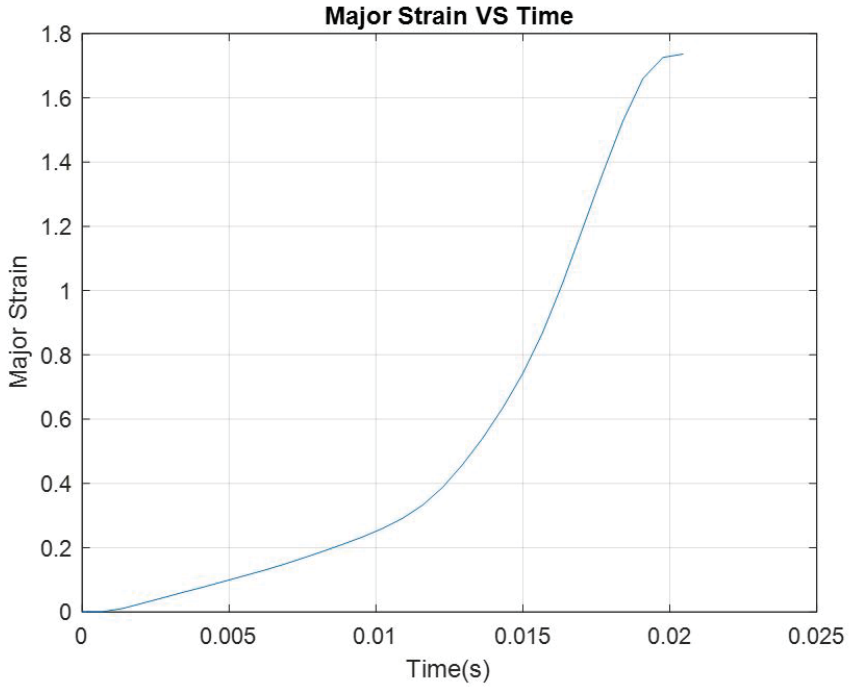

Figure A.6: Major Strain vs Time

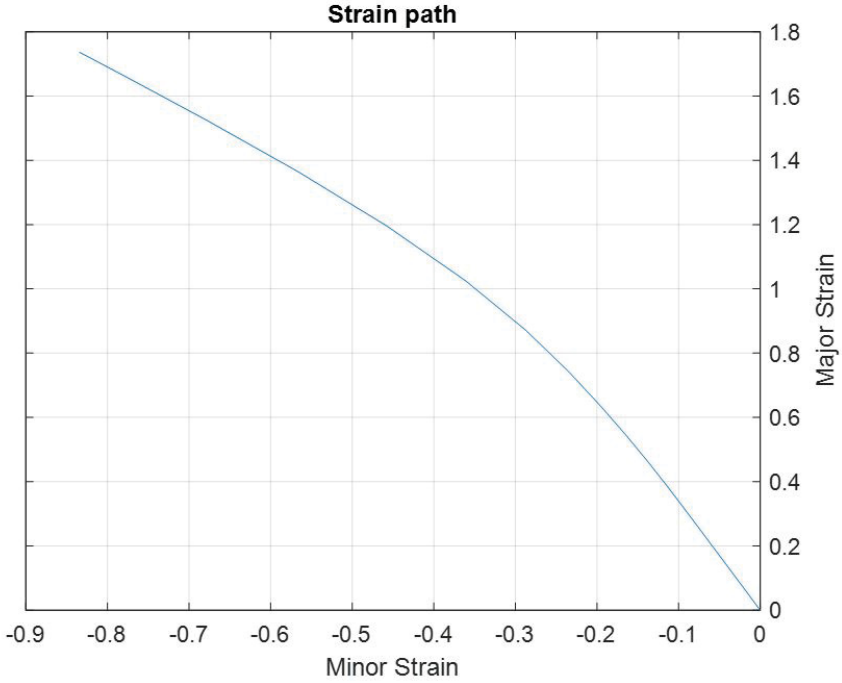

Figure A.7: Strain Path

Tensile test with Failure Model (GISSMO)

All the test results corresponding to tensile test with failure models are shown below. Initially, effective strain path seen in the specimen one stage before failure is shown in figure A.8 and effective strain path as soon as failure is initiated is shown in

figure A.9. Continuously, Von Mises stresses seen in the specimen before and after failure are shown in figureA.11 and figure A.11 respectively. Next, minor strain of the specimen before failure and as soon as failure begins is shown in figure A.12 and figure A.13 respectively. Also for Major strain the corresponding figures are plotted and shown in figure A.14 and figure A.15.

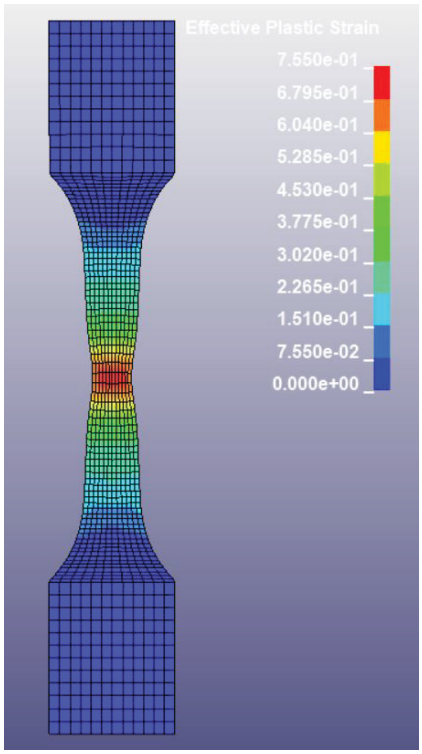

Figure A.8: Effective Plastic Strain - Before failure

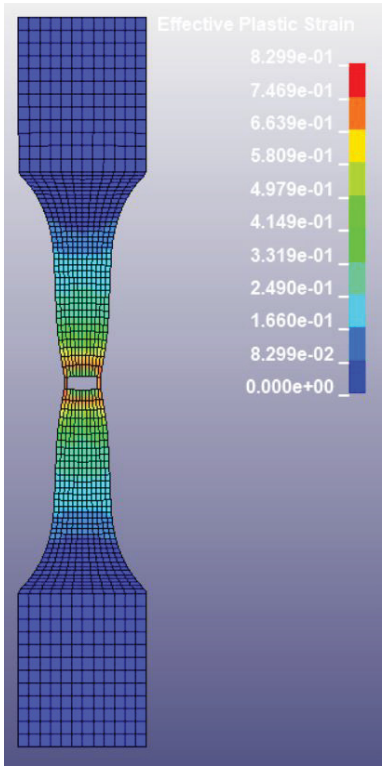

Figure A.9: Effective Plastic Strain - after failure

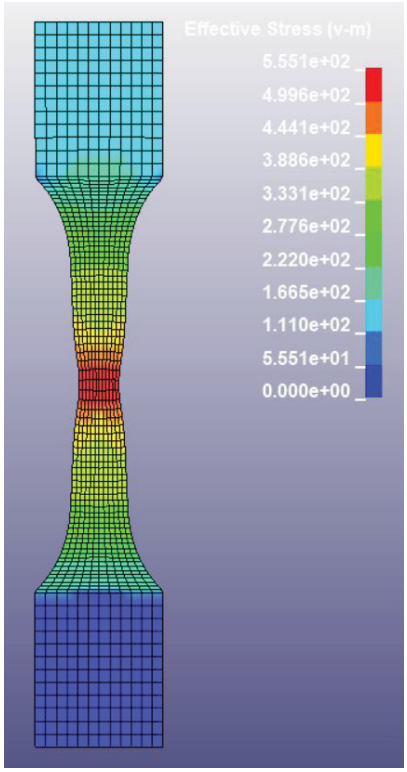

Figure A.10: Von Mises Stresses - Before failure

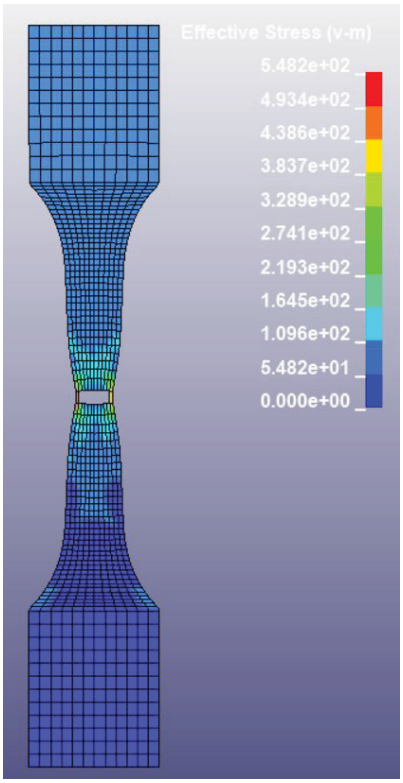

Figure A.11: Von Mises Stresses - After failure initiated

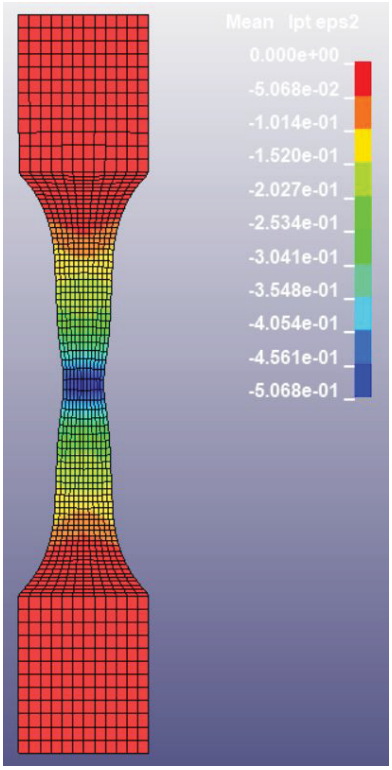

Figure A.12: Minor Strain - Before failure initiation

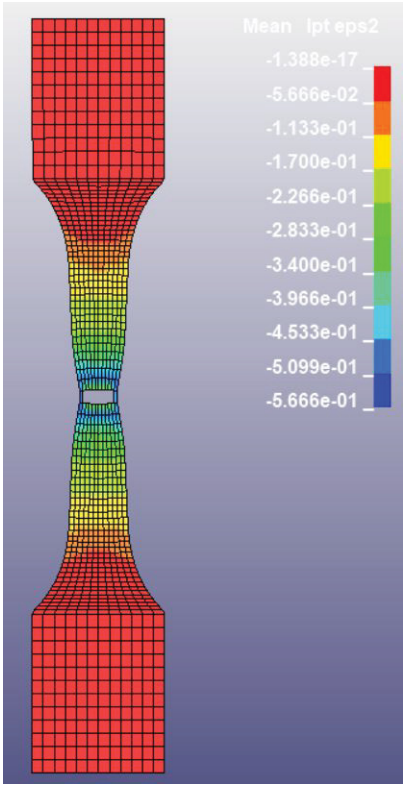

Figure A.13: Minor Strain - as soon as failure initiation

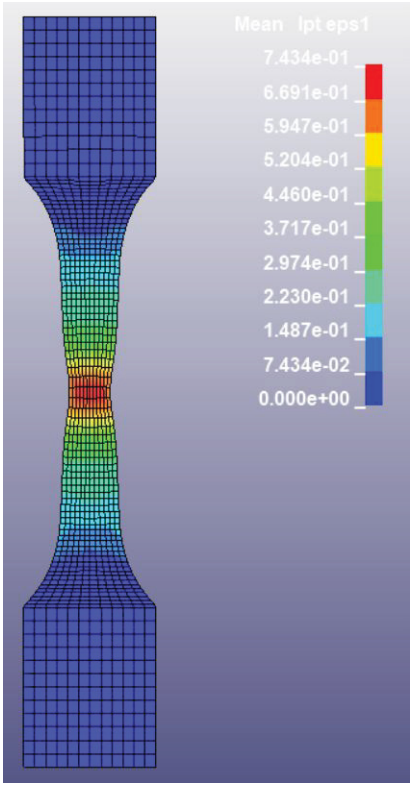

Figure A.14: Major Strain - before failure initiation

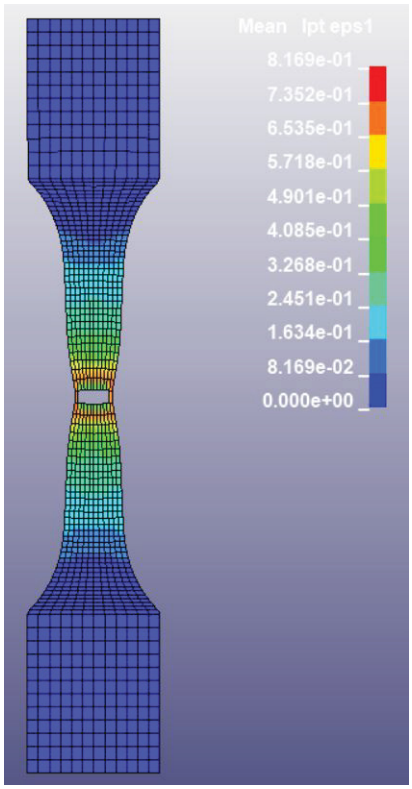

Figure A.15: Major Strain - As soon as failure initiation

In addition to results based on fringes shown from figure A.8 - A.15, few graphs corresponding to strains and strain paths have been plotted and show below. Minor strain Vs time graph for the entire simulation is shown in figure A.16. Furthermore figure A.17 corresponds to major strain vs time graph.

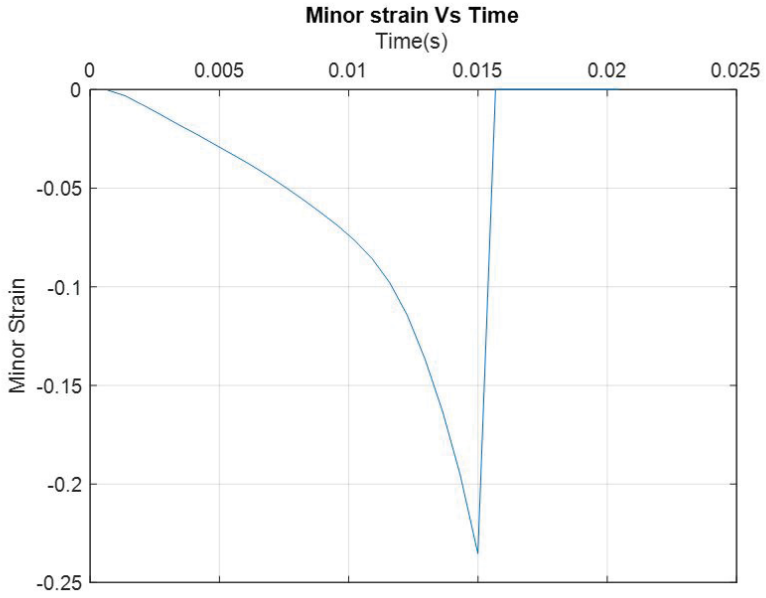

Figure A.16: Minor Strain VS Time

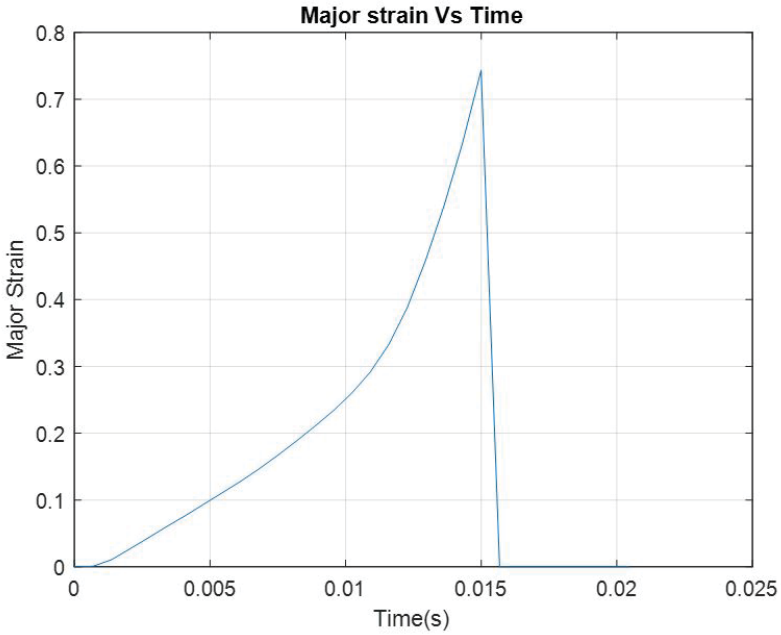

Figure A.17: Major Strain vs Time

Finally, the observed strain path for the element in center for tensile testing FE-simulation is shown is figure A.18.

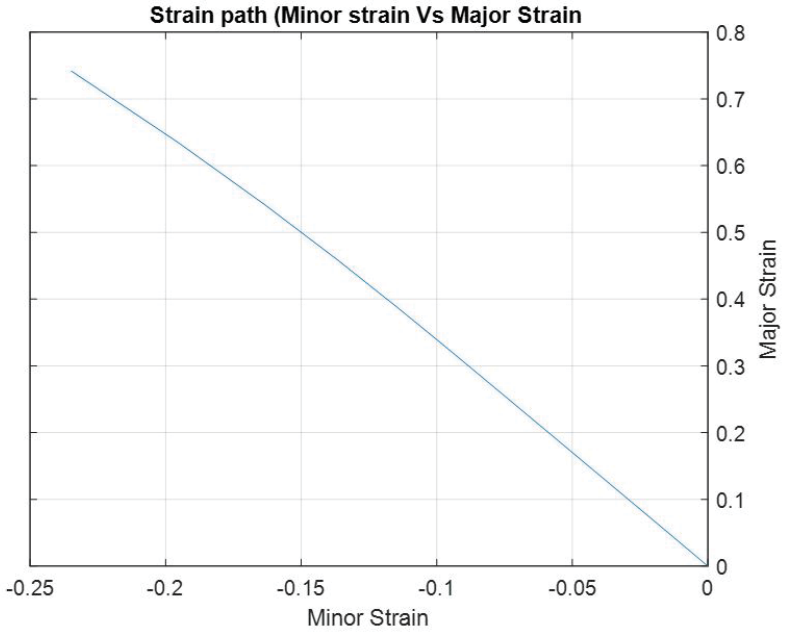

Figure A.18: Strain Path

A.0.2 Shear Test

Findings of FE-simulation of shear test or 45-degree tensile test are categorized in two two section based on the inclusion of failure model, GISSMO.

Shear test without Failure Model (GISSMO)

All the test results corresponding to shear test without failure models are shown below. Initially, effective strain path seen in the specimen at the end of the simulation is shown in figure A.19. Continuously, Von Mises stresses seen in the specimen at the end of the simulation is shown in figure A.20. Next, minor strain and major strain of the specimen at the end of the simulation is shown in figure A.21 and figure A.22 respectively.

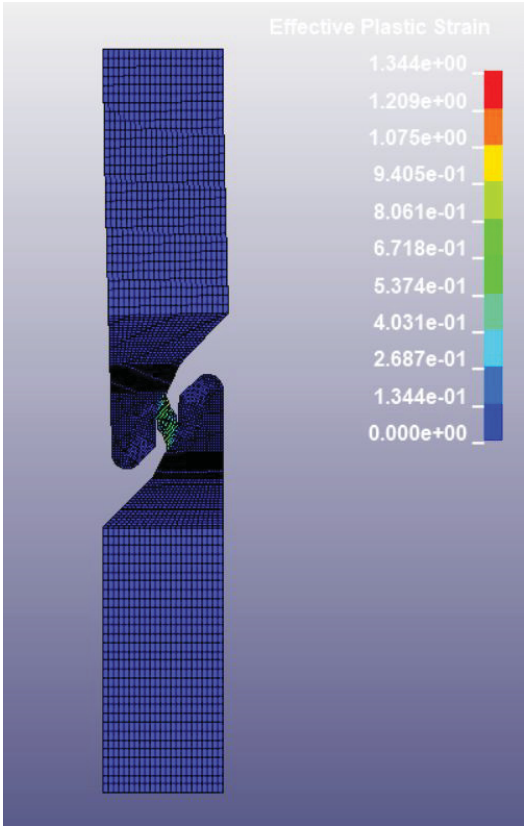

Figure A.19: Effective Plastic Strain

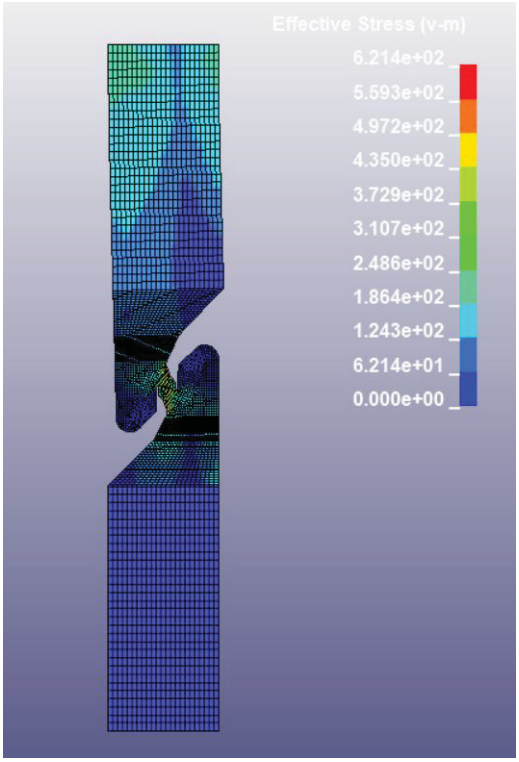

Figure A.20: Von Mises Stress

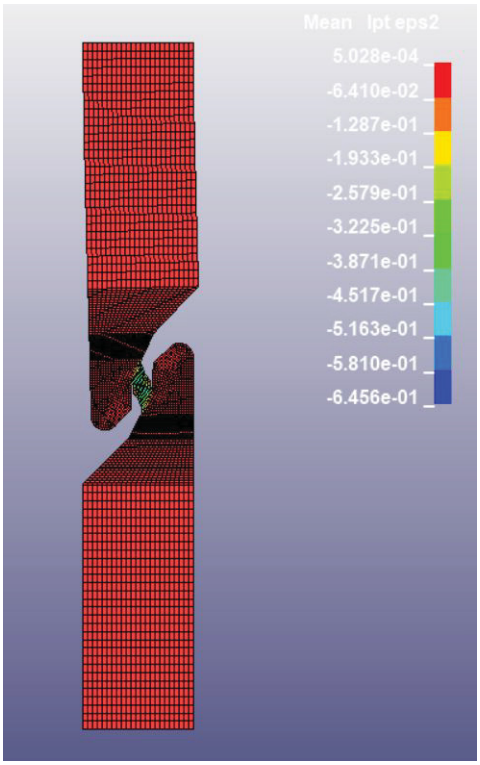

Figure A.21: Minor Strain

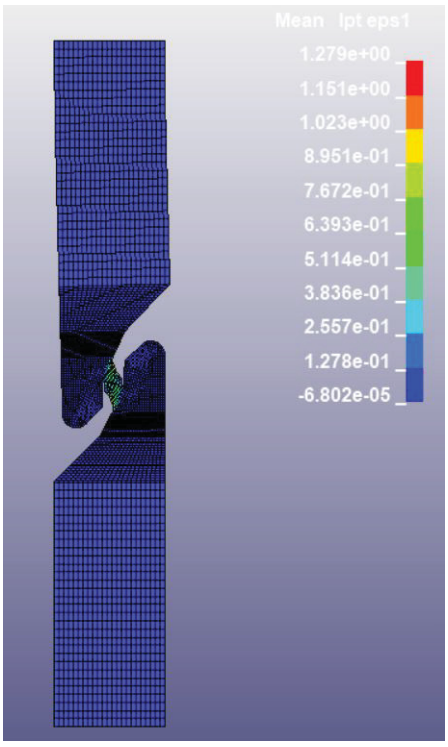

Figure A.22: Major Strain

In addition to results based on fringes shown from figure A.19 - A.22, few graphs corresponding to strains and strain paths have been plotted and show below with further details. Minor strain Vs time graph for the entire simulation is shown in figure A.23. Furthermore figure A.24 corresponds to major strain vs time graph.

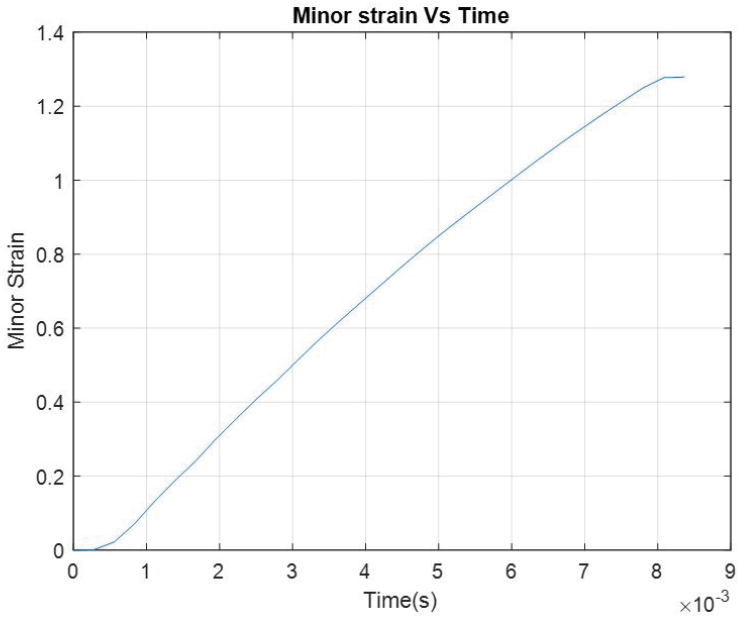

Figure A.23: Minor Strain VS Time

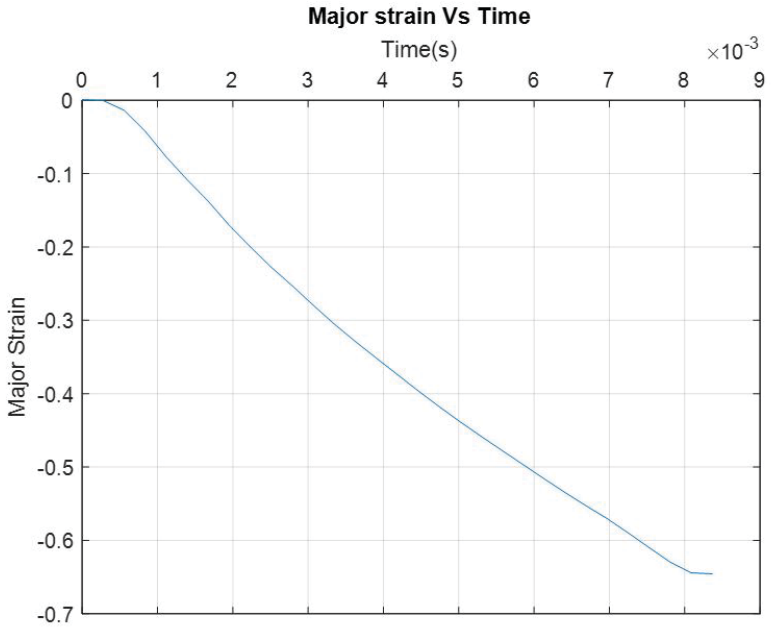

Figure A.24: Major Strain vs Time

Finally, the observed strain path for the element in center for shear testing FE-simulation is shown is figure A.25.

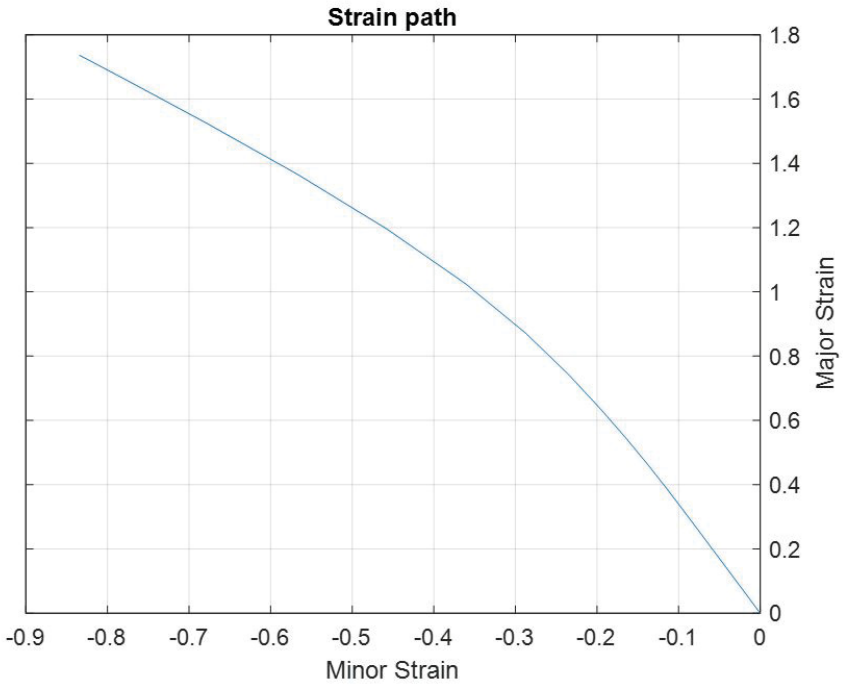

Figure A.25: Strain Path

Shear Test with Failure Model (GISSMO)

All the test results corresponding to shear test or 45-degree tensile test FE-simulation with failure models are shown below. Initially, effective strain path seen in the specimen one stage before failure is shown in figure A.26 and effective strain path as soon as failure is initiated is shown in figure A.27. Continuously, Von Mises stresses seen in the specimen before and after failure are shown in figureA.29 and figure A.28 respectively. Next, minor strain of the specimen before failure and as soon as failure begins is shown in figure A.30 and figure A.31 respectively. Also for Major strain the corresponding figures are plotted and shown in figure A.32 and figure A.33.

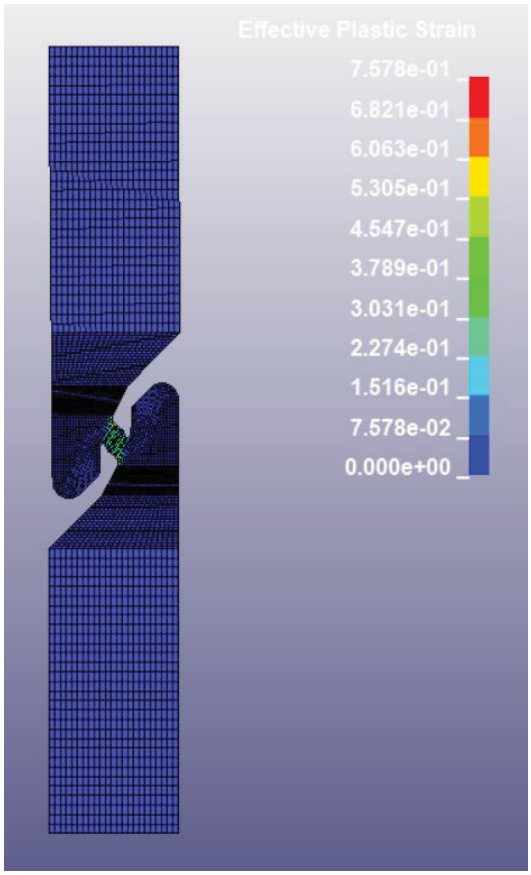

Figure A.26: Effective Plastic Strain - Before failure

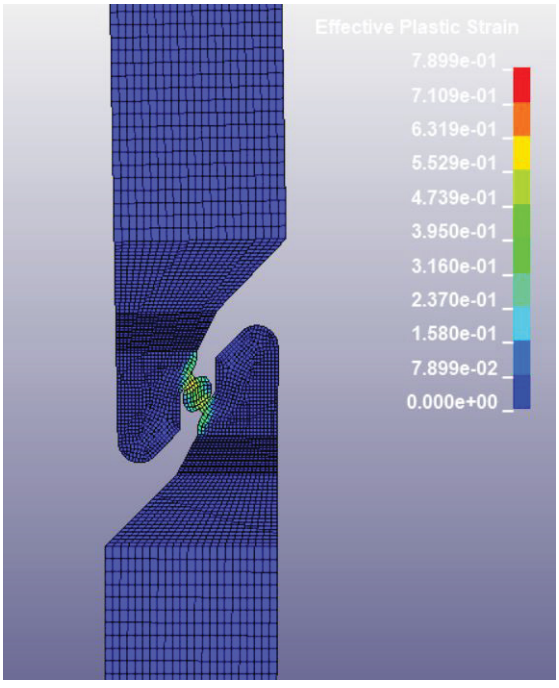

Figure A.27: Effective Plastic Strain - after failure

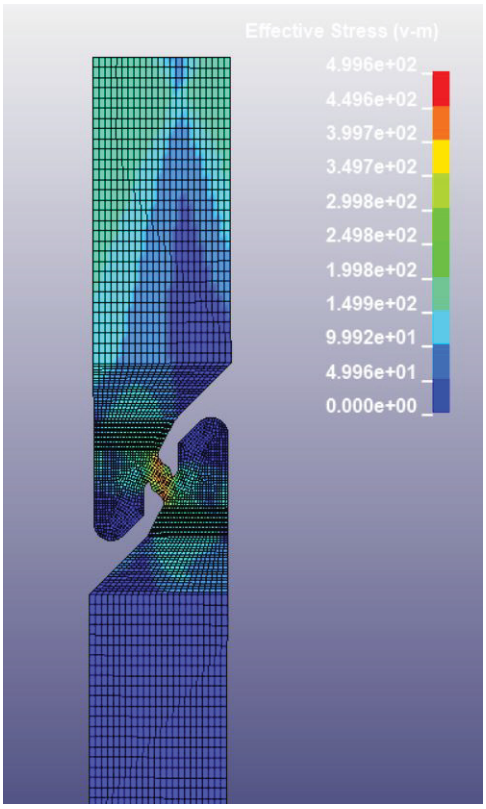

Figure A.28: Von Mises Stresses - Before failure

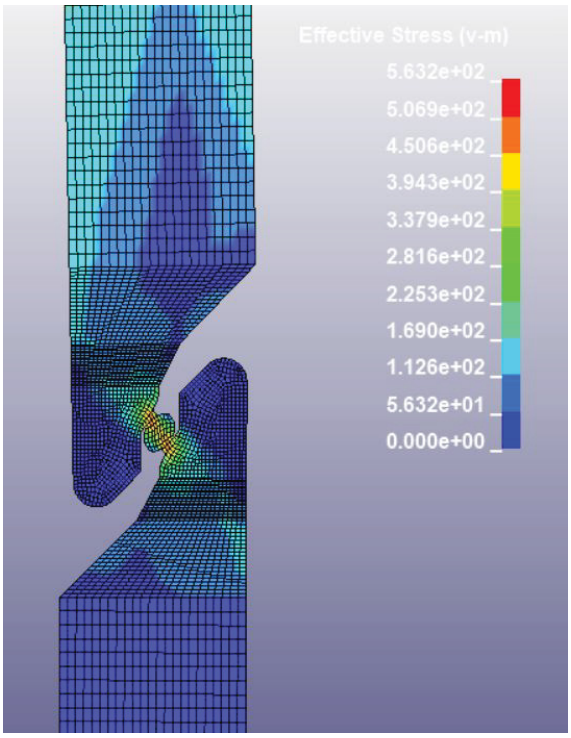

Figure A.29: Von Mises Stresses - After failure initiated

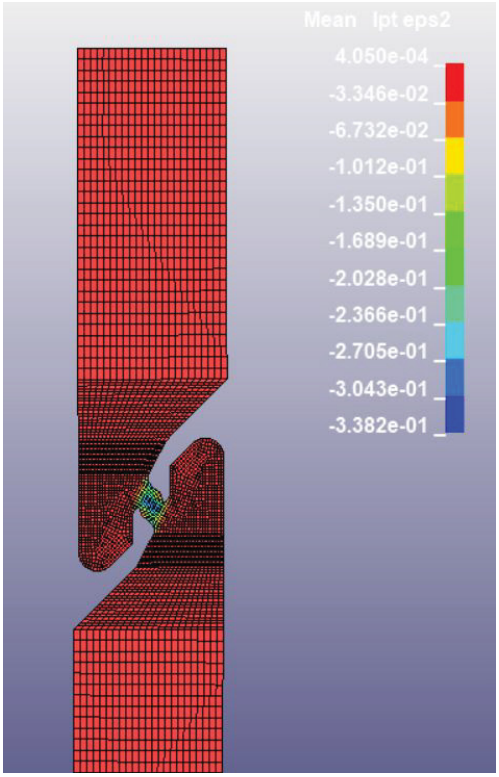

Figure A.30: Minor Strain - Before failure initiation

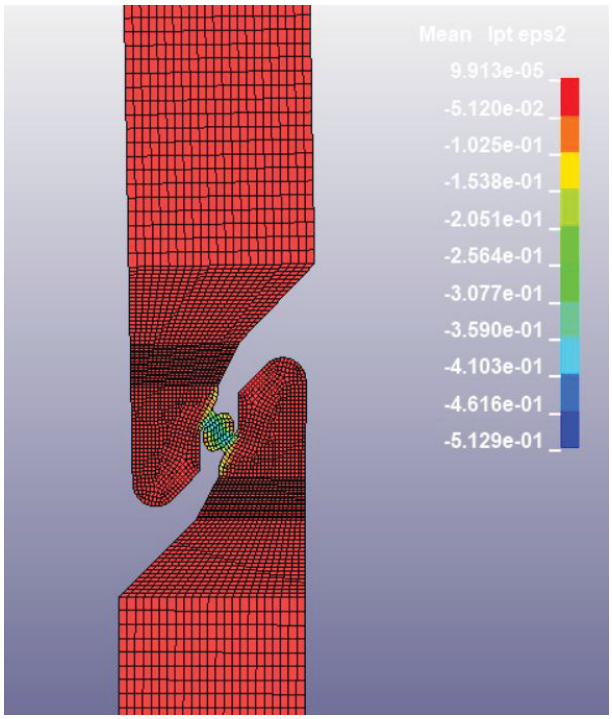

Figure A.31: Minor Strain - as soon as failure initiation

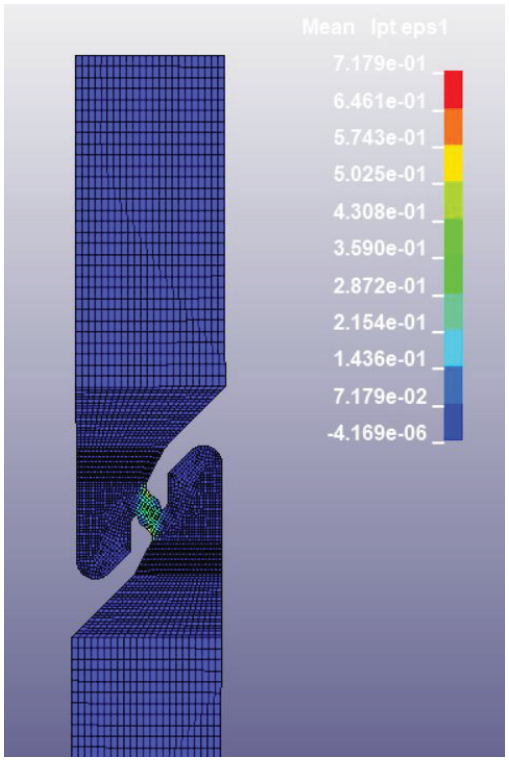

Figure A.32: Major Strain - before failure initiation

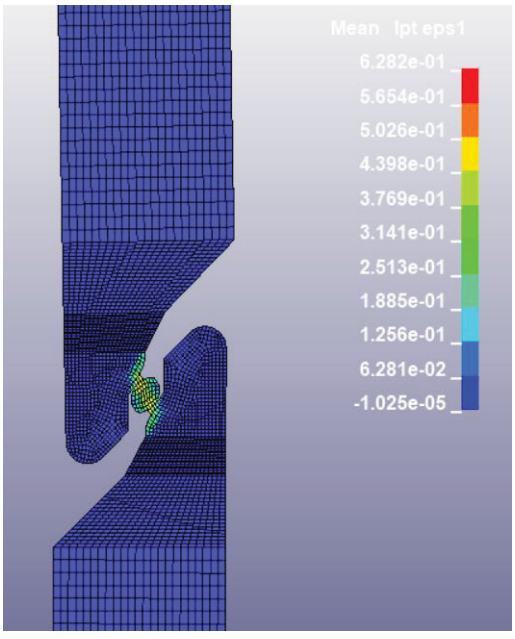

Figure A.33: Major Strain - As soon as failure initiation

In addition to results based on fringes shown from figure A.26 - A.33, few graphs corresponding to strains and strain paths have been plotted and show below. Minor strain Vs time graph for the entire simulation is shown in figure A.34. Furthermore figure A.35 corresponds to major strain vs time graph.

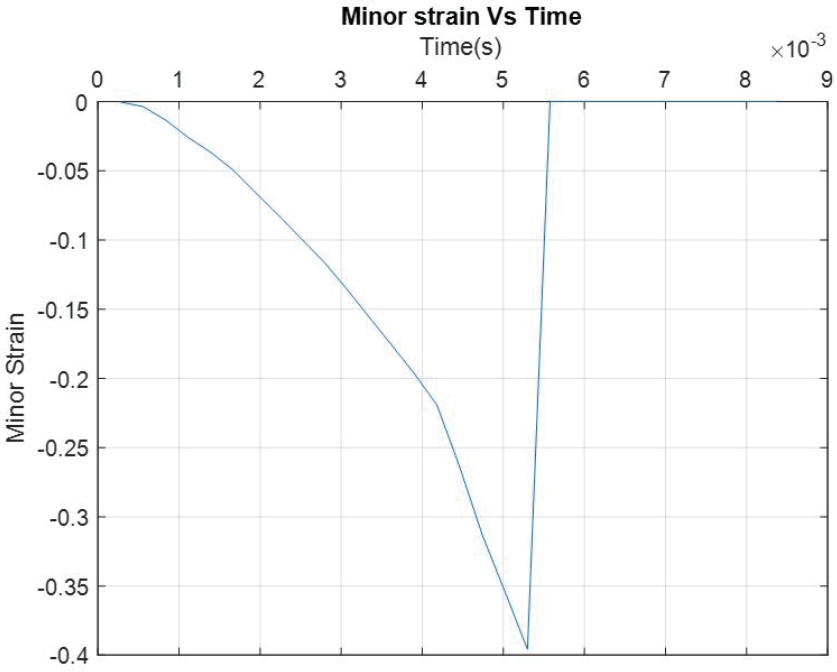

Figure A.34: Minor Strain VS Time

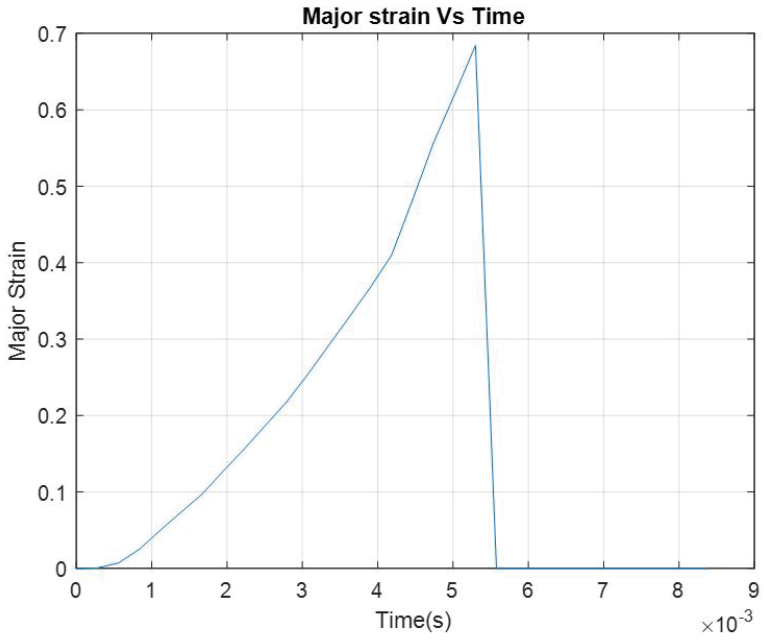

Figure A.35: Major Strain vs Time

Finally, the observed strain path for the element in center for shear testing FE-simulation is shown is figure A.36.

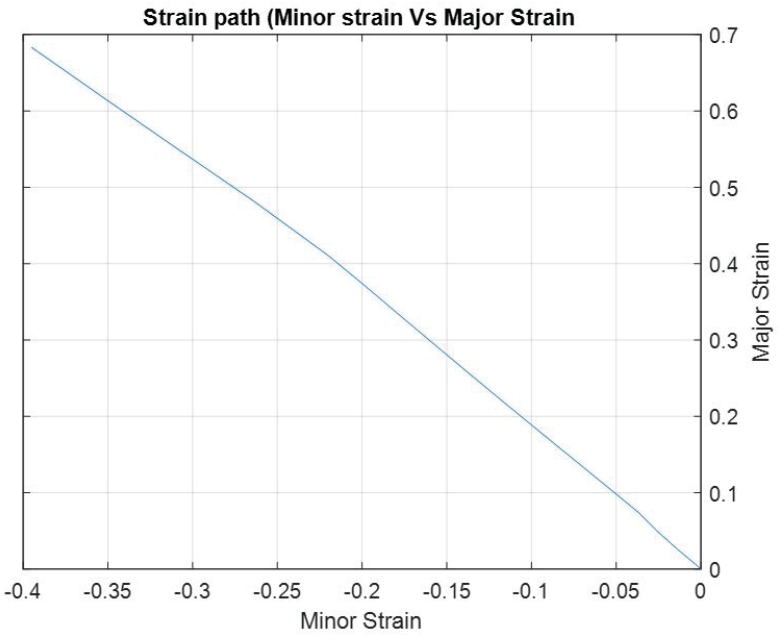

Figure A.36: Strain Path

A.0.3 Plane-Strain test

Findings of FE-simulation of Plane-strain test are categorized in two two section based on the inclusion of failure model, GISSMO.

Plane-strain test without Failure Model (GISSMO)

All the test results corresponding to shear test without failure models are shown below. Initially, effective strain path seen in the specimen at the end of the simulation is shown in figure A.37. Continuously, Von Mises stresses seen in the specimen at the end of the simulation is shown in figure **??**. Next, minor strain and major strain of the specimen at the end of the simulation is shown in figure A.39 and figure A.40 respectively.

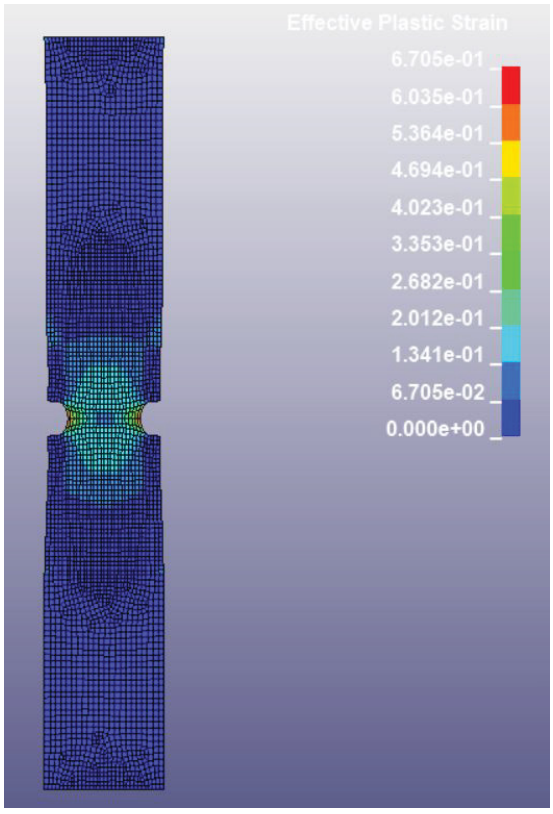

Figure A.37: Effective Plastic Strain

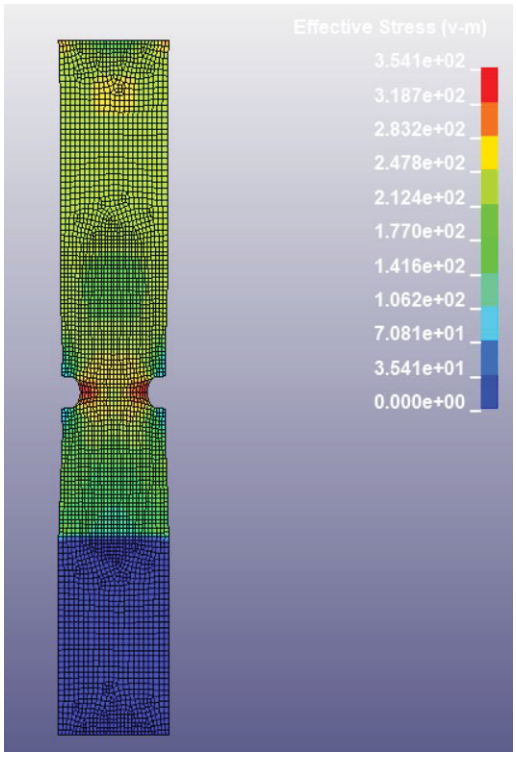

Figure A.38: Von Mises Stress

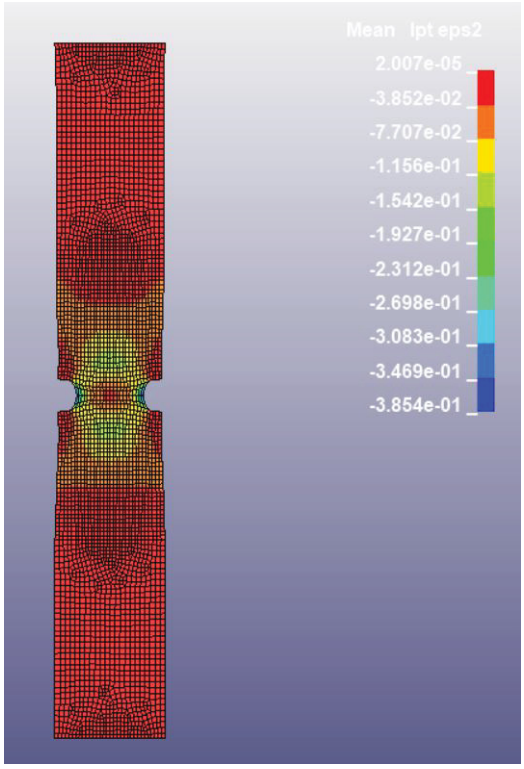

Figure A.39: Minor Strain

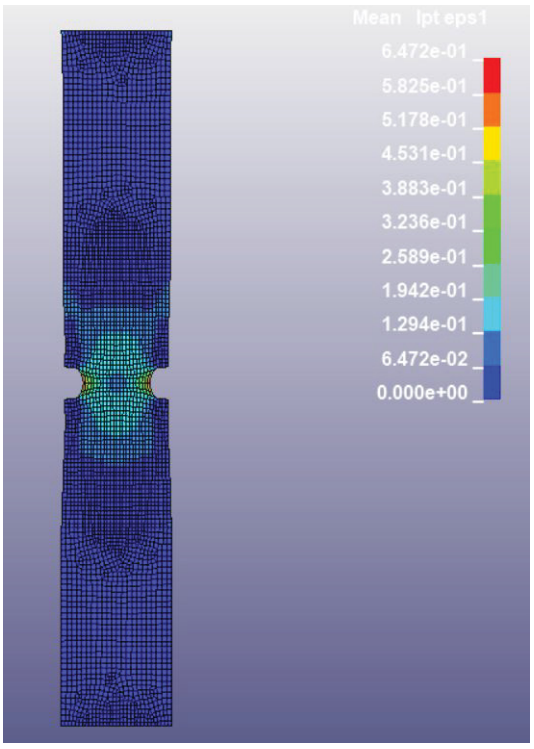

Figure A.40: Major Strain

In addition to results based on fringes shown from figure A.37 - A.40, few graphs corresponding to strains and strain paths have been plotted and show below with further details. Minor strain Vs time graph for the entire simulation is shown in figure A.41. Furthermore figure A.42 corresponds to major strain vs time graph.

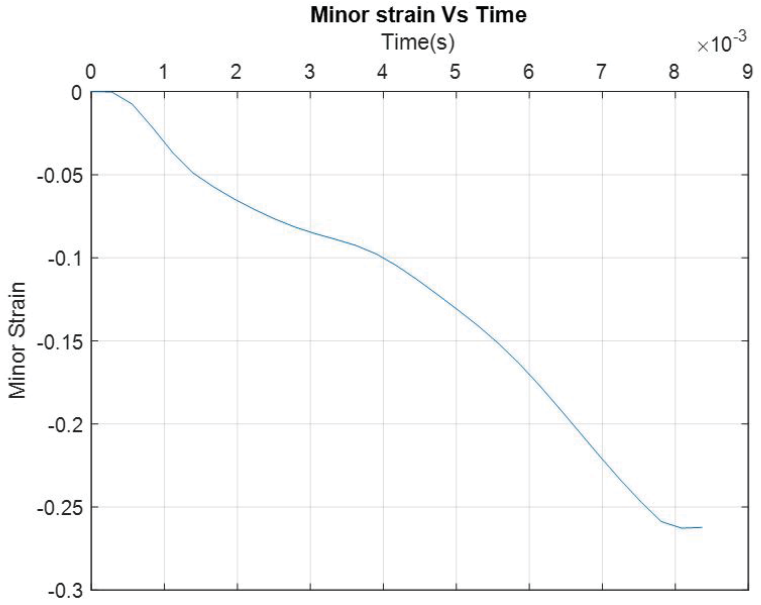

Figure A.41: Minor Strain VS Time

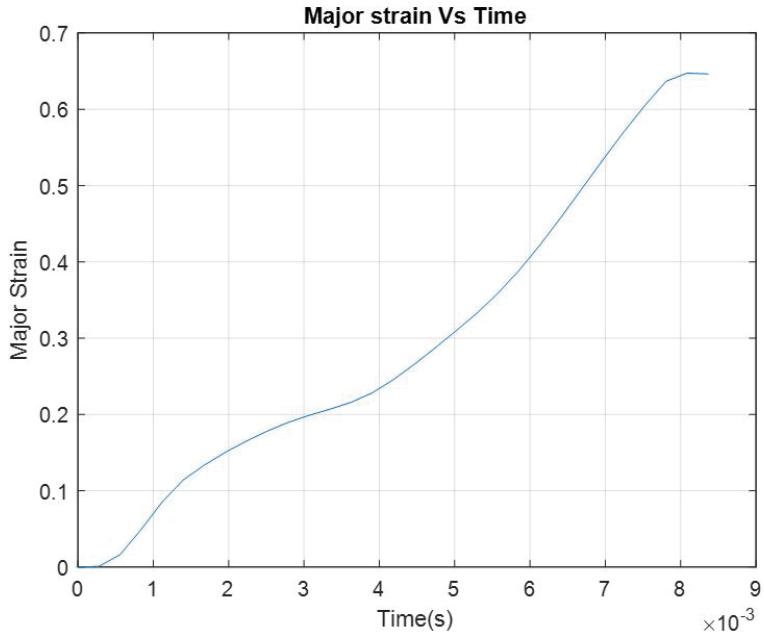

Figure A.42: Major Strain vs Time

Finally, the observed strain path for the element in center for shear testing FE-simulation is shown is figure A.43.

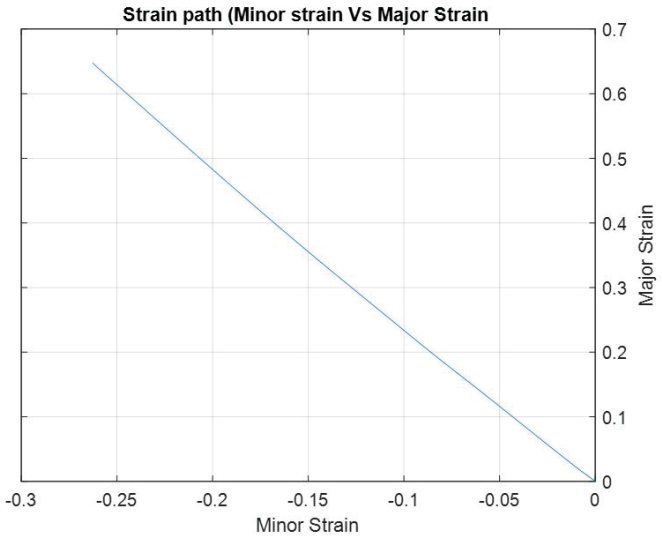

Figure A.43: Strain Path

Plane-strain Test with Failure Model (GISSMO)

All the test results corresponding to plane-strain test FE-simulation with failure models are shown below. Initially, effective strain path seen in the specimen one stage before failure is shown in figure A.44 and effective strain path as soon as failure is initiated is shown in figure A.45. Continuously, Von Mises stresses seen in the specimen before and after failure are shown in figureA.47 and figure **??** respectively. Next, minor strain of the specimen before failure and as soon as failure begins is shown in figure A.48 and figure A.49 respectively. Also for Major strain the corresponding figures are plotted and shown in figure A.50 and figure A.51.

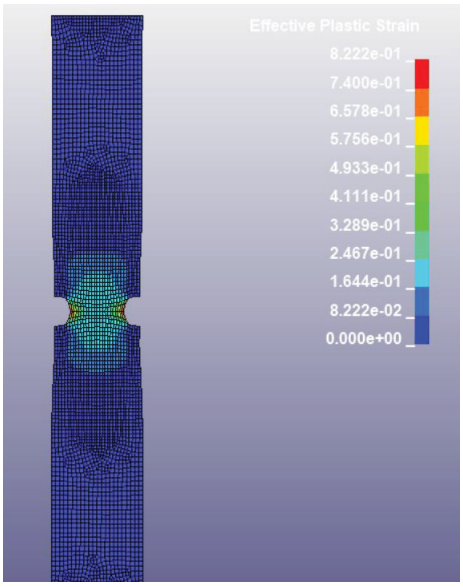

Figure A.44: Effective Plastic Strain - Before failure

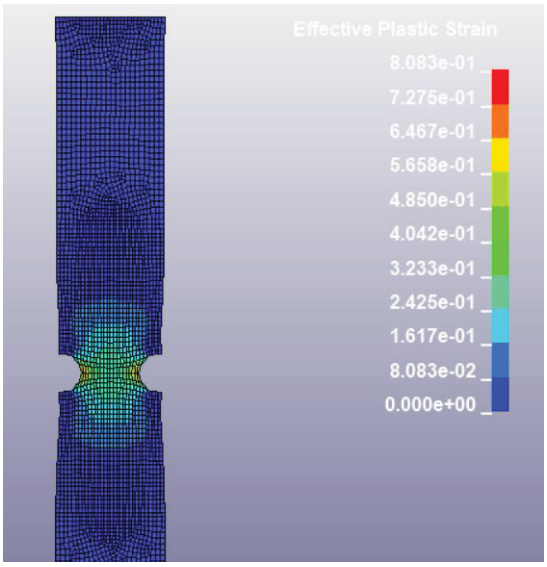

Figure A.45: Effective Plastic Strain - after failure

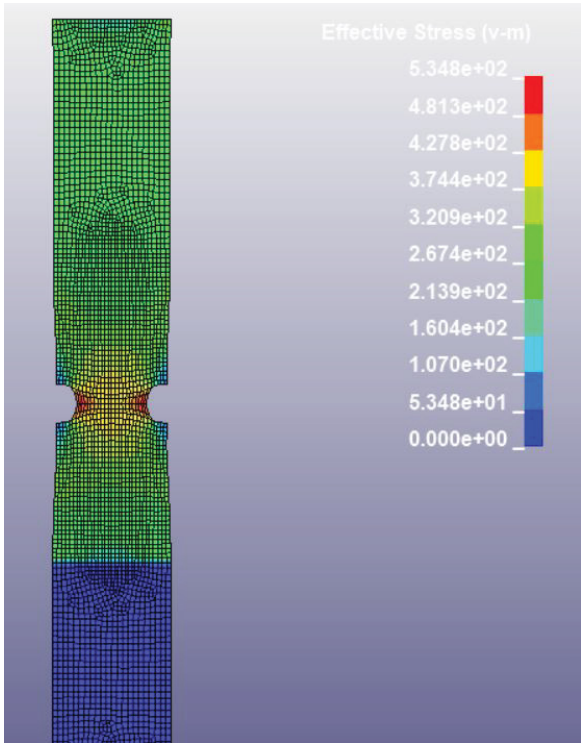

Figure A.46: Von Mises Stresses - Before failure

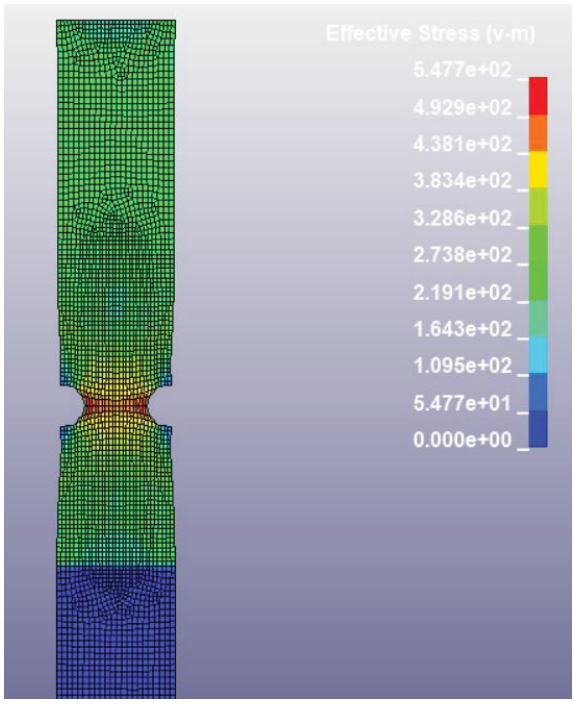

Figure A.47: Von Mises Stresses - After failure initiated

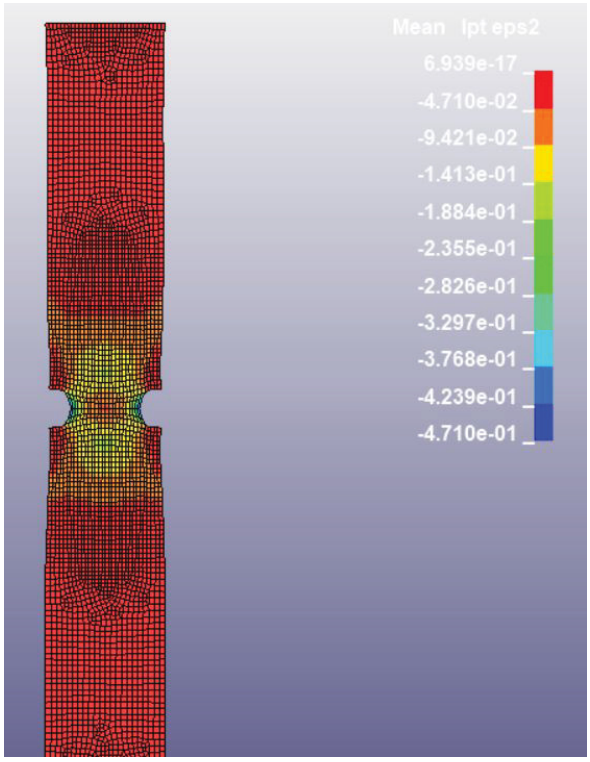

Figure A.48: Minor Strain - Before failure initiation

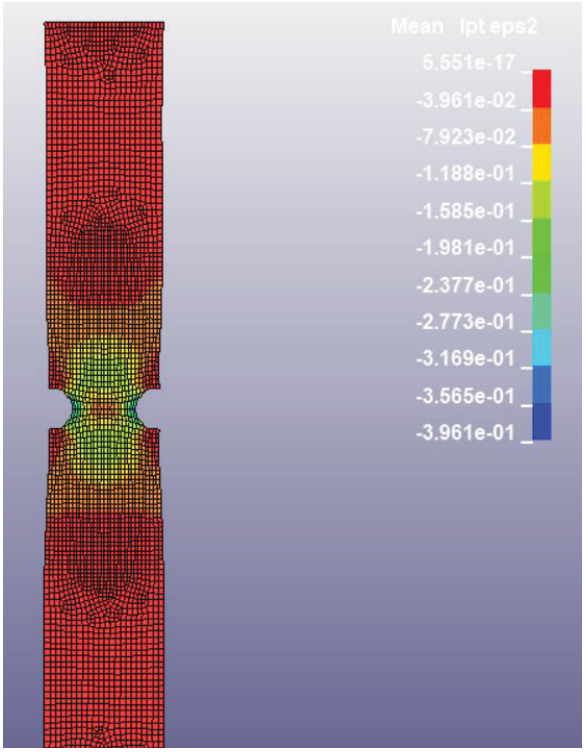

Figure A.49: Minor Strain - as soon as failure initiation

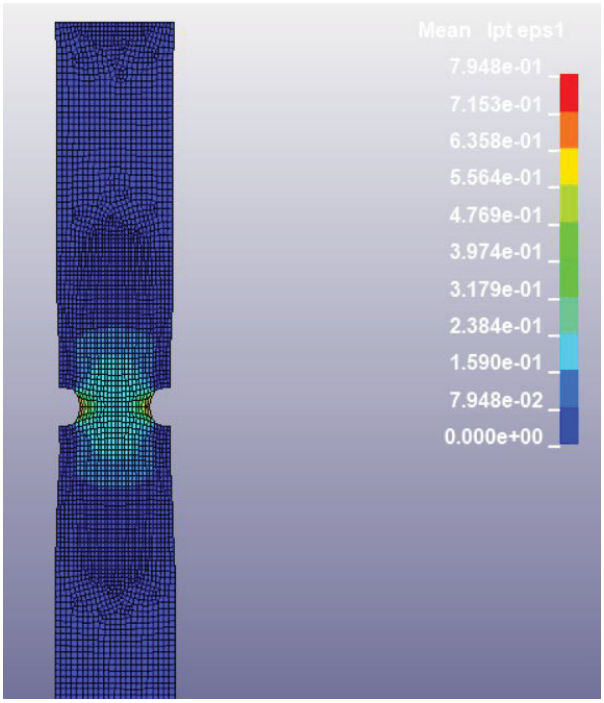

Figure A.50: Major Strain - before failure initiation

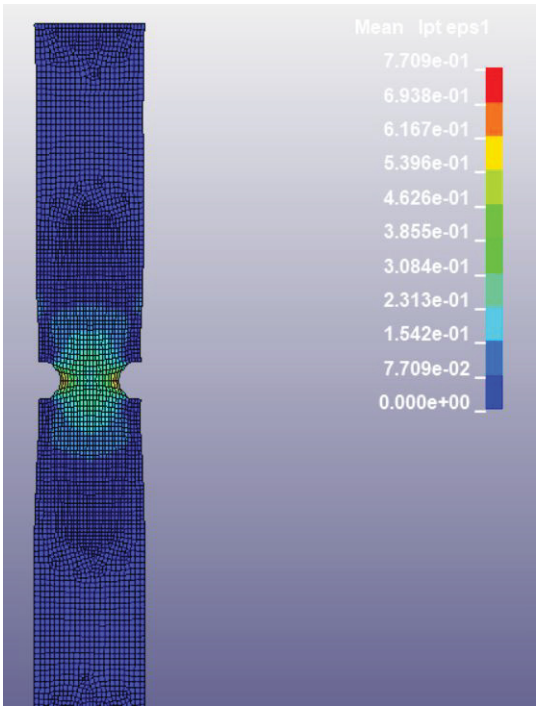

Figure A.51: Major Strain - As soon as failure initiation

In addition to results based on fringes shown from figure A.44 - A.51, few graphs corresponding to strains and strain paths have been plotted and show below. Minor strain Vs time graph for the entire simulation is shown in figure A.52. Furthermore figure A.53 corresponds to major strain vs time graph.

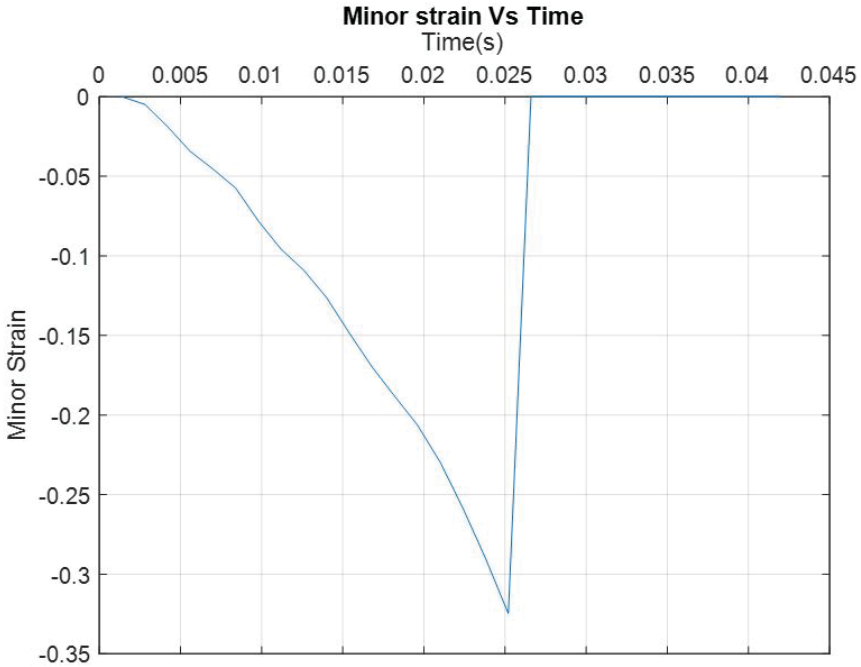

Figure A.52: Minor Strain VS Time

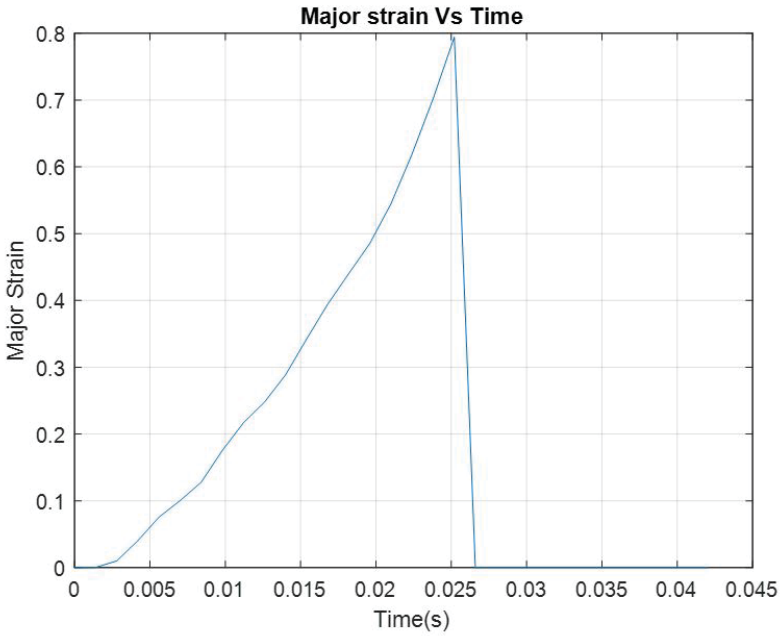

Figure A.53: Major Strain vs Time

Finally, the observed strain path for the element in center for shear testing FE-simulation is shown is figure A.54.

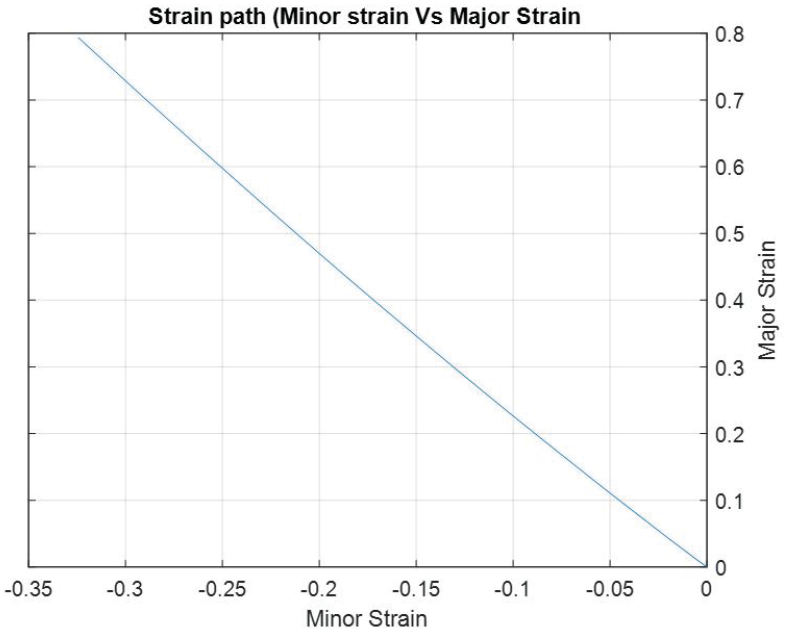

Figure A.54: Strain Path

A.0.4 Nakajima Test

In this subsection, FE-simulation results for Nakajima testing for the specimen width of 200mm. During FE-Simulation, failure model was included. Initially, effective strain path seen in the specimen one stage before failure is shown in figure A.55 and effective strain path as soon as failure is initiated is shown in figure A.56. Continuously, Von Mises stresses seen in the specimen before and after failure are shown in figureA.58 and figure A.58 respectively. Next, minor strain of the specimen before failure and as soon as failure begins is shown in figure A.59 and figure A.60 respectively. Also for Major strain the corresponding figures are plotted and shown in figure A.61 and figure A.62.

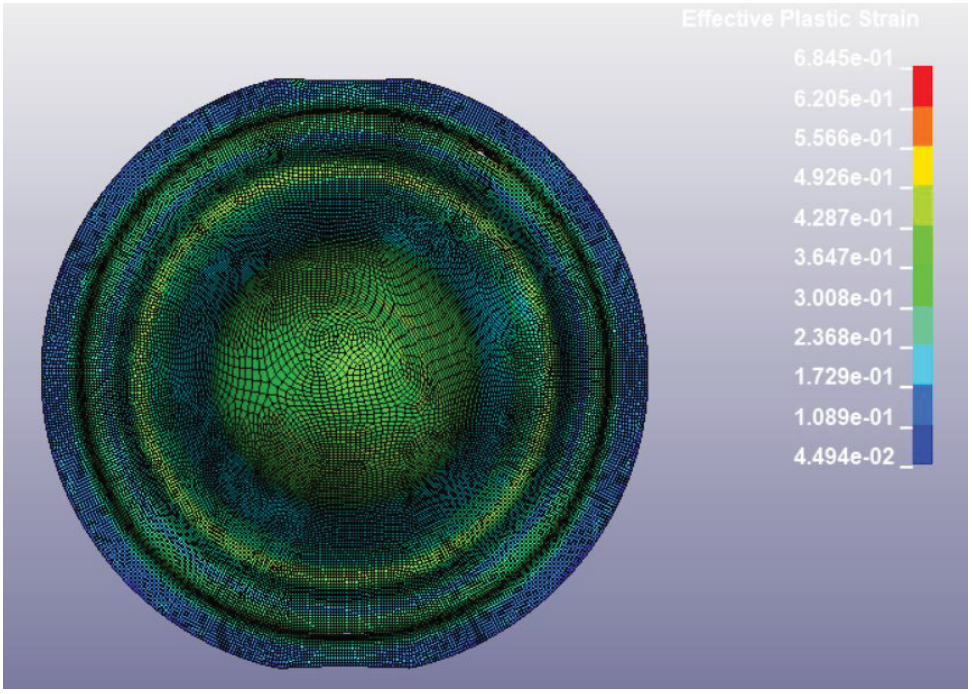

Figure A.55: Effective Plastic Strain - Before failure

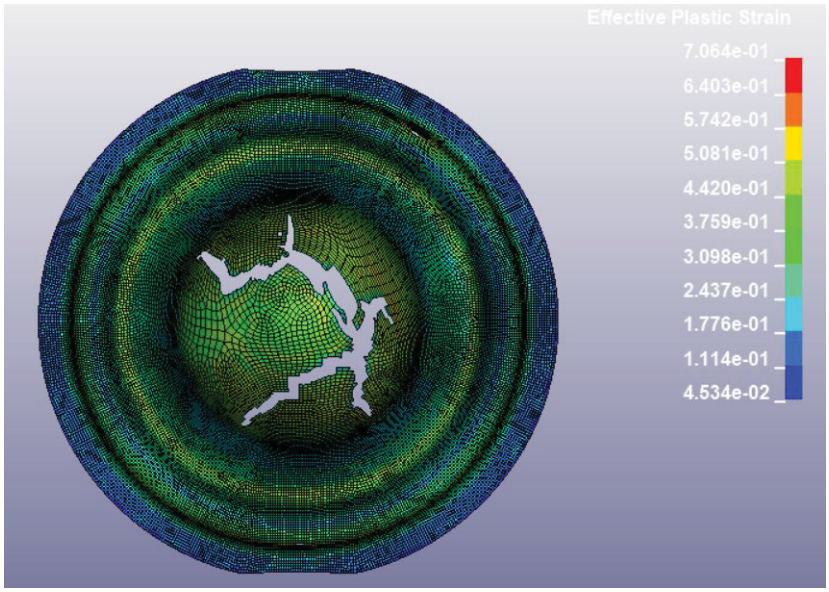

Figure A.56: Effective Plastic Strain - after failure

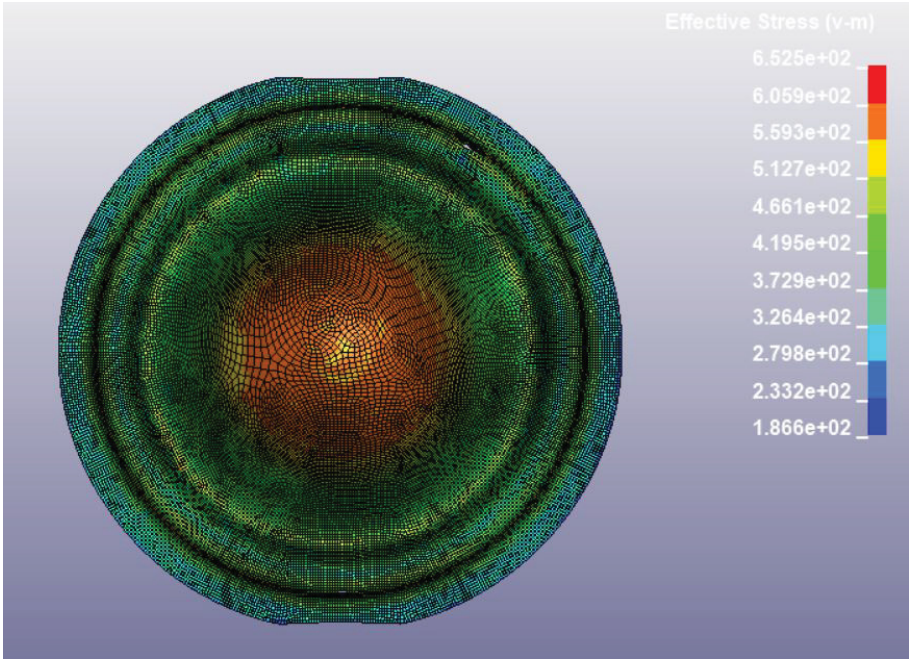

Figure A.57: Von Mises Stresses - Before failure

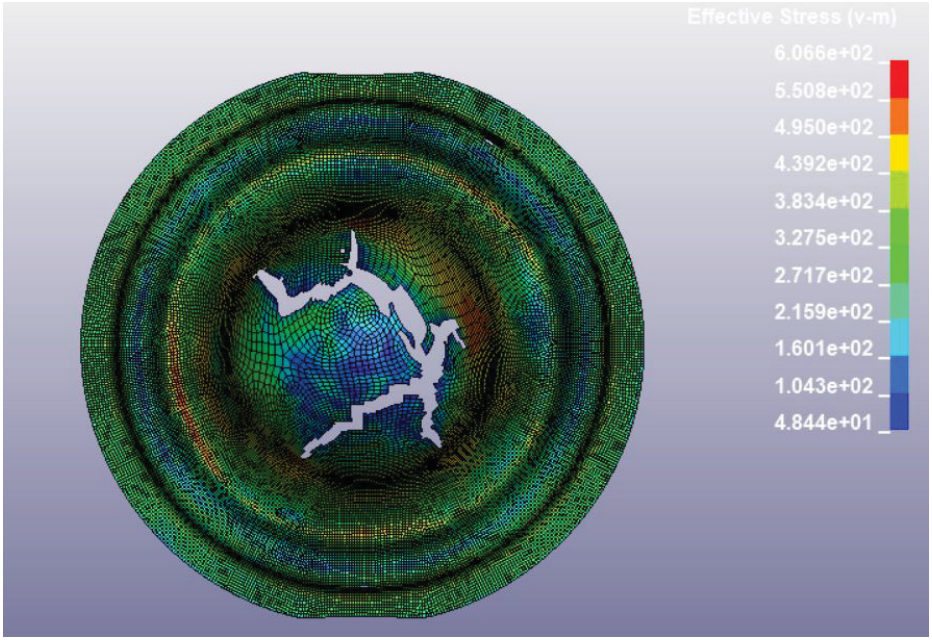

Figure A.58: Von Mises Stresses - After failure initiated

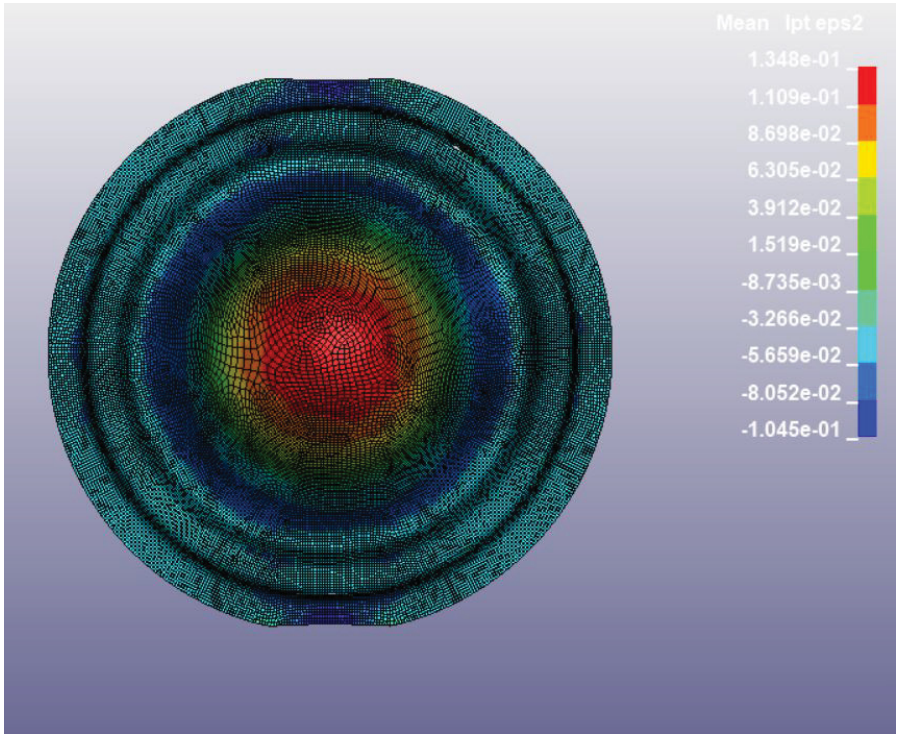

Figure A.59: Minor Strain - Before failure initiation

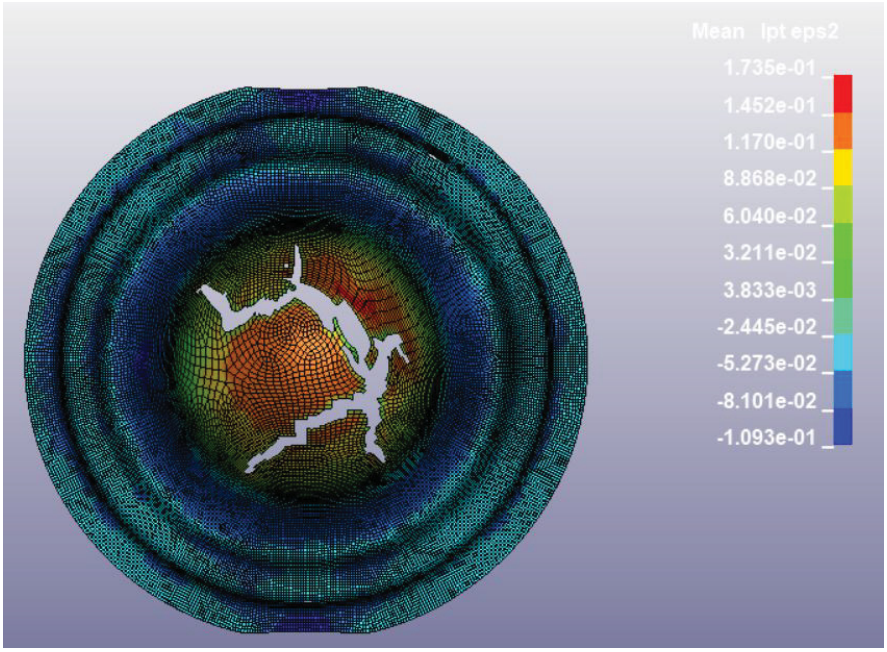

Figure A.60: Minor Strain - as soon as failure initiation

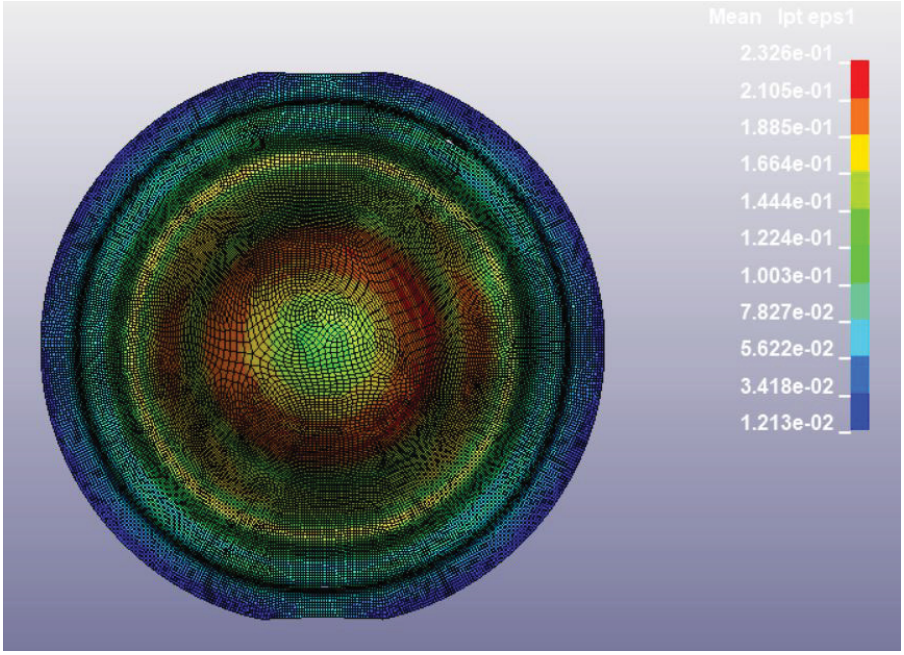

Figure A.61: Major Strain - before failure initiation

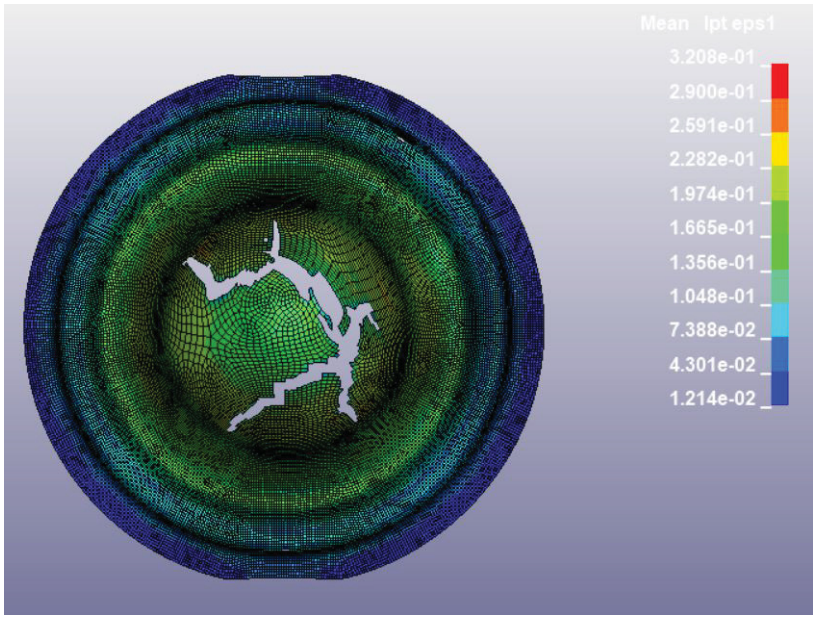

Figure A.62: Major Strain - As soon as failure initiation

In addition to results based on fringes shown from figure A.55 - A.62, few graphs corresponding to strains and strain paths have been plotted and show below. Minor strain Vs time graph for the entire simulation is shown in figure A.63. Furthermore figure A.64 corresponds to major strain vs time graph.

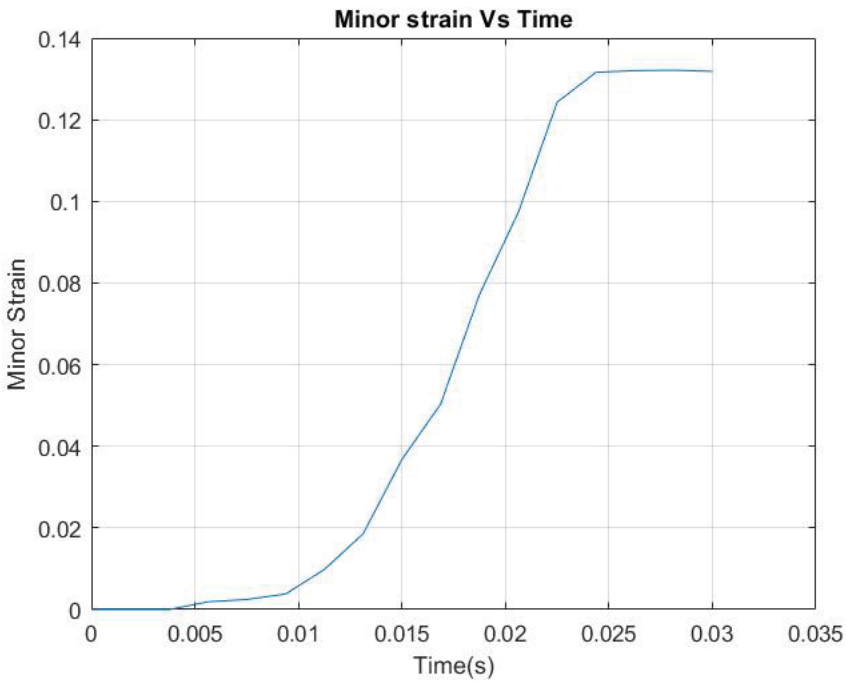

Figure A.63: Minor Strain VS Time

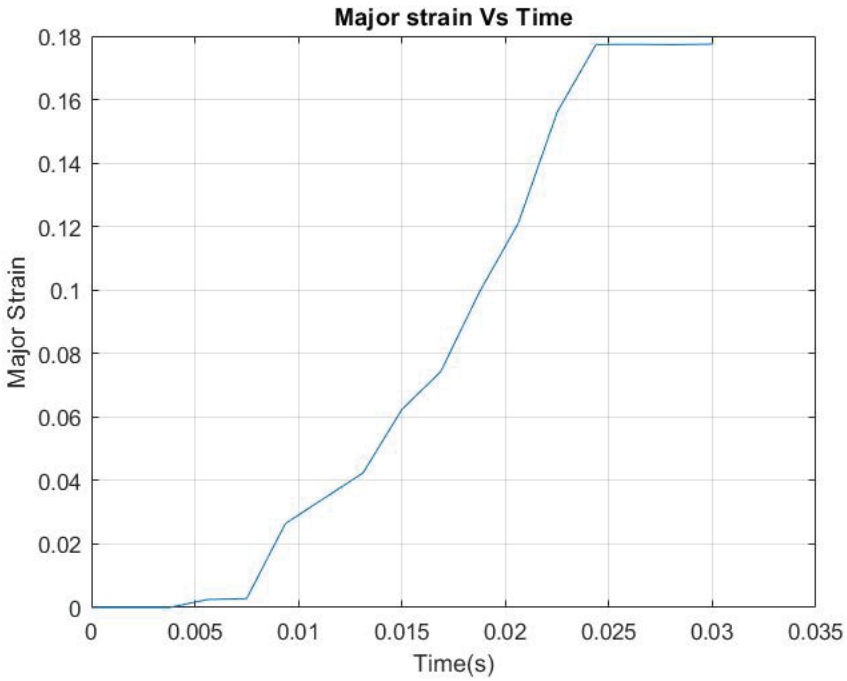

Figure A.64: Major Strain vs Time

Finally, the observed strain path for the element in center for shear testing FE-simulation is shown is figure A.65.

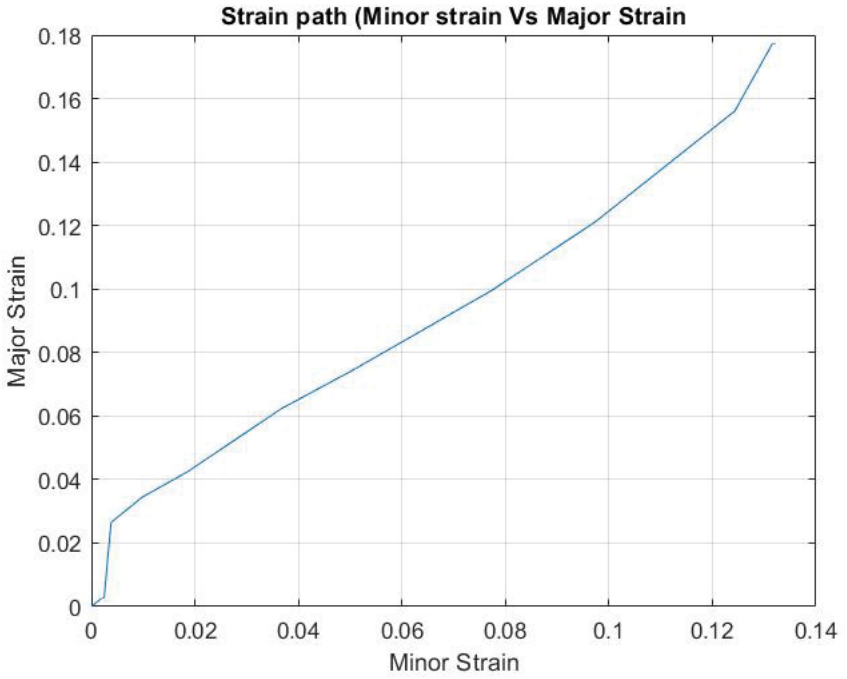

Figure A.65: Strain Path

Faculty of Engineering, Blekinge Institute of Technology, 371 79 Karlskrona, Sweden